

Preparation of the polyurethane resins with enhanced resistance against flammability

Bc. Peter Srnec

Master's thesis
2019



Tomas Bata University in Zlín
Faculty of Technology

Univerzita Tomáše Bati ve Zlíně

Fakulta technologická

Ústav inženýrství polymerů

akademický rok: 2018/2019

ZADÁNÍ DIPLOMOVÉ PRÁCE

(PROJEKTU, UMĚLECKÉHO DÍLA, UMĚLECKÉHO VÝKONU)

Jméno a příjmení: **Bc. Peter Srnec**
Osobní číslo: **T18696**
Studijní program: **N2808 Chemie a technologie materiálů**
Studijní obor: **Inženýrství polymerů**
Forma studia: **prezenční**

Téma práce: **Příprava polyuretanových pryskyřic se zvýšenými nároky na hořlavost**

Zásady pro vypracování:

Polyuretanové pryskyřice jsou polymerní materiály, které se skládají s dvou hlavních komponent; (i) izokyanátu a (ii) polyolu. Tyto materiály jsou velmi flexibilní s pohledu jejich zpracovatelnosti a zajímavé z důvodu jejich poměrně nízké ceny. Mají dobré mechanické vlastnosti, které jsou modulovatelné s ohledem na jejich finální aplikaci, použitím různých typů izokyanátů a polyolů. Jejich velkou nevýhodou, je poměrně nízká odolnost vůči hořlavosti a značné uvolňování plynů, které brání jejich frekventovanému použití v především dopravních prostředcích.

Student se bude v rešeršní části zabývat polyuretany obecně. Podrobně se bude věnovat pryskyřicím na bázi polyuretanu. Popíše různé typy plniv, které se používají jako retardéry hoření. Nedílnou součástí rešeršní práce bude popsat principy hořlavosti a zejména metody jejich hodnocení obecně a konkrétně pro dopravní prostředky. V experimentální části připraví student polymerní materiály na báze polyuretanu obsahující retardéry hoření. Tyto systémy bude charakterizovat pomocí různých analytických metod, spektroskopických technik, termických metod a nakonec zhodnotí jejich hořlavost a mechanické vlastnosti.

Rozsah diplomové práce:

Rozsah příloh:

Forma zpracování diplomové práce: **tištěná/elektronická**

Seznam odborné literatury:

1. HORROCKS, A. R., PRICE, D., *Advances in fire retardant materials*, Woodhead publishing materials, CRC Press Boston, 2008, ISBN 978-1-4200-7961-6
2. SONNENSCHNEIN, M.F., *Polyurethanes, Science, Technology, Market and Trends*, John Wiley and Sons Inc., 2015, ISBN 978-1-118-73783-5.

Vedoucí diplomové práce:

Ing. Miroslav Mrlík, Ph.D.
Centrum polymerních systémů

Datum zadání diplomové práce:

2. ledna 2019

Termín odevzdání diplomové práce:

14. května 2019

Ve Zlíně dne 18. února 2019

L.S.

doc. Ing. Roman Čermák, Ph.D.
děkan

doc. Ing. Tomáš Sedláček, Ph.D.
ředitel ústavu

Příjmení a jméno:

Obor:

PROHLÁŠENÍ

Prohlašuji, že

- beru na vědomí, že odevzdáním diplomové/bakalářské práce souhlasím se zveřejněním své práce podle zákona č. 111/1998 Sb. o vysokých školách a o změně a doplnění dalších zákonů (zákon o vysokých školách), ve znění pozdějších právních předpisů, bez ohledu na výsledek obhajoby ¹⁾;
- beru na vědomí, že diplomová/bakalářská práce bude uložena v elektronické podobě v univerzitním informačním systému dostupná k nahlédnutí, že jeden výtisk diplomové/bakalářské práce bude uložen na příslušném ústavu Fakulty technologické UTB ve Zlíně a jeden výtisk bude uložen u vedoucího práce;
- byl/a jsem seznámen/a s tím, že na moji diplomovou/bakalářskou práci se plně vztahuje zákon č. 121/2000 Sb. o právu autorském, o právech souvisejících s právem autorským a o změně některých zákonů (autorský zákon) ve znění pozdějších právních předpisů, zejm. § 35 odst. 3 ²⁾;
- beru na vědomí, že podle § 60 ³⁾ odst. 1 autorského zákona má UTB ve Zlíně právo na uzavření licenční smlouvy o užití školního díla v rozsahu § 12 odst. 4 autorského zákona;
- beru na vědomí, že podle § 60 ³⁾ odst. 2 a 3 mohu užít své dílo – diplomovou/bakalářskou práci nebo poskytnout licenci k jejímu využití jen s předchozím písemným souhlasem Univerzity Tomáše Bati ve Zlíně, která je oprávněna v takovém případě ode mne požadovat přiměřený příspěvek na úhradu nákladů, které byly Univerzitou Tomáše Bati ve Zlíně na vytvoření díla vynaloženy (až do jejich skutečné výše);
- beru na vědomí, že pokud bylo k vypracování diplomové/bakalářské práce využito softwaru poskytnutého Univerzitou Tomáše Bati ve Zlíně nebo jinými subjekty pouze ke studijním a výzkumným účelům (tedy pouze k nekomerčnímu využití), nelze výsledky diplomové/bakalářské práce využít ke komerčním účelům;
- beru na vědomí, že pokud je výstupem diplomové/bakalářské práce jakýkoliv softwarový produkt, považují se za součást práce rovněž i zdrojové kódy, popř. soubory, ze kterých se projekt skládá. Neodevzdání této součásti může být důvodem k neobhájení práce.

Ve Zlíně

.....

¹⁾ zákon č. 111/1998 Sb. o vysokých školách a o změně a doplnění dalších zákonů (zákon o vysokých školách), ve znění pozdějších právních předpisů, § 47 Zveřejňování závěrečných prací:

(1) Vysoká škola nevydělečně zveřejňuje disertační, diplomové, bakalářské a rigorózní práce, u kterých proběhla obhajoba, včetně posudků oponentů a výsledku obhajoby prostřednictvím databáze kvalifikačních prací, kterou spravuje. Způsob zveřejnění stanoví vnitřní předpis vysoké školy.

(2) Disertační, diplomové, bakalářské a rigorózní práce odevzdané uchazečem k obhajobě musí být též nejméně pět pracovních dnů před konáním obhajoby zveřejněny k nahlížení veřejnosti v místě určeném vnitřním předpisem vysoké školy nebo není-li tak určeno, v místě pracoviště vysoké školy, kde se má konat obhajoba práce. Každý si může ze zveřejněné práce pořizovat na své náklady výpisy, opisy nebo rozmnoženiny.

(3) Platí, že odevzdáním práce autor souhlasí se zveřejněním své práce podle tohoto zákona, bez ohledu na výsledek obhajoby.

²⁾ zákon č. 121/2000 Sb. o právu autorském, o právech souvisejících s právem autorským a o změně některých zákonů (autorský zákon) ve znění pozdějších právních předpisů, § 35 odst. 3:

(3) Do práva autorského také nezasahuje škola nebo školské či vzdělávací zařízení, užije-li nikoli za účelem přímého nebo nepřímého hospodářského nebo obchodního prospěchu k výuce nebo k vlastní potřebě dílo vytvořené žákem nebo studentem ke splnění školních nebo studijních povinností vyplývajících z jeho právního vztahu ke škole nebo školskému či vzdělávacího zařízení (školní dílo).

³⁾ zákon č. 121/2000 Sb. o právu autorském, o právech souvisejících s právem autorským a o změně některých zákonů (autorský zákon) ve znění pozdějších právních předpisů, § 60 Školní dílo:

(1) Škola nebo školské či vzdělávací zařízení mají za obvyklých podmínek právo na uzavření licenční smlouvy o užití školního díla (§ 35 odst. 3). Odpírá-li autor takového díla udělit svolení bez vážného důvodu, mohou se tyto osoby domáhat nahrazení chybějícího projevu jeho vůle u soudu. Ustanovení § 35 odst. 3 zůstává nedotčeno.

(2) Není-li sjednáno jinak, může autor školního díla své dílo užít či poskytnout jinému licenci, není-li to v rozporu s oprávněnými zájmy školy nebo školského či vzdělávacího zařízení.

(3) Škola nebo školské či vzdělávací zařízení jsou oprávněny požadovat, aby jim autor školního díla z výdělku jím dosaženého v souvislosti s užitím díla či poskytnutím licence podle odstavce 2 přiměřeně přispěl na úhradu nákladů, které na vytvoření díla vynaložily, a to podle okolností až do jejich skutečné výše; přitom se přihlíádne k výši výdělku dosaženého školou nebo školským či vzdělávacím zařízením z užití školního díla podle odstavce 1.

ABSTRAKT

Teoretická časť tejto práce sa zaoberá základnou teóriou o polyuretánoch, presnejšie o ich stavebných jednotkách, chemických reakciách a aplikáciách. Reakcia polyuretánu na tepelnú dekompozíciu a všeobecná reakcia materiálov voči horeniu a procesov horenia sú diskutované a spolu s kapitolami zameranými na rôzne typy retardérov horenia. Ich funkčný mechanizmus a spôsoby vyhodnocovania sú použité na určenie ich vplyvu na mechanické a chemické vlastnosti a mieru odolnosti a retardácie horenia.

Pre túto prácu bol pripravený odlievateľný polyuretán s aditívnym intumescenčným retardérom horenia a reaktívnym horenie retardujúcim polyolom, vo rôznych koncentráciách. Vplyv týchto komponent na schopnosť matrice odolávať horeniu bol vyhodnotený kónickým kalorimetrom (podľa ISO 5660-1:2002) a testom horľavosti plastových materiálov pre súčiastky v zariadeniach a spotrebičoch (podľa UL94). Kinetika vytvrdzovacích reakcií bola vyhodnotená pomocou dynamického skenovacieho kalorimetru s použitím dynamického skenu na vyrovnanie rýchlosti reakcie k rýchlosti ohrevu. Rotačná reológia nastavená na konštantnú frekvenciu a s konštantné namáhanie s teplotným profilom od 25°C do 150°C bola použitá na vyhodnotenie spracovateľnosti vytvrdzujúcej sa živice. Dynamická mechanická analýza bola použitá na sledovanie visko-elastických vlastností živice po dokončení vytvrdzovacej reakcie.

Kľúčové slová: kónický calorimeter, DSC, DA, rotačná reometria, vytvrdzovacia reakcia, kinetika, MARHE, heat release rate, polyol, izokyanát, UL94, retardér horenia, intumescencia, produkcia dymu.

ABSTRACT

Theoretical part of this thesis concerns basic theory about polyurethanes, more precisely its building blocks, their chemistry and applications. Reaction of polyurethane to thermal decomposition and overall reaction of materials to fire and fire dynamics are discussed, and together with chapters aimed at various types of flame retardants, their modes of action and

evaluation methods used to determine their impact on mechanical and chemical properties and flame resisting and retarding performance.

For this work cast polyurethane was prepared with additive intumescent flame retardant and reactive flame-retardant polyol in increasing concentrations. Impact of these components on the flame retarding performance of the matrix was evaluated by the cone calorimetry (according ISO 5660-1:2002) and by the test for flammability of plastic materials for parts in devices and appliances (according UL94). Kinetics of the curing reaction were evaluated by dynamic scanning calorimetry using dynamic scan to align the curing speed to the speed of temperature change. Rotational rheology in constant frequency and under constant shearing with temperature sweep from 25°C to 150°C was used to determine the processability of the curing resin. Dynamic mechanical analysis was performed to determine the viscoelastic behaviour of the resin after the curing reaction was performed.

Keywords: cone calorimeter, DSC, DMA, rotational rheometry, curing reaction, kinetics, MARHE, heat release rate, polyol, isocyanate, UL94, flame retardant, intumescence, smoke production

ACKNOWLEDGEMENTS

I would like to express my thankfulness to Tomáš Plachý and Miroslav Mrlík, for they have endless patience.

I hereby declare that the print version of my Bachelor's/Master's thesis and the electronic version of my thesis deposited in the IS/STAG system are identical.

16.5.2019 in Zlín

Peter Srnec

CONTENTS

| | |
|--|-----------|
| INTRODUCTION | 10 |
| I. THEORY | 12 |
| 1 POLYURETHANE (PUR) | 13 |
| 1.1 BUILDING BLOCKS | 15 |
| 1.2 POLYOLS | 15 |
| 1.3 POLYETHER POLYOLS | 15 |
| 1.3.1 POLYESTER POLYOLS | 17 |
| 1.3.2 OTHER POLYOLS | 19 |
| 1.4 ISOCYANATES | 20 |
| 1.4.1 TOLUENE BASED ISOCYANATES (TDI) | 20 |
| 1.4.2 ANILINE AND FORMALDEHYDE BASED ISOCYANATES – MDI AND PMDI | 21 |
| 1.4.3 ALIPHATIC ISOCYANATES | 22 |
| 1.5 CHAIN EXTENDERS | 23 |
| 2 FLAME RETARDANT SYSTEMS (FRS) | 24 |
| 2.1 MODES OF ACTION | 24 |
| 2.1.1 PHYSICAL MODE OF ACTION | 24 |
| 2.1.2 CHEMICAL MODE OF ACTION | 25 |
| 2.1.3 CHARRING AND INTUMESCENCE | 25 |
| 2.2 SYNERGISTIC AND ANTAGONISTIC EFFECT OF FLAME RETARDANTS | 26 |
| 2.3 MINERAL FLAME RETARDANTS | 27 |
| 2.4 HALOGENATED FLAME RETARDANTS (HFR) | 29 |
| 2.5 PHOSPHOROUS – BASED FLAME RETARDANTS | 30 |
| 2.6 NITROGEN – BASED FLAME RETARDANTS | 31 |
| 2.7 NANOMETRIC PARTICLES | 32 |
| 3 BEHAVIOUR OF POLYMER UNDER THERMAL STRAINING | 34 |
| 3.1 THERMAL DECOMPOSITION | 34 |
| 3.2 CHEMISTRY MECHANISM OF DEGRADATION | 35 |
| 3.3 THERMAL RESPONSE OF COMMON POLYMERS | 36 |

| | | |
|--------|---|-----------|
| 3.3.1 | POLYETHYLENE (PE)..... | 36 |
| 3.3.2 | POLYPROPYLENE (PP) | 36 |
| 3.3.3 | POLYVINYLCHLORIDE (PVC)..... | 37 |
| 3.3.4 | POLYSTYRENE (PS) | 37 |
| 3.3.5 | POLYETHYLENETEREHPHTALATE (PET) | 37 |
| 3.3.6 | POLYMETHYLMETHACRYLATE (PMMA) | 37 |
| 3.3.7 | POLYOXYMETHYLENE (POM)..... | 38 |
| 3.3.8 | NYLON 6 AND NYLON 6,6 | 38 |
| 3.3.9 | POLYCARBONATE (PC)..... | 38 |
| 3.3.10 | FLUOROPOLYMERS | 39 |
| 3.3.11 | ELASTOMERS..... | 39 |
| 3.4 | THERMAL RESPONSE OF POLYURETHANE THERMOSETS | 39 |
| 4 | FLAMMABILITY AND MECHANISM OF COMBUSTION | 42 |
| 4.1 | REACTION OF MATERIAL TO FIRE | 42 |
| 4.2 | HEAT RELEASE RATE (HRR)..... | 43 |
| 4.3 | PEAK HEAT RELEASE RATE (PHRR)..... | 45 |
| 4.4 | AVERAGE HEAT RELEASE RATE | 45 |
| 4.5 | TIME TO IGNITION..... | 45 |
| 4.6 | FLAME SPREAD RATE | 45 |
| 4.7 | LIMITING OXYGEN INDEX..... | 46 |
| 4.8 | SMOKE GENERATION, DENSITY AND TOXICITY..... | 46 |
| 4.9 | MASS LOSS..... | 47 |
| 4.10 | FIRE RESISTANCE | 47 |
| 4.11 | MECHANISM OF COMBUSTION | 48 |
| 4.11.1 | FLAME STRUCTURE..... | 48 |
| 4.11.2 | COMBUSTION CYCLE..... | 49 |
| 5 | EVALUATION METHODS..... | 51 |
| 5.1 | CONE CALORIMETER..... | 51 |
| 5.2 | ROTATIONAL RHEOMETRY | 54 |
| 5.3 | FLAMMABILITY INVESTIGATION ACCORDING TO UL-94 | 56 |
| 5.4 | DYNAMIC MECHANICAL ANALYSIS (DMA)..... | 58 |
| 5.5 | DIFFERENTIAL SCANNING CALORIMETRY (DSC)..... | 59 |
| 5.6 | FOURIER-TRANSFORM INFRARED SPECTROSCOPY (FTIR) | 61 |
| II. | ANALYSIS | 62 |
| 6 | EXPERIMENT..... | 63 |
| 6.1 | MATERIALS..... | 63 |
| 6.1.1 | POLYURETHANE COMPONENTS | 63 |
| 6.1.2 | ADDITIVE..... | 63 |
| 6.2 | SAMPLE FABRICATION..... | 63 |
| 6.3 | SAMPLE PREPARATION..... | 64 |

| | | |
|------------|---|-----------|
| 6.3.1 | SAMPLE DENOTATION AND COMPOSITION | 64 |
| 6.4 | EXPERIMENT METHODOLOGY | 65 |
| 6.4.1 | FTIR..... | 65 |
| 6.4.2 | ROTATIONAL RHEOMETRY | 66 |
| 6.4.3 | DYNAMIC SCANNING CALORIMETRY (DSC)..... | 66 |
| 6.4.4 | DYNAMIC MECHANICAL ANALYSIS (DMA)..... | 66 |
| 6.4.5 | CONE CALORIMETRY | 66 |
| 6.4.6 | UL94 | 66 |
| 7 | RESULTS AND DISCUSSION | 67 |
| 7.1 | FTIR..... | 67 |
| 7.2 | ROTATIONAL RHEOLOGY | 67 |
| 7.3 | DSC | 76 |
| 7.4 | DMA..... | 78 |
| 7.5 | CONE CALORIMETER..... | 80 |
| 7.6 | UL94..... | 87 |
| | CONCLUSION..... | 90 |
| | BIBLIOGRAPHY | 92 |
| | LIST OF ABBREVIATIONS | 98 |
| | LIST OF FIGURES..... | 102 |
| | LIST OF TABLES | 105 |
| | APPENDICES | 106 |

INTRODUCTION

Polyurethanes are one of the most used class of thermosetting polymers and polymers in general, due to the fact that polyurethanes may have variety of mechanical properties and can vary from elastomers to resins. Therefore, they can be effectively used in many applications from simple cushioning, tubing, textiles or adhesives to small components of electronic appliances or profiles in automotive and public transportation. This variability in applications is given by the large number of possible combinations in reactions of isocyanates and polyols [1].

In the case of thermosetting polyurethanes, the crucial parameter influencing the applicability of the system is the reaction kinetics. The curing reaction has to be accurate. Fast reaction does not allow for the system to change into the well-defined shape, while long reaction time is unsuitable from the technological point of view (amount of the samples).

Another parameter is mechanical performance, since the flame retardants are from the class of powders or liquids, they can influence the mechanical properties significantly and thus the sustainability of the mechanical properties is very crucial to provide sufficient mechanical performance at least comparable to those obtained for neat polyurethane system

Because the polyurethanes are widely used in the public transportation, the requirements on the resistance against flammability are on the highest level. Due to the fact, that the halogen-based flame retardants release toxic volatiles while burning, these FR systems are not that frequent. Various inorganic fillers such as aluminium trihydrate or magnesium hydroxide are usually applied instead. On the other hand, since 2013 the limits for flammability of the components used in railway carriages were significantly tightened [2], the utilization of other flame retardants, such as intumescent additives or individual parts of isocyanates or polyols with flame retardant directly in their chemical structure seem to be very attractive way to sufficiently improve this property.

This work is therefore focused on the preparation of the polyurethane material, modified with flame retardants in multiple concentrations. Presence of individual flame retardants was confirmed by FTIR (Fourier transform infrared spectroscopy). Reaction kinetics were investigated using DSC as evaluation of the plotting the Heat flow against time and using viscoelastic properties where viscoelastic moduli as well as viscosity of the various systems were plotted against time at elevated temperature. Furthermore, evaluation of viscoelastic properties such as viscoelastic moduli measured using DMA (dynamic mechanical analysis) in the tensile mode at

broad temperature range provide the information about glass transition temperature and how it is changing with various flame retardants. Finally, the and flammability of the prepared composite systems was measured by cone calorimeter as well as using UL-94 method, as it is the most utilized flammability test nowadays. The results from cone calorimeter and UL 94 test as a complementing method to the cone calorimetry test were investigated, compared and correlation between them was discussed.

I. THEORY

1 POLYURETHANE (PUR)

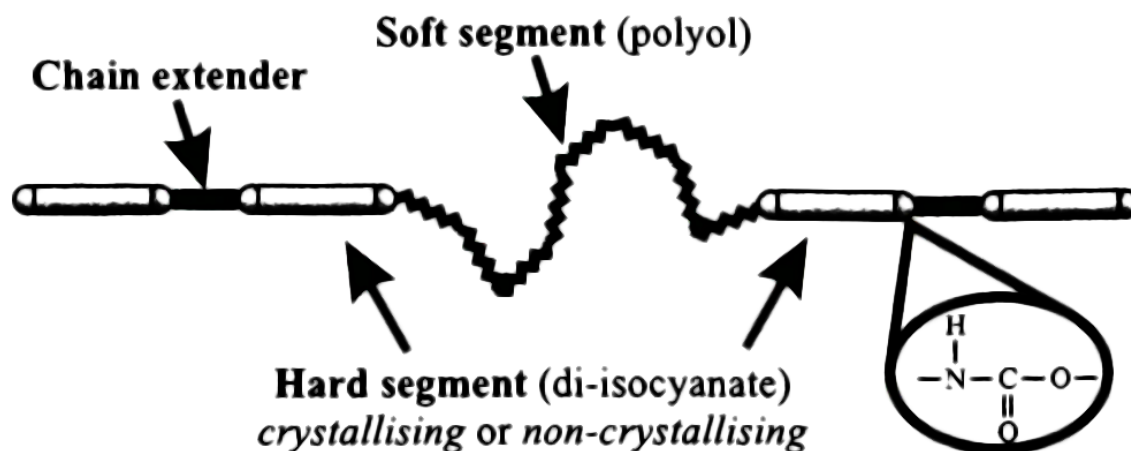


Fig. 1: Schematic representation of polyurethane chain and its segmented character [3].

PURs are class of thermosetting polymers, which have extensive versatility of applications such as heat insulation, soft foam for cushioning, adhesives, coatings, structural foam, fibres and many more. Polyurethane is not one exact polymer that can be characterised by specific formula. Instead every polymer that contains repeating urethane unit can be considered as polyurethane. Polyurethanes are produced in two ways. The first one is one-shot process, in which all components are mixed together. The second process is the prepolymer process, where prepolymer is prepared first and then chain extenders are added [4]. The polymerisation follows polyaddition mechanism, where functional groups of R-OH and R'-NCO react with each other to produce PUR. If the hydroxyl group would be swapped for amine group, R-NH, then the product of the reaction would be polyurea. Contrary to polycondensation, polyaddition does not produce any side product. Reaction is driven by the free hydrogen that is easily removed from functional group of polyol or isocyanate and leaves unhindered electron pair [5]. Reaction of isocyanates with polyols at standard conditions is slow and therefore needs to be catalysed [6]. Generalized reaction mechanism is shown in fig. 2. The common used catalysts are: diazobicyclo[2.2.2]octane (DABCO), Dibutyltin dilaurate (DBTDL), Triethylene diamine (TEDA), 1,8-diazabicyclo (5.4.0) undec-7-ene (DBU), Tin (II) 2-ethylhexanoate (T-9), Bis (dimethylamino) ether, Dibutyltindimercaptide (UL-22), Pentamethyl diethylenetriamine, Dimethylpiperazine and Penthamethyldipropylenetriamine. Catalysis does not only enhance formation of

polyurethanes, but also accelerates a number of side reactions that can determine the resulting product. Polymerisation of PURs has few characteristics [7]:

- Single reaction (propagation) is responsible for the formation of polymer
- Monomer system contains A, B or C functional groups that can react randomly
- Monomers are depleted at the early stages of reaction
- M_w rises slowly, high M_w is achieved only with high conversion
- Broad distribution of M_w during reaction until the end, when all oligomers have reacted
- Successful reaction requires precise stoichiometric ratios
- Monomers with high purity are required
- Reactions are reversible.

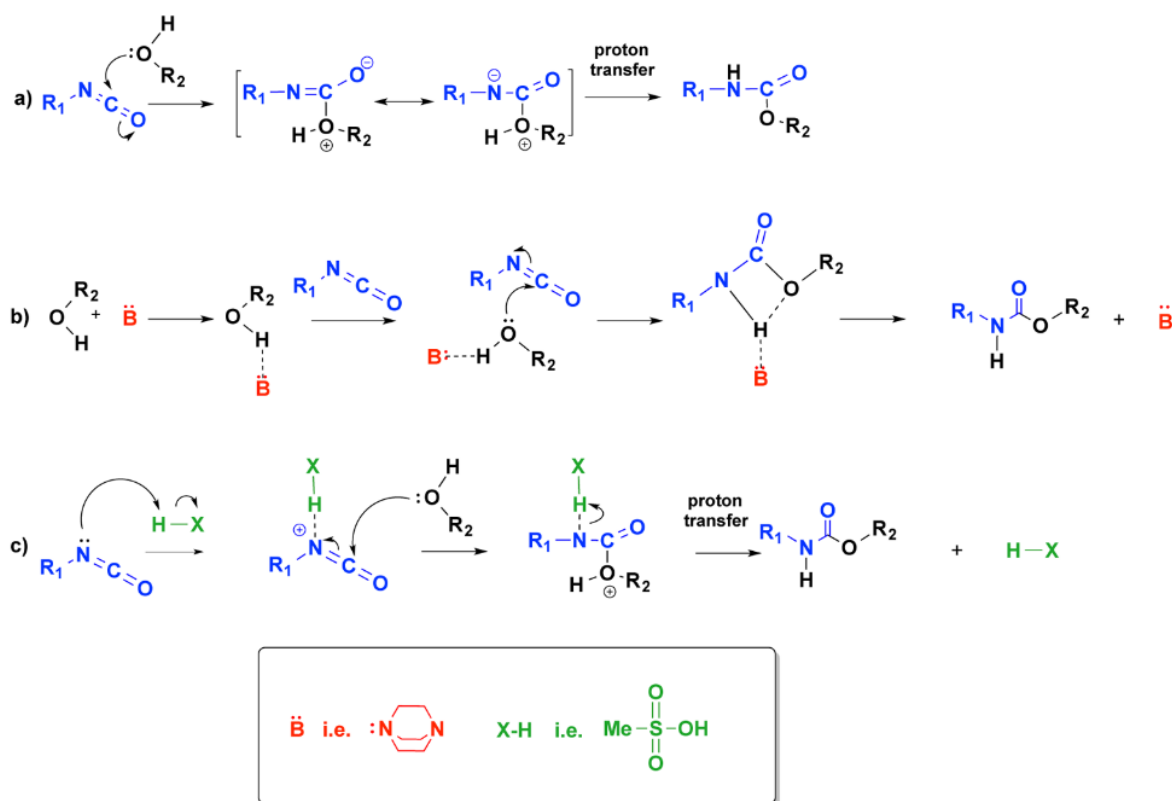


Fig. 2: Mechanisms of isocyanate and alcohol reaction a) without catalyst b) with base or nucleophilic activator and c) acid or electrophilic activator [8].

1.1 Building blocks

Versatility of PURs comes from the amount of building blocks that can be used for synthesis. Polyurethanes therefore have significantly different structure depending on application in which they are going to be used.

The building blocks are divided to three major classes:

- a) Polyols
- b) Isocyanates
- c) Chain extenders

1.2 Polyols

Polyols are polymer backbones, made up of molecules containing multiple hydroxyl groups in their structure. Polyols have high weight ratio in PURs, ranging from 90 wt% to 30 wt% in flexible sealants, flexible foams and rigid insulation foams, respectively.[6] Polyols have wide range of functionality, based on their backbone composition and hydroxyl functionality. Two of the main groups are based on ether and ester. Others can be derived from tetrahydrofuran (THF) and they are used in high-performance applications. Polyols have significant impact on the processing and final properties of polyurethane. Polyols represent the soft segment of polyurethane chain as shown in fig. 1.

1.3 Polyether polyols

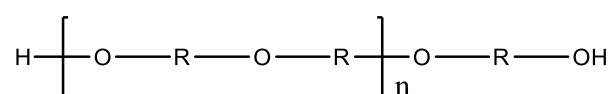


Fig. 3: Polyether [6].

Polyether polyols (see fig. 3) are products of exothermic reaction between starter molecules (initiators) and cyclic ethers. The Starter molecules are for example ethylene glycol, propylene glycol, glycerine, pentaerythritol, trimethylolpropane. Cyclic ethers can be ethylene oxide (oxirane), 1,2 propylene oxide (methyloxirane), 1,2 butylene oxide (ethyloxirane) or THF. Polyether polyols have functionality that is directly related to the functionality of initiators of their synthesis. For example, diol initiator will make the resulting polyol have functionality of two.

Synthesis of polyether polyols can be seen on fig. 4. The most important polyether polyols are poly butadiene oxide glycol, polytetra-methylene ether glycol (PTMEG), polypropylene oxide glycol and polybutylene oxide glycol (see fig. 5). [7] Polyether polyols produce high quality PUR foams and elastomers. Polyether polyols have one subcategory of amine terminated polyethers, in these polyethers the terminal hydroxyl group is swapped with primary or secondary amino groups. Polyether polyols have disadvantage in high flammability caused by volatility of their monomers. This property is modified by usage of flame retardants.

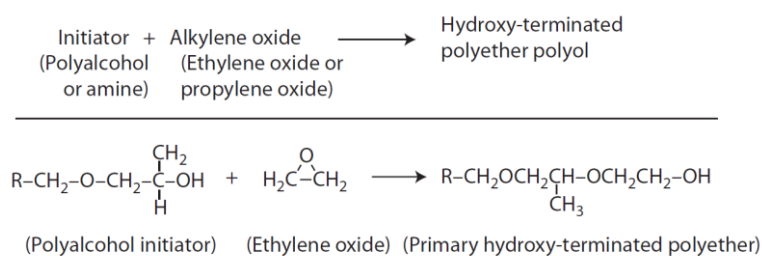


Fig. 4: Schematic synthesis of polyether polyol [7].

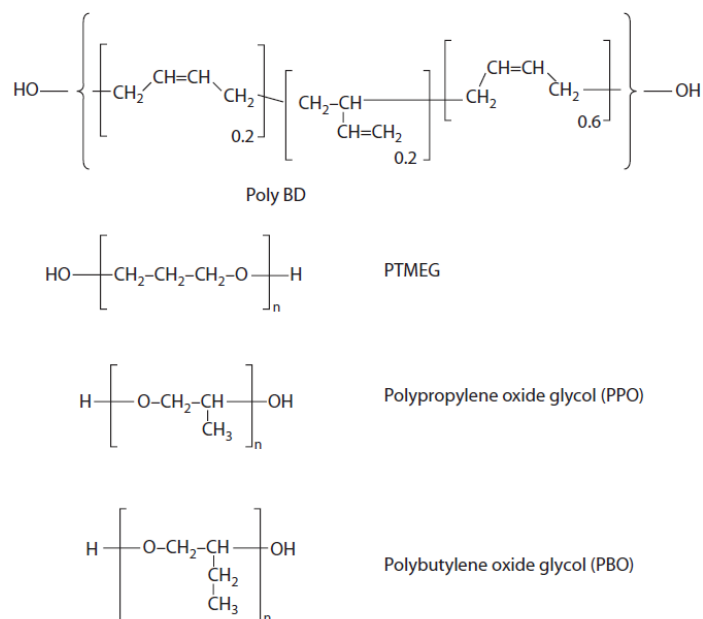


Fig. 5.: Common polyether polyols [7].

1.3.1 Polyester polyols

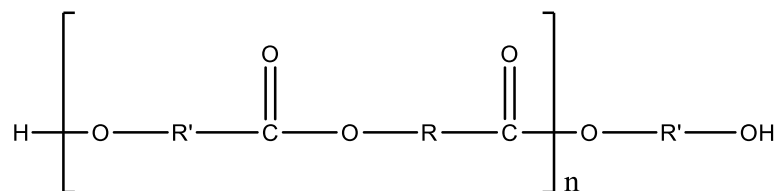


Fig. 6: Polyester [6].

Polyester polyols (see fig. 6) are esters of polyalkylene glycols, for example polybutylene terephthalate (PBT), adipate and caprolactane polyesters. They can be derived from aliphatic or aromatic diacids, depending on their application. Polyester polyols are used in making of coating, adhesives and rigid foams. Aromatic polyesters have advantage in flame retardancy (enhanced charring) [9], gas permeability, structural integrity and thermal insulation. Therefore, they are best employed in insulation foams. Aliphatic polyesters have better tensile strength, abrasion resistance, UV resistance and flexibility in low temperatures. Their use is preferred in coatings, elastomers and even artificial leather.

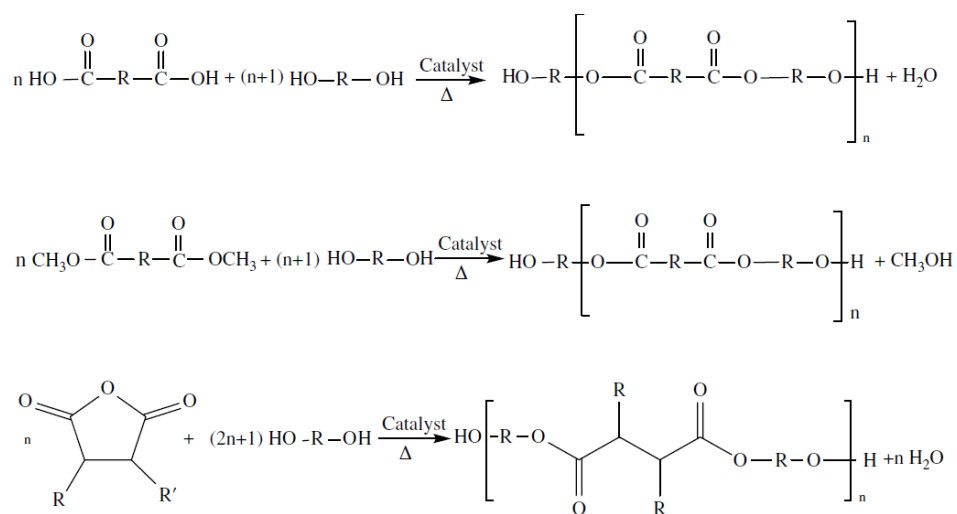


Fig. 7: Synthesis of polyester polyol [6].

Polyesters are produced by condensation polymerisation between polyhydroxy and polyacid monomers (see fig. 7). Huge number of possible building blocks gives relative freedom to designing specific PUR.

Caprolactane polyesters are products of ring-opening polymerization, where caprolactane monomer reacts with a glycol (diethylene glycol, ethylene glycol). Polyesters of this type have higher hydrolytic stability and are used in applications where this property is sought for.

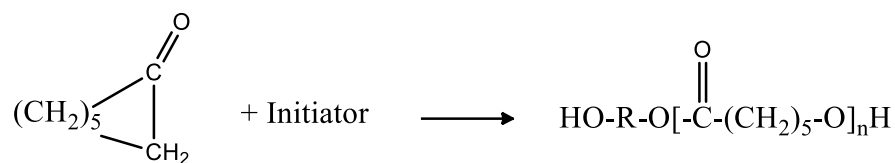
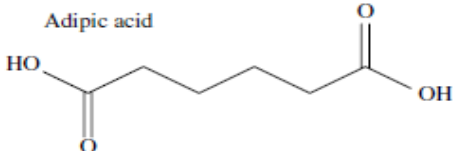

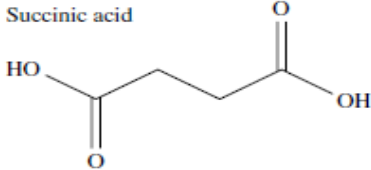
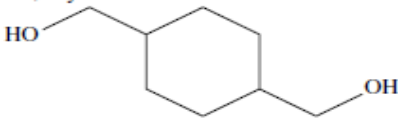
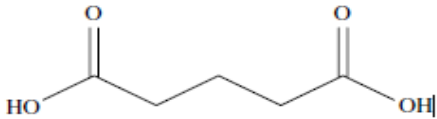
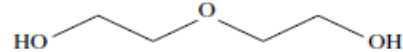
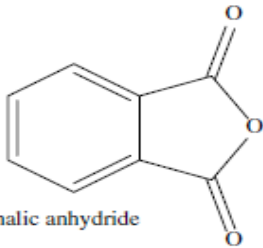

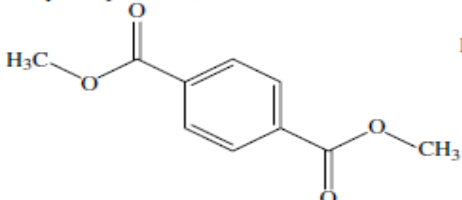



Fig. 8: Synthesis of caprolactane polyester [7].

Polyalkylene glycol adipates are products of condensation polymerisation between alkylene glycol and diester or diacid. Table 1. Shows some of the most commonly used glycols, polyols and acids

Tab. 1: Some of the most commonly used glycols, polyols and acids for polyester polyol production [6].

| Examples of acids and anhydrides | Examples of glycols and diols |
|---|--|
| <p>Adipic acid</p>  | <p>Ethylene glycol</p>  |
| <p>Succinic acid</p>  | <p>1,4 cyclohexane dimethanol</p>  |
| <p>Glutaric acid</p>  | <p>Diethylene glycol</p>  |
| <p>Phthalic anhydride</p>  | <p>1,4 -Butane diol</p>  |
| <p>Dimethyl terephthalate (DMT)</p>  | <p>1,6-Hexane diol</p>  |

1.3.2 Other polyols

Polycarbonate polyols

Produced at small volumes due to their expensive price, polycarbonate polyols are high performance backbones for PURs.

Polycarbonate polyols can be prepared from reaction of phosgene or dimethyl carbonate (DMC) with diol monomer or mixture of various diol monomers. These reactions can be seen in fig. 9.

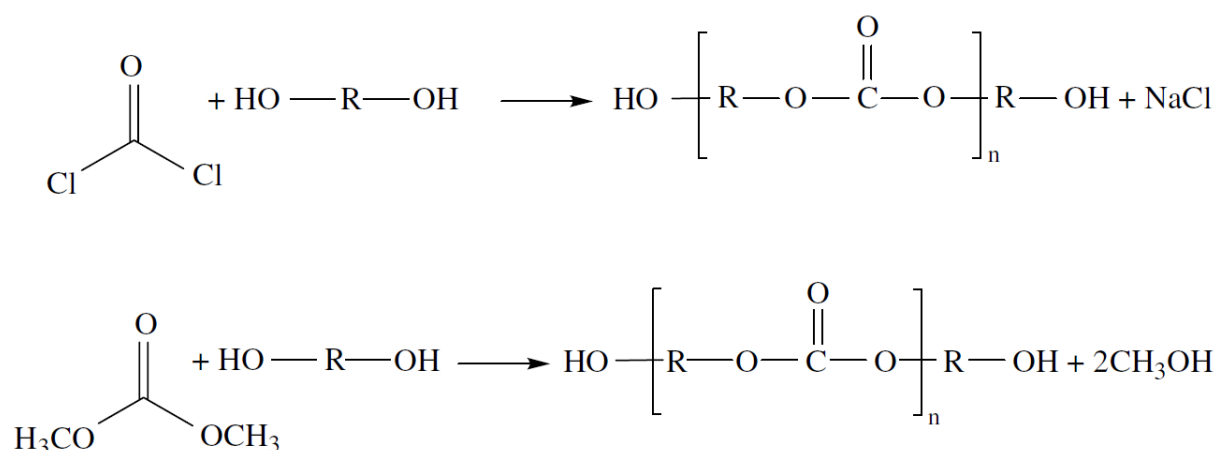


Fig. 9: Preparation of PC polyol from phosgene and dimethyl carbonate [6].

Preparation with usage of DMC is easier, because of its low cost and availability. Disadvantage of this preparation is caused by evolution of methanol, which forms azeotrope that cannot be separated by conventional methods. Alternative method to production is a reaction inside of autoclave under elevated temperature and pressure.

Polyacrylic polyols

Polyacrylic polyols have good properties in hardness, UV stability and resistance to water and acids. Use of polyacrylic polyols is most of the time limited to the coating applications, predominantly in automotive surface finishes. Polyester polyols are also used in coating applications, but in comparison to the polyacrylic polyols, they are used where hydrolytic stability is not as important and cost is principal.

Polyacrylic polyols are prepared with radical initialization. Acrylic monomers can be utilized if they have hydroxyl functionalized monomers in their backbone. For example: Hydroxyethyl methacrylate, hydroxyl butylacrylate and hydroxyethyl acrylate.

1.4 Isocyanates

Isocyanates are chemicals with high reactivity and versatility. They are capable of many reactions, but their main significance is related to PURs. Isocyanates are affinitive to active hydrogens, such as those contained in alcohol and amine functionalized molecules of polyols. Isocyanate monomers must have at least two functional groups to promote addition polymerisation. Two widely used isocyanates are toluene-based diisocyanates (TDI) and aniline and formaldehyde-based isocyanates (MDI). TDI and MDI cover 90% of isocyanate production, the remaining 10% are covered by aliphatic isocyanates.

1.4.1 Toluene based isocyanates (TDI)

TDI based isocyanates used in PURs find their application in flexible foams, coatings and several small specific applications. TDI is produced in three steps as shown in fig. 10. The first step is nitration of toluene, followed by hydrogenation to form polyamine, which then reacts with phosgene to create final product, the TDI.

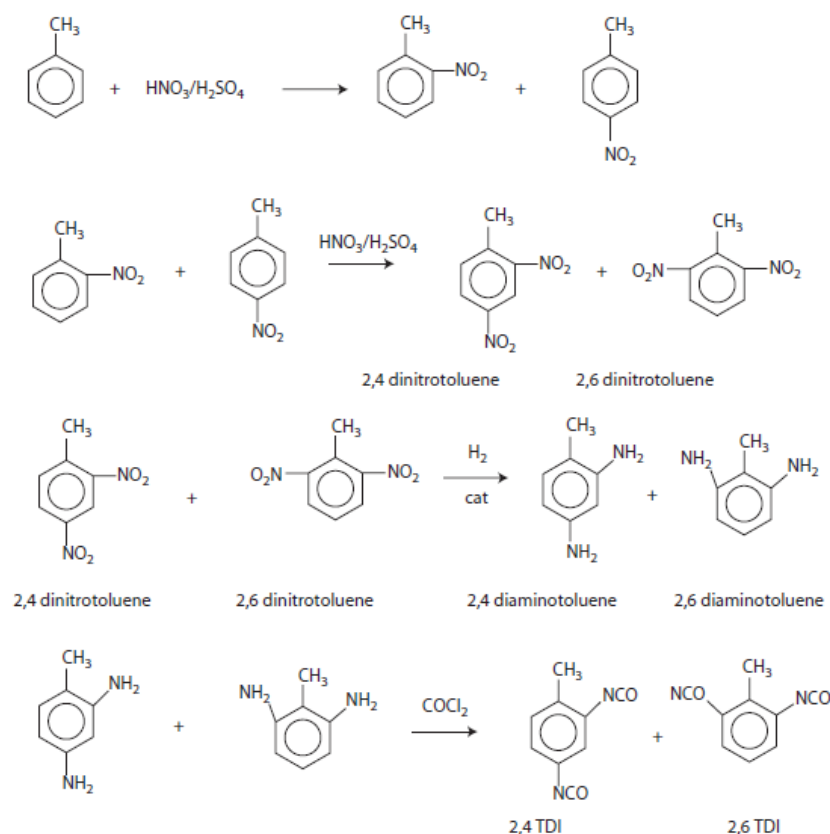


Fig. 10: Production of TDI [7].

1.4.2 Aniline and Formaldehyde based isocyanates – MDI and pMDI

MDI and pMDI (polymeric form of MDI) diisocyanates are applied in production of similar products, such as: rigid foams, adhesives, sealants, coatings, elastomers and flexible foam [7]. Production of MDI is similar yet more complex than the production of TDI. Generally utilized process to produce MDI and pMDI (that is the second product of the reaction) is composed of three steps: nitration, hydrogenation and phosgenation. Schematic representation of MDI and pMDI production can be seen on fig. 11. Differences between MDI and pMDI can be seen in table 2.

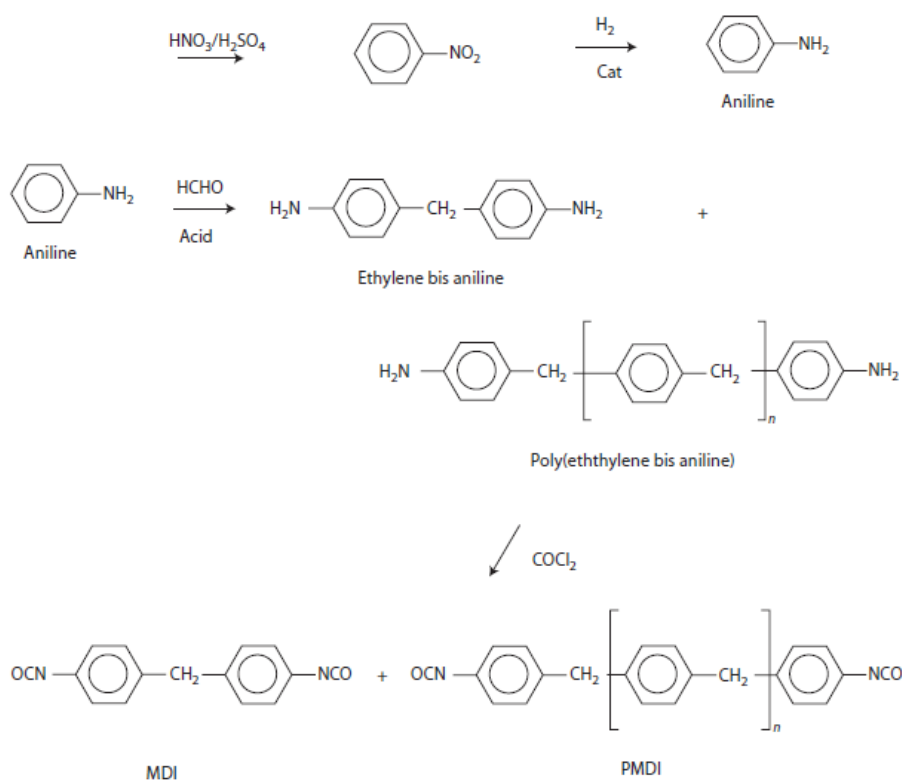


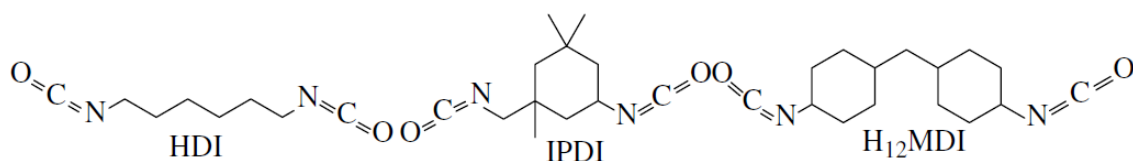
Fig. 11: MDI and pMDI production schematic [7].

Tab. 2: Differences between MDI and pMDI [7].

| Property | MDI | pMDI |
|--------------------------------------|-------|---------|
| Physical form | Solid | Liquid |
| Molecular weight | 250 | ≈450 |
| Equivalent weight | 125 | ≈225 |
| Functionality | 2 | 2+ |
| Boiling point, °C at 760 mm Hg | 170 | N/A |
| Flash point, °C (Cleveland open cup) | 213 | 210–230 |
| Fire point, °C (Cleveland open cup) | N/A | 220–250 |

1.4.3 Aliphatic Isocyanates

Aliphatic isocyanates are mostly used as coatings. In comparison to aromatic isocyanates, aliphatic ones have better weather colouring stability and all around weathering resistance. Another different property is slow reactivity of aliphatic isocyanates. Some of the widely used aliphatic isocyanates are: hexamethylene diisocyanate (HDI), isophorone diisocyanate (IPDI) and 4,4'-diisocyanatodicyclohexylmethane (H₁₂MDI) which is a hydrogenated version of MDI. Structures of these aliphatic isocyanates are in fig. 12.

**Fig. 12:** Structures of common aliphatic isocyanates [6].

HDI is prepared by phosgenation of hexane diamine, which is prepared by using hydrogenation of adiponitrile.


IPDI is prepared by aldol condensation of acetone, forming isophorone isomers. These isophorone isomers are then converted into isophorone nitrile by reacting with HCN. Following conversion to diamine is done by reductive amination, after which reaction with phosgene forms isocyanates.

H₁₂MDI is prepared by hydrogenation of 4,4'-MDA – precursor to production of MDI. MDA is distilled from mixture with pMDA right before addition of phosgene that converts MDA to MDI. The hydrogenation is performed in alcohol or dioxane media, utilizing ruthenium or rhodium on alumina catalyst.

1.5 Chain extenders

Chain extenders are low-molecular weight diols or diamines that connect isocyanate groups in PUR structure. [6] Polyisocyanate and chain extender groups together form the hard segment (HS) of the polyurethanes. Soft segment (SS) is made of polyol parts. Chain extenders with functionality higher than two are considered cross-linkers. Content of HS is important for the mechanical properties and thermal and hydrolytic stability [7] [10]. Another important property of chain extenders, is their effect on kinetics of phase separation between SS and HS. Phase separation takes place during addition polymerization between isocyanates and polyols, as the two are immiscible [11]. There is large number of possible chain extenders, table 3 contains the common types.

Tab. 3: Common chain extenders [7].

| Trivial Name | Chemical Name | Structure |
|--------------|--|---|
| 1,4 BD | 1,4-Butanediol | $\text{HO}-(\text{CH}_2)_4-\text{OH}$ |
| CHDM | 1,4-Cyclohexanedimethanol |  |
| Glycerine | 1,2,3-Propanetriol | $\begin{array}{c} \text{OH} \\ \\ \text{HO}-\text{CH}_2-\text{CH}-\text{CH}_2-\text{OH} \end{array}$ |
| 1,6 HD | 1,6-Hexanediol | $\text{HO}-(\text{CH}_2)_6-\text{OH}$ |
| HQEE | Hydroquinone di (B hydroxyethyl ether) | $\text{HOCH}_2\text{CH}_2-\text{O}-\text{C}_6\text{H}_4-\text{O}-\text{CH}_2\text{CH}_2-\text{OH}$ |
| MPD | 2-methyl-1, 3 propanediol | $\begin{array}{c} \text{CH}_3 \\ \\ \text{HOCH}_2-\text{CH}-\text{CH}_2-\text{OH} \end{array}$ |
| Quadrol | <i>N,N,N',N'</i> tetrakis (2-hydroxyethyl) ethyl diamine | $\begin{array}{c} \text{HOCH}_2\text{CH}_2 \\ \diagdown \\ \text{NCH}_2\text{CH}_2\text{N} \\ \diagup \\ \text{HOCH}_2\text{CH}_2 \end{array} \begin{array}{c} \text{CH}_2\text{CH}_2\text{OH} \\ \diagup \\ \text{NCH}_2\text{CH}_2\text{N} \\ \diagdown \\ \text{CH}_2\text{CH}_2\text{OH} \end{array}$ |
| Sorbitol | D-glucitol | $\begin{array}{c} \text{OH} \quad \text{OH} \quad \text{OH} \quad \text{OH} \quad \text{OH} \\ \quad \quad \quad \quad \\ \text{HOCH}_2-\text{CH}-\text{CH}-\text{CH}-\text{CH}-\text{CH}-\text{CH}_2\text{OH} \\ \\ \text{OH} \end{array}$ |
| TMP | Trimethylolpropane | $\begin{array}{c} \text{CH}_2-\text{OH} \\ \\ \text{HO}-\text{CH}_2-\text{CH}-\text{CH}_2-\text{OH} \\ \\ \text{CH}_2\text{CH}_3 \end{array}$ |

2 FLAME RETARDANT SYSTEMS (FRS)

Since polymers are often easily combustible materials, flame retardant systems are used to interfere with combustion process by either preventing fuel availability, reducing heat entering reaction externally or from reaction itself, or by limiting the amount of O_2 that drives thermooxidation. FRS can be introduced to polymer by mechanical compounding of additives or chemical reaction during polymerization, when the FRS becomes an integrated part of a polymer chain. Mechanically compounded FRS additives do not interfere with the chemistry or chemical properties of polymer below their decomposition temperature. Therefore, this type of FR must be selected with emphasis on its decomposition temperature and the temperature of polymer matrix in which it will be performing. Chemically introduced FRS possesses some advantages over mechanically introduced. Their dispersion in the system is more homogenous and there is no phase separation. Additives might show migration to the surface of the matrix, which is not possible for the chemically introduced FRS, therefore material does not lose flame retarding abilities over time. The last advantage is the lower concentration needed to sufficiently perform flame retardation [12].

2.1 Modes of action

Both additive and reactive FRS utilize two possible modes of action to interfere with the combustion process. The first mode of action is physical, the second one is chemical [13].

2.1.1 Physical mode of action

Flame retardants that utilize physical mode of action undergo endothermic decomposition that decreases the heat released during combustion. Two common retardants with this behaviour are $Al(OH)_3$ and $MgOH$. This effect of decreasing released heat by endothermic decomposition is called “heat sink”.

Another physical retardation of combustion is added by production of inert gases from decomposition of retardants. These gases dilute the volatiles and combustible gases released from polymer and therefore reduce the risk of ignition and further spreading of fire.

In some retardant systems formation of solid layer may occur. This solid layer physically separates the polymer fuel and volatiles it releases from combustion. Other than solid layer, protective gas layer that significantly limits gas transfer in combustion may form on top of the fuel.

2.1.2 Chemical mode of action

This type of flame retardants relies on chemical reaction between retardant and combusting fuel. Interaction can take place in both gaseous and condensed phase.

In gas phase the mechanism works by releasing radicals (e.g. Cl^{\bullet} or Br^{\bullet}), these radicals can then reduce heat released during combustion by reacting with other highly reactive radicals from combustion (e.g. H^{\bullet} and OH^{\bullet}). The lower amount of released heat decreases temperature which cannot turn material to fuel.

Retardation in condensed phase has two possible pathways. The first one is based on catalysing chain rupture in polymer, where polymer drips away from fire. The second mechanism forms carbonized or vitreous layer at the top of the polymer. This “charring” is caused by transformation of degrading polymer chains and acts as a physical insulation between gas and condensed phase.

2.1.3 Charring and intumescence

Char formation or charring is a flame retarding effect, which builds a carbonaceous layer on the top of the polymer fuel. Polyimides, polyaramides, polyarylenes or thermosets are an example of polymers with inherent flame retardation, given by their ability to yield high amount of char upon combustion. Flame retardation by charring works through lowering the heat of combustion, insulating polymer, limitation of gas transfer and in some cases release of water and carbon dioxide. [14]

Polymers that do not char properly are modified with char generating additives:

- a) Source of acid – inorganic acid or acid salt decomposing to produce acid. Phosphoric or polyphosphoric acid are ideal examples.
- b) Carbonizing agent – carbohydrate that undergoes dehydration by the acid and forms char (e.g. pentaerythritol).

If a blowing agent is added as a third additive, effect of intumescence would be achieved. Blowing agent decomposes and releases gas that expands carbonizing layer. Effect of intumescence compared to charring can be seen on fig. 13. Scheme of expanded intumescence layer can be seen in fig. 14. Intumescence also works as an insulating barrier, permits the access of flame to polymer and limits oxygen diffusion [13] [15] [16] [17] [18].

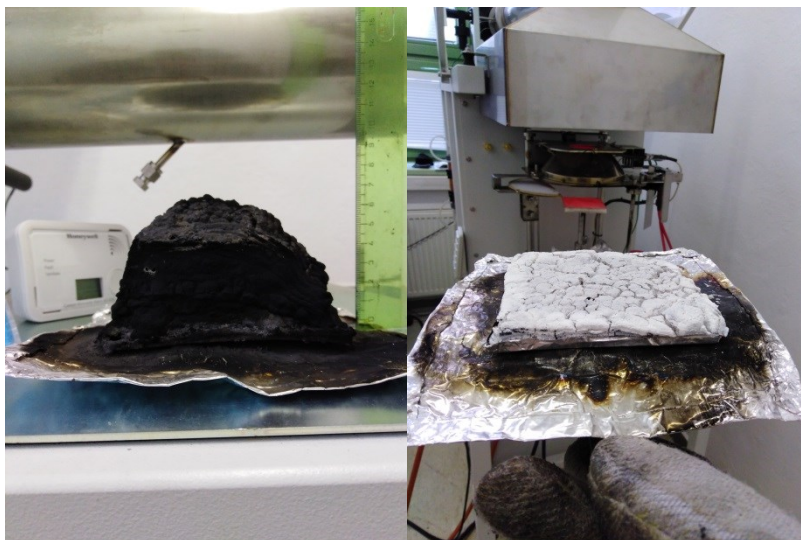


Fig. 13: Effect of intumescence and charring.

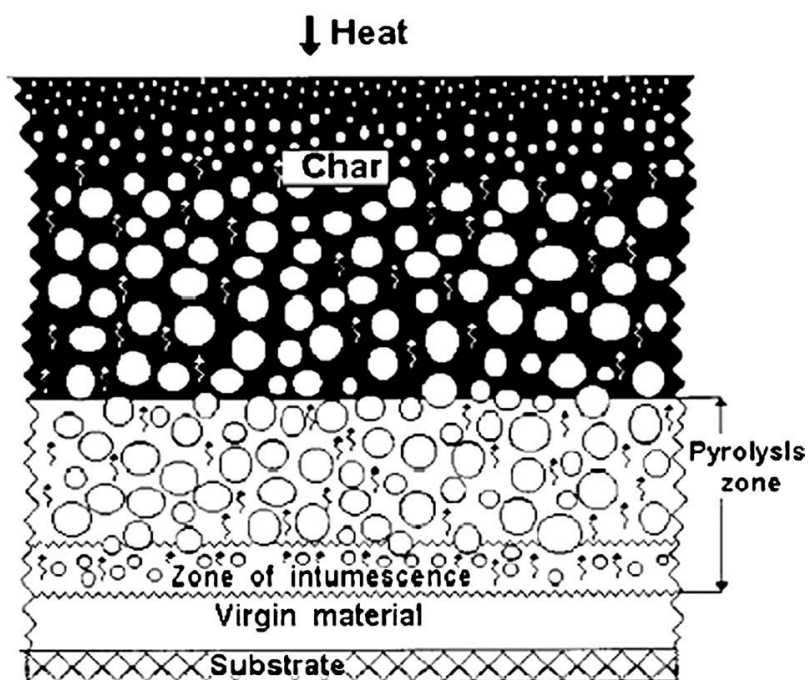


Fig. 14: Expansion of intumescent used in coating of PUR foam [19].

2.2 Synergistic and antagonistic effect of flame retardants

Synergy is an effect, when two or more FRS in a mixture attain enhanced performance, which would not be possible for each flame retardant alone. Synergy works in both physical and chemical modes of actions and in gas and condensed phase. As an example of synergy in gas phase can be shown enhanced flame retardation of halogenated flame retardants (HFR) mixed with antimony oxide Sb_2O_3 . Antimony oxide reacts with the hydric acids produced from HFRs and

forms heavy antimony oxihalides. These antimony oxihalides reside in flame for longer time and form SbX_3 , where X is chloride or bromide, which scavenges radicals released from burning material. [13] Another example of synergism in condensed phase is shown by Chen et al. [20] and Li et al. [21] on combination of expandable graphite and phosphorous flame retardant in rigid polyurethane foam. Chen, in his work prepares combination of expandable graphite and guanidinium phosphate as a system along with combination of red phosphorus and guanidinium phosphate FR system. Fig. 15 shows excerpt of Chens results.

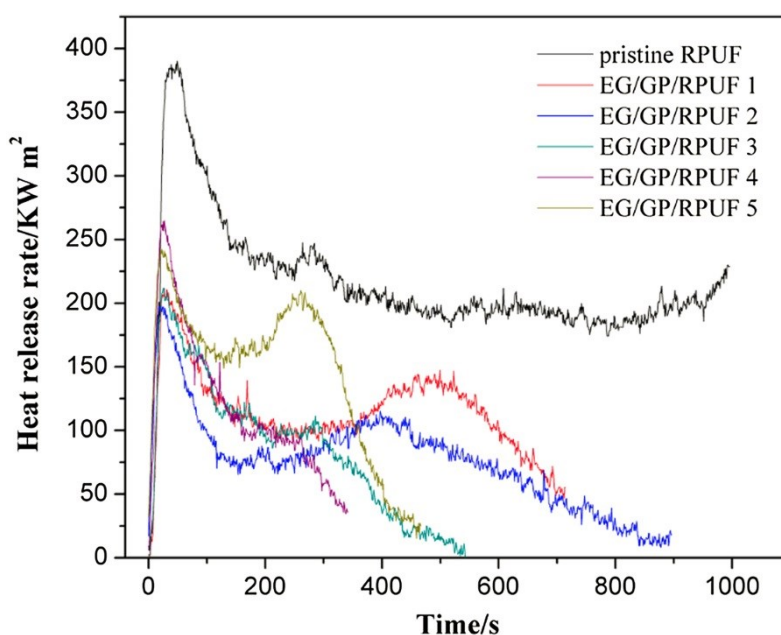


Fig. 15: HRR results on neat rigid PUR foam and rigid PUR foam filled with FR mixture of expandable graphite and guanidinium phosphate in various concentrations [20].

Antagonistic effect is the opposite to synergism and occurs when one FR blocks mode of action of other FR in mixture. For example, this effect was researched by Gerard et al. [22] on combination of APP and carbon nanotubes.

2.3 Mineral flame retardants

Mineral flame retardants are inorganic fillers of active or inactive type. Flammability of polymer matrix can be decreased just by the lower amount of flammable material and adjusted physical properties. Minerals that are often used for flame retardation have usually additional mode of action to those mentioned beforehand (e.g. heat sink or gas dilution). [13] Inorganic hydroxides make up 50% of FRS sold globally, they offer low cost, low toxicity and low corrosivity. [23] Most widely used are metal hydroxides such as:

Alumina Trihydrate (ATH), decomposes in the range of 180 – 200 °C and produces alumina and water. ATH uses heat sink as its mode of action, during endothermal decomposition it consumes 1050 kJ/kg [24]. Effect of ATH on HRR can be seen in fig. 16. Additionally, the released water dilutes the gases from combustion, layer of aluminium oxide is created on top of the polymer and protects it from further decomposition and chokes back the smoke production.

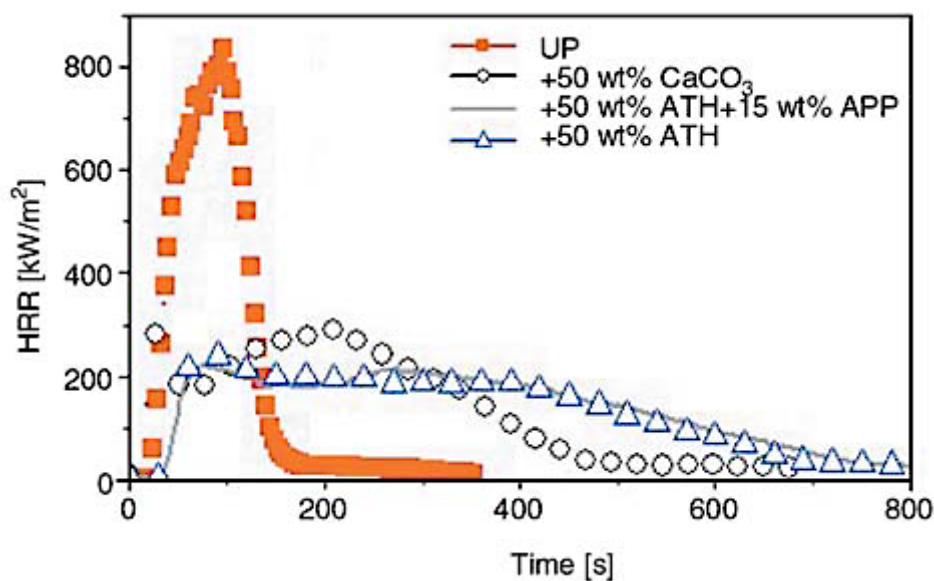


Fig. 16: Effect of ATH and APP on unsaturated polyester resin [25].

Magnesium Hydroxide (MDH), has decomposition temperature about 350 °C which makes it suitable for number of polymers. [26] Mode of action of MDH is essentially the same as of ATH, but in its endothermic decomposition it consumes 1300 kJ/kg of energy. To meet desired FR abilities of MDH, high volume, about 50 wt.% is needed. This amount of MDH might have effects on mechanical attributes of polymer matrix which creates a problem that can be assessed by surface modification of MDH (see fig. 17) [27].

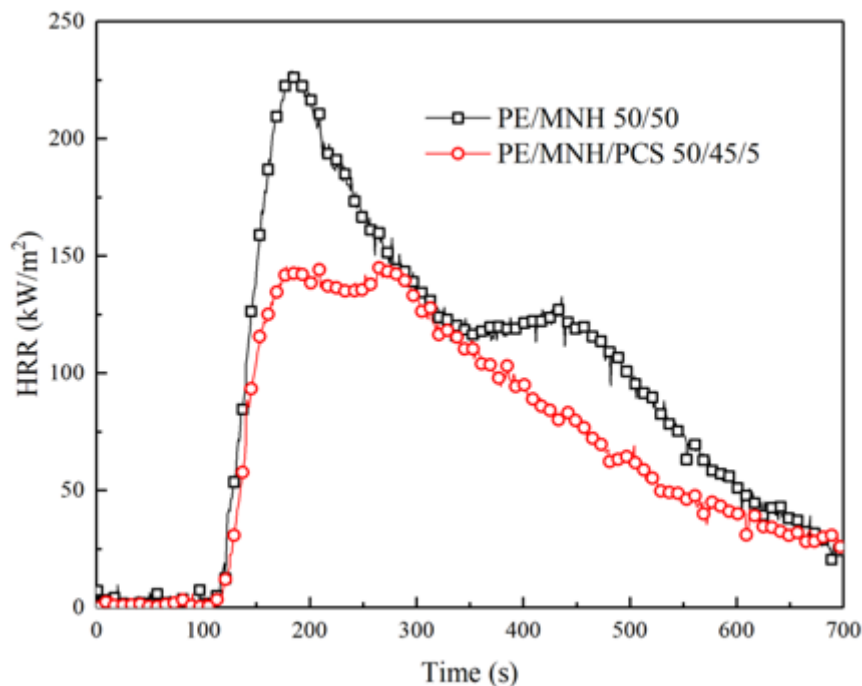


Fig. 17: HRR data of neat MDH and MDH modified with polycarbosilane [27].

2.4 Halogenated flame retardants (HFR)

Category of halogenated flame retardants is represented mostly by bromine (BFR) and chlorine (CFR) based flame retardants. Other halogens, iodine and fluorine are not used in large scale. Iodine is expensive and its compounds are unstable to heat and light. Fluorine is applicable to flame retardancy because of its non-combustible nature in the form of fluoropolymers (Teflon, wire insulation), but decomposition products of fluorine compounds are too stable to interfere combustion reactions, therefore it cannot be used as a flame retardant. [13]

Combination of HFR with Sb_2O_3 shows strong synergy, that produces antimony trichloride or tribromide. [14] Synergistic effect can be also achieved by using nanoclays and zinc hydroxystannate. [28]

The most common bromine-based halogen flame retardants (BFR) are:

Tetrabromobisphenol-A (TBBPA), which is applied as a reactive FR in epoxy resins or as an additive in ABS and HIPS. TBBPA is prone to discoloration due to reaction with light and it is recommended to use it in low cost applications. Polybromodiphenylether (PBDE), is the second most used BFR. As a FR additive it is used in forms of penta- (5), octa- (8) and deca- (10) bromodiphenylethers. Penta- and octa- were used for polyolefins, nylons and polyesters until

they were discarded and only deca-bromodiphenylether is still used outside of EU in few countries.

Hexabromocyclododecane (HBCD) and Tetrabromophthalic anhydride (TBPA) are less used BFRs that are used for PS, textiles and polyesters respectively.

An example for chlorine based halogenated fire retardants (CFR) might be chloroparaffins and Dechlorane plus (DP). Chloroparaffins are for a long period of time used in elastomers, rubbers and polyolefins. Chloroparaffins provide thermal stability to 230 °C and as an addition to the synergy with Sb_2O_3 , improved fire retarding performance of aluminium trihydroxide and magnesium dihydroxide is occurring when combined. Dechlorane plus (DP) is compound used in nylons and polyolefins. Mode of action of DP is charring, flame inhibition is secondary. DP works well with bromine additives as it has synergy with Cl and Br compounds.

HFRs and their use is controversial due to the possessed toxicity. Residual amounts of HFRs are nowadays found in living organisms from around the world. Salamova and Hites [29] report bioaccumulation of various HFRs by analysing tree bark, Gagné et. al [30] examine the presence and activity of Dechlorane plus in marine organisms. Overall toxicity and distribution of BFRs are researched by Kefeni et. al [31]

2.5 Phosphorous – based flame retardants

Phosphorus-based flame retardants (PFR) is large group of flame retardants, and can be divided into three categories, Inorganic, organic and halogen containing [32]. PFR may be used as additives or as reactive comonomers to be incorporated into polymer. Mode of action is dependent on the structure of polymer matrix.

PFRs are known to be more effective in matrices that contain oxygen or nitrogen, such as: polyesters, polyamides, polyurethanes or cellulose. Mode of action in condensed phase is characteristic for mentioned polymers and for phosphorous compounds with high oxygenation, such as phosphates [33]. This mechanism utilizes production of phosphorous acid, which is a product of the most PFRs to further decompose into pyrophosphate structures, while releasing water during this process. Water dilutes the oxidizing gases in the gas phase and the phosphorus acid additionally catalyses dehydration of terminal alcohols, that leads to creation of double carbon bonds. At elevated temperatures, there is possibility of production of char. If PFRs are used in polyolefins that do not contain nitrogen nor oxygen in their chain, addition of highly charring

additive is advised. If the PFRs have low oxygenation, generation of active radicals PO_2^\bullet , PO^\bullet or HPO^\bullet and mode of action in gas phase is prevalent. Free radicals released from PFRs are from 5 to 10 times more effective in inhibiting the H^\bullet and OH^\bullet than bromine and chlorine radicals respectively.

Synergistic behaviour might be achieved by combination of PFRs with nitrogen compounds, carbon nanotubes or montmorillonite. [34] [35]

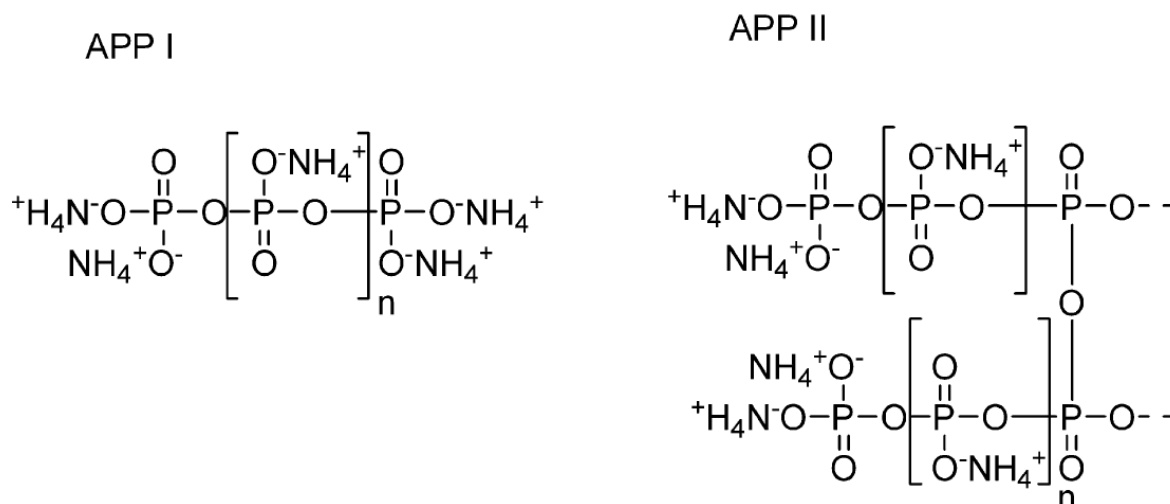


Fig. 18: Structure of APP I and APP II [13]

Ammonium polyphosphate (APP) is a salt of polyphosphoric acid and ammonia $[\text{NH}_4\text{.PO}_3]_n$. Its properties are dependent on polymerisation degree. APP exist in two crystal forms, APP I and APP II, (see fig. 18) with chains referred to as short if the number of polymerisation degree n is less than 100 and long, if the n is more than 100. Long chain APP is more thermally stable at 300 [°C] in comparison to short chain APP that is thermally stable only up to 150 [°C].[13] The polyphosphoric acid released from APPs has good reactivity with Oxygen and Nitrogen containing polymers, in which it is catalysing charring. APPs are commonly used as a source for acid and gas in IFR systems. Commercially available APPs are Exolit from Clariant or Budit from Budenheim.

2.6 Nitrogen – based flame retardants

Melamine (Mel) is crystalline product with good thermal stability up to 345 °C. At 350 °C melamine undergoes sublimation, during which high amount of energy is absorbed and tem-

perature decreased. Melamine dilutes combustible gases by producing ammonia in its decomposition reaction. The released ammonia also forms thermally stable condensates melam, melem and melon.

Melamine tends to form salts in reaction with organic or inorganic acids (e.g. boric acid, cyanuric acid, phosphoric and polyphosphoric acid) its effect on HRR is shown on fig. 19.

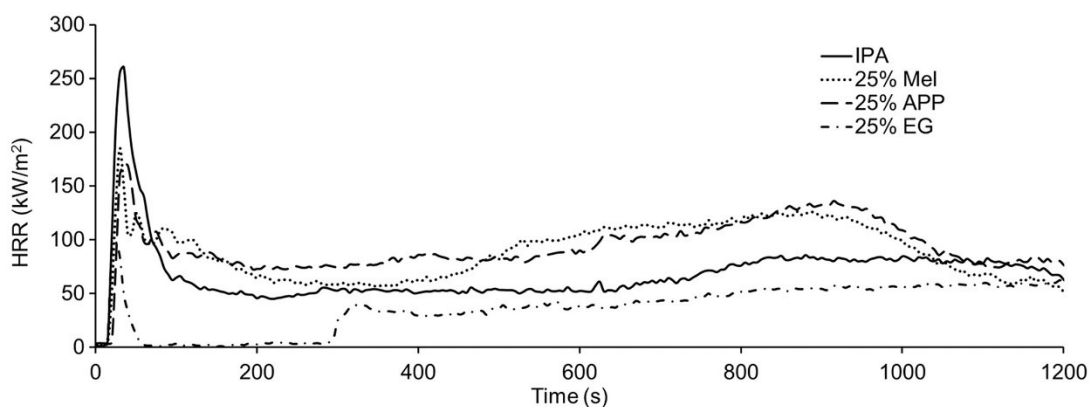


Fig. 19: Effect of Melamine (Mel), APP and expandable graphite (EG) on HRR of speciality polyol [36].

Melamine polyphosphate (MPP) is a derivative of melamine. Thermal decomposition of MPP is occurring at about 360 °C [12] and has low solubility in water. At temperatures above 350 °C MPP undergoes endothermic sublimation [37], therefore acting as a heatsink. To add up to this retardation, MPP also releases phosphoric acid, which promotes charring, and melamine, which acts as a blowing agent. Therefore, MPP is also IFR. In comparison to APP, melamine polyphosphate is more thermally stable and not as susceptible to hydrolysis as APP, on the other hand, MPP is less effective in its flame retarding abilities.

2.7 Nanometric particles

Nanometric particles are relatively new class of FRs. As additives, they increase flame retarding performance and mechanical and thermal properties of polymer matrix. Mechanism of flame retardation by nanometric particles takes place in condensed phase and its effectivity depends on geometric shape and chemical composition of particles. As nanometric particles are considered layered materials (e.g. nanoclay), particulate material (e.g. polyhedral oligosilsesquioxane) and fibrous material (e.g. carbon nanotubes). These materials are non-toxic

and environmentally friendly. [38] On the following fig. 20, effect of montmorillonite (MMT) and nanosilica on HRR of polystyrene (PS) is depicted.

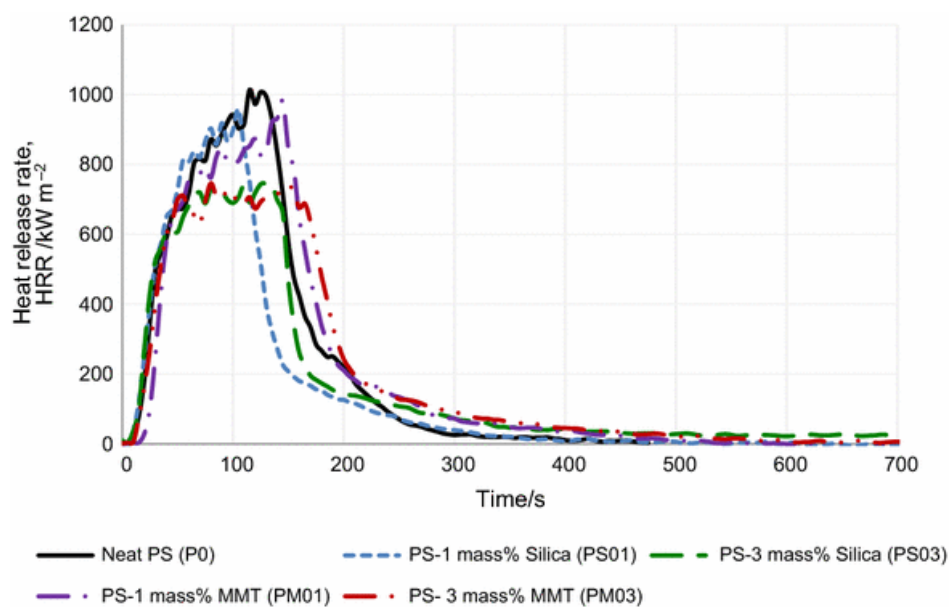


Fig. 20: HRR of neat PS and PS filled with MMT and nanosilica [38].

3 BEHAVIOUR OF POLYMER UNDER THERMAL STRAINING

Based on thermal response, polymers are sorted to three groups:

- a) Polymers with complete breaking of the main chain (thermoplastics)
- b) Polymers that experience breaking off side groups and form volatiles and soot
- c) Cross-linked polymers that form char as main product of degradation.

Combustion process of charring polymers may follow by two pathways, flaming combustion and or smouldering combustion. Flaming combustion can be achieved when volatile products of thermal degradation release enough heat in their gas phase combustion, to produce heat flux needed to initiate solid fuel degradation and flame spread. The smouldering combustion occurs when the temperature or heat flux are below certain levels and can precede flaming combustion in charring polymers. Smouldering combustion takes place in the solid phase of fuel rather than in the gas phase. No visible flame can be observed in this type of combustion, instead we observe the material to be glowing. [39, 40]

3.1 Thermal decomposition

Thermal decomposition is process occurring in polymers at elevated temperatures, when polymer is exposed to radiant heat flux from fire or located in a high temperature environment. Thermal decomposition can be observed by changes in chain conformation, molecular weight, crystallinity, flexibility, cross-linking, branching, colour changes, different densities, crack formation, shape deformation. The result of these changes shows itself in physical properties (mechanical, electrical, thermal, magnetic) and aesthetic properties. [41] If the focus is kept on the molecular weight, number of mechanisms can be distinguished, that result in decrease or increase of the molecular weight M_w . Mechanisms reducing M_w are:

- a) Random chain scission – Occurs randomly throughout the length of the chain, weak bonds with irregularities are the most susceptible to the scission. Propagation works via free radical. Produces oligomers of different length. If polymers are not depolymerising, they tend to break to smaller and smaller fragments. This type of scission can be used for statistical fragmentation. [42]
- b) Chain-end scission (depolymerisation/unzipping) – Decomposition where the individual units of monomers or volatile fragments are removed from the chain end until complete depolymerisation of polymer molecule. For example, polymers of polymethacrylate and

polystyrene type undergo this type of scission. Process propagates via free radical. Reaction is antagonistic to polymerisation, and in enclosed system, it works until equilibrium between monomer and polymer is reached. [42]

- c) Chain stripping – Works in two steps, in the first step side groups are eliminated, this leaves polyene molecule on the main chain. The second step is scission into smaller molecules, char formation or formation of cyclized molecules. [42]

Other mechanisms that increase M_w are:

- d) Cross-linking – Bonding of parallel chains, this process is important in formation of char. Cross-linking is usually temporary process. Many thermosets at elevated temperature, from 100 – 150°C, forego cross-linking referred as post-curing to decomposition that occurs at temperatures between 250 – 400°C.
- e) Cyclization – Important for char formation. Char is highly porous, its basic building blocks are aromatic rings. Polymers containing high number of aromatic rings yield more char and the yield is increasing linearly with concentration of multiple-bonded aromatic rings in polymer. [43] [39]

3.2 Chemistry mechanism of degradation

Multistep free-radical reaction is common mechanism of chain scission. Individual steps of this reaction are:

Initiation – formation of free radicals, while polymer backbone is breaking to small molecules. Occurs randomly on chain (random chain scission) or on chain ends (chain-end scission). In air atmosphere, these free radicals will react with oxygen and produce peroxides and hydroperoxides with high reactivity.

Propagation – cross-linking, main-chain unsaturation, intra or inter molecular hydrogen transfer and further decomposition of polymer backbone, or chain-end scission, will take place in this step. Production of the char in this step is a result of cross-linking reactions and cyclization reactions of the side groups.

Termination – radical coupling, disproportionation and hydrogen transfer from one radical to another, are the mechanisms that occur in this step. Thermo-oxidation of this step, that occurs if the degradation takes place in air atmosphere, may produce several by-products.

3.3 Thermal response of common polymers

This chapter focuses on the thermal response and properties of commonly used polymers, to give quick insight on behaviour of everyday use plastics.

3.3.1 Polyethylene (PE)

Polyethylene (see fig. 21) degrades via random chain scission. During its degradation formation of propane, propene, ethane and other alkene type decomposition products takes place. Thermal stability is influenced by the type of macromolecular structure. LDPE for instance, has high degree of branching and this steric displacement raises the rate of hydrogen transfer. As a result, LDPE is not as thermally stable as HDPE is. In air atmosphere, decomposition starts at 250 °C.

3.3.2 Polypropylene (PP)

Like PE, PP degrades (see fig. 21) by random chain scission with free radical transfer. PP is less stable than PE because of its methyl group, that speeds up the secondary free-radical production. Decomposition produces pentane, 2-methyl-1-pentane and 4-dimethyl-1-heptane.

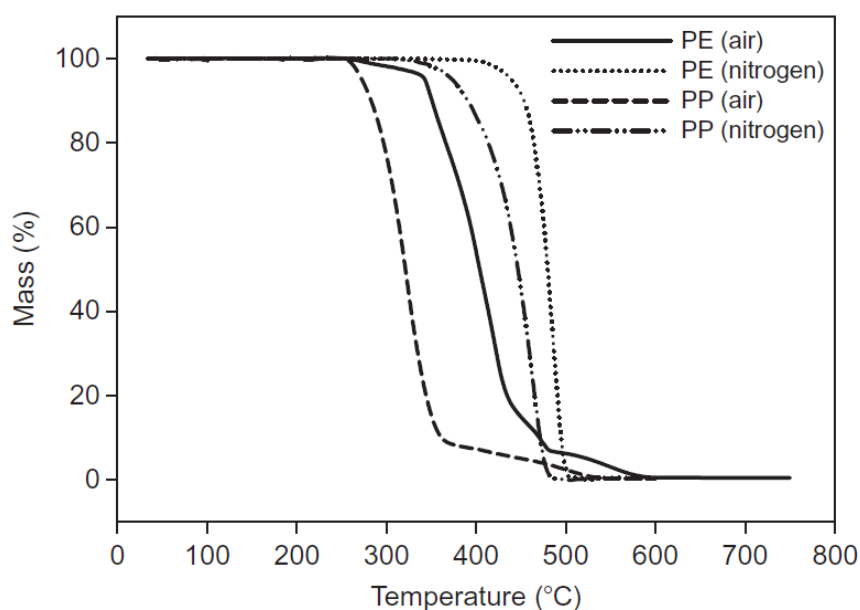


Fig. 21: TGA scan of PE and PP [41].

3.3.3 Polyvinylchloride (PVC)

Polyvinylchloride is not stable as PE and PP, the thermally sensitive Cl group in the building block produces highly unstable secondary free radicals and releases toxic HCl. Thermal decomposition starts with the end groups of the macromolecule and oxygen then initiates decomposition within the backbone. HCl production initiates formation of double bond in the main chain, this process reveals itself by colour change of the polymer.

3.3.4 Polystyrene (PS)

Product of the degradation is PS monomer. Degradation follows scission of the chain-end radicals. Radical transfer followed by scission results in decreasing amounts of dimer, trimer, tetramer and pentamer.

3.3.5 Polyethyleneterephthalate (PET)

In an air atmosphere, thermal decomposition has onset at 350°C (see fig. 22) and leads to complete combustion and depletion of material at 560°C. Thermal decomposition is initiated by scission of an alkyl-oxygen bond following random chain scission.

3.3.6 Polymethylmethacrylate (PMMA)

Thermal degradation has onset at 285°C in the air atmosphere (see fig. 22). Thermal stability is again influenced by macromolecular structure of PMMA given by used polymerization method. PMMA prepared with free-radical polymerization has lower thermal stability than PMMA prepared ionically.

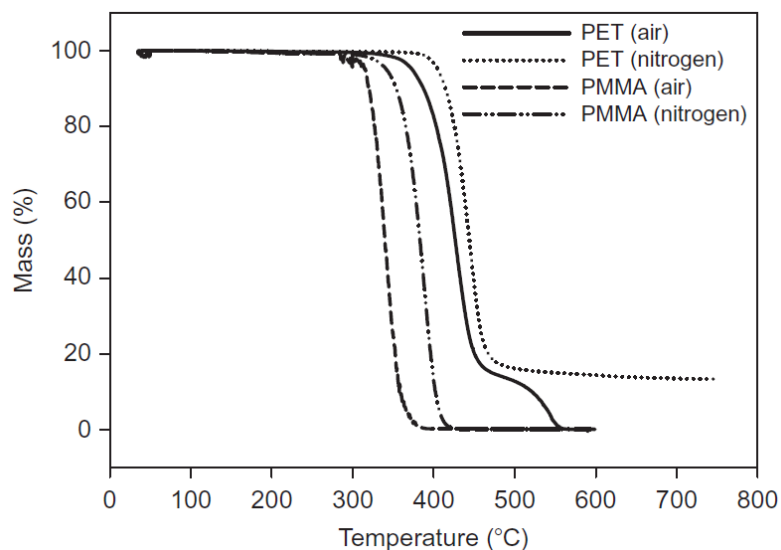


Fig. 22: TGA scan for PET and PMMA [41].

3.3.7 Polyoxymethylene (POM)

Thermal degradation onsets at 275°C and follows process of unzipping, with release of formaldehyde. Degradation starts at the unstable chain ends and then continues by random-chain scission, other products are carbon monoxide and methanol.

3.3.8 Nylon 6 and Nylon 6,6

Thermal degradation of nylon 6 (see fig. 23) involves two steps, a) intramolecular backbiting process and b) hydrogen transfer reaction, leading to scission of C-N bond to the amide group. Intramolecular backbiting is dominant over hydrogen transfer. Nylon 6,6 degrades through the same mechanism. Both nylons produce char, though nylon 6,6 yields more amount.

3.3.9 Polycarbonate (PC)

Thermal degradation in atmosphere has onset at 420°C (see fig. 23). Condensation and hydrolysis reactions compete against each other during degradation of PC. Condensation reaction produces char if volatile products of degradation are removed during reaction. Preserving these volatile products makes chain scission reactions predominant and reduces formation of char. Major products of degradation are carbon dioxide, bisphenol A and phenol.

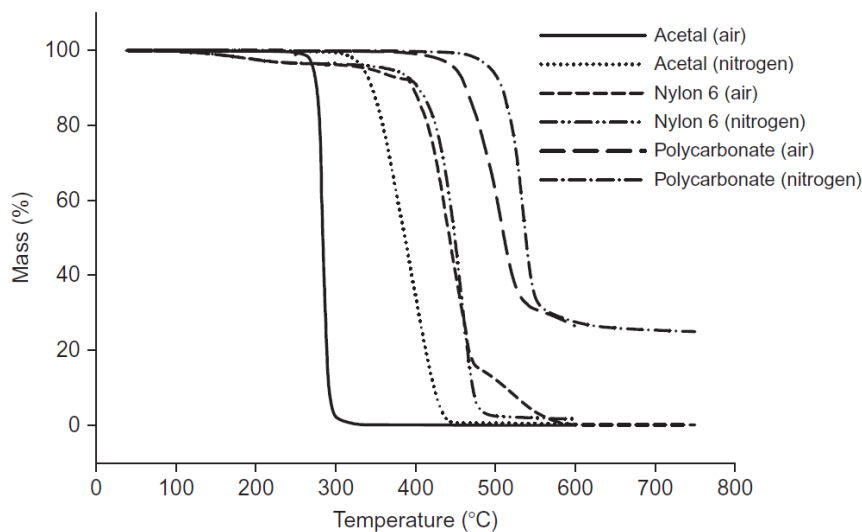


Fig. 23: TGA scan for Acetal, Nylon 6 and PC under air and nitrogen atmosphere [41].

3.3.10 Fluoropolymers

High strength of C-F bond gives high chemical and physical resistance, and thermal stability to polymers from fluoropolymer family. Polytetrafluorethylene (PTFE) is thermally stable in temperatures over 400°C. If the degradation of PTFE occurs inside inert atmosphere, degradation leads almost completely to production of a monomer, working by free radical decomposition mechanism. Products of degradation in air atmosphere are carbon monoxide, carbon dioxide and other volatiles, but no monomer is produced this time.

3.3.11 Elastomers

Unsaturated elastomers are more prone to thermal degradation. Between these rubbers we include natural rubber, isoprene rubber, styrene-butadiene rubber, nitrile rubber, butadiene rubber, chloroprene rubber and butyl rubber. Thermal decomposition follows random-chain scission with intramolecular hydrogen transfer. Decomposition of rubbers is affected by the curing system used in various types of elastomers. The other group of elastomers, the saturated ones, are more stable against thermal degradation. Saturated elastomers are ethylene propylene rubber, ethylene propylene diene rubber, silicone rubber, fluoroelastomers, etc.

3.4 Thermal response of polyurethane thermosets

Polyurethanes are compound of soft and hard segments, made of polyether or polyester and of diisocyanate, respectively. During thermal degradation, PURs show phase separation between

these hard segments domains that act as a physical crosslink and soft segments that act as a matrix. In general Polyurethanes follow decomposition mechanism shown in figure 24. Initial degradation of urethane bonding may follow three pathways:

- a) Dissociation to isocyanate and alcohol
- b) Dissociation to primary amine, olefin and carbon dioxide
- c) Formation of secondary amine and elimination of carbon dioxide

Polyurethanes start to degrade in the range of 200 – 300°C. During degradation, residue is formed as well as yellowish smoke that contains nitrogen. The yellow smoke contains HCN and Acetonitrile, residue continues to break into smaller segments with rising temperature.

Decomposition under inert atmosphere produces no volatile products, initial step of the degradation is depolymerisation. Primary products are two monomers, from which several other products are formed in secondary reactions. These products are: carbon dioxide, butadiene, tetrahydrofuran, dihydrofuran, water, carbodiimide and urea amide.

Decomposition under oxygen atmosphere is initiated by scission of the polyurethane molecule into primary amine, carbon dioxide and propenyl ether like compounds that form propene later on. Mechanism of this decomposition is on fig 24 and fig. 25 [36] [42].

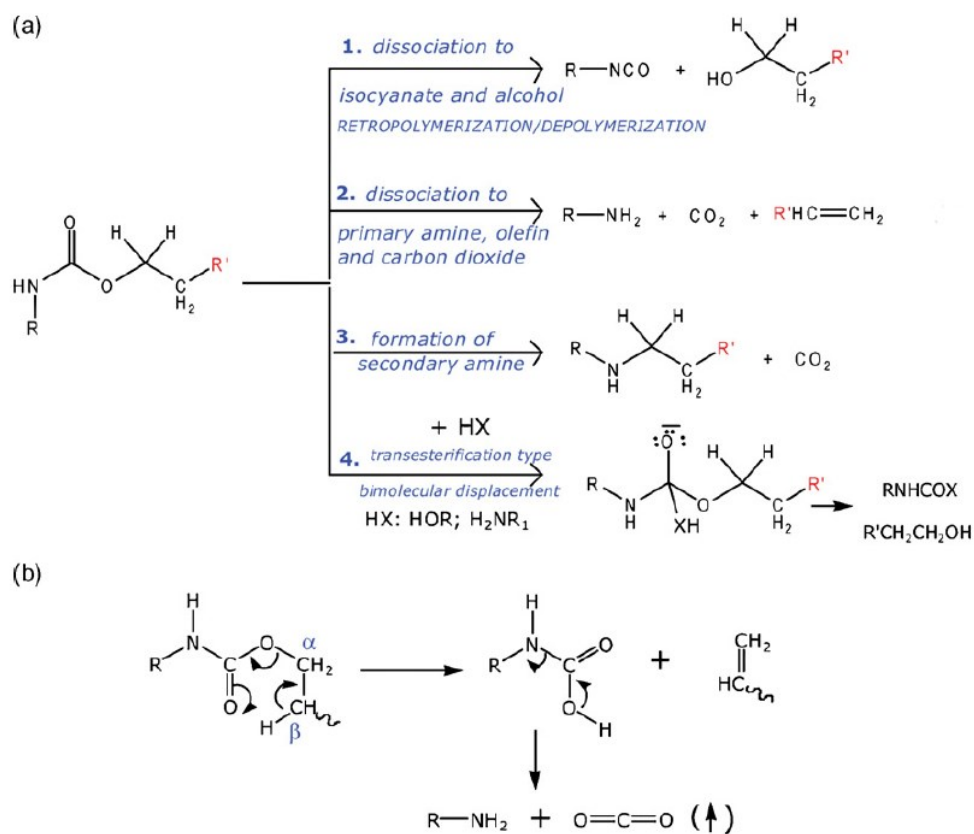


Fig. 24: Mechanics of PUR thermal degradation [44].

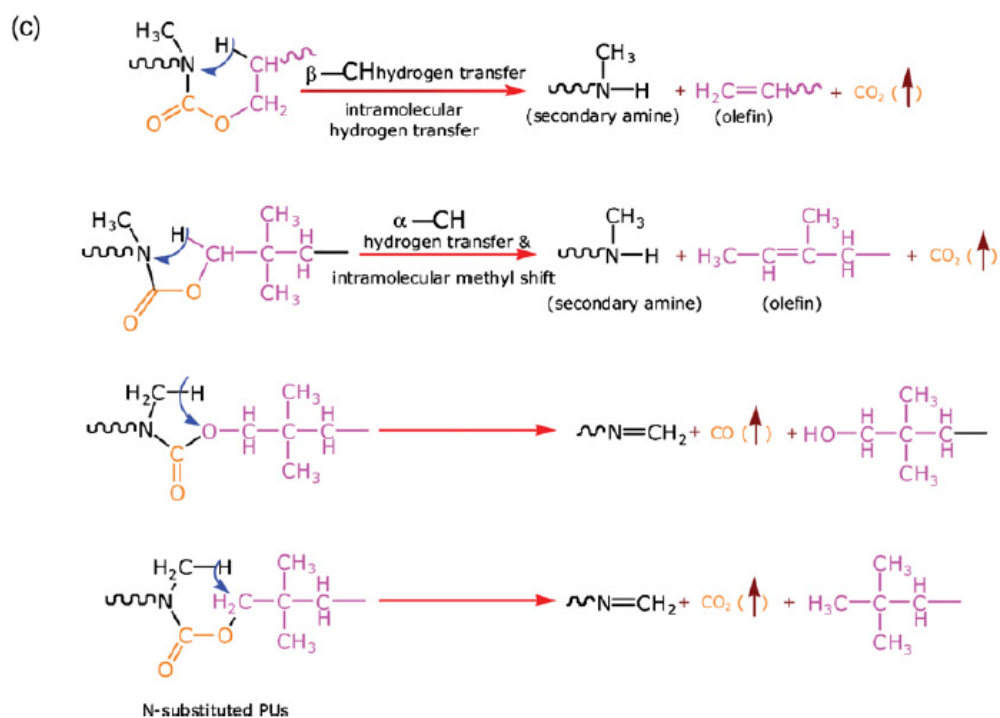


Fig. 25: Mechanics of N substituted PUR thermal degradation [44].

4 FLAMMABILITY AND MECHANISM OF COMBUSTION

The flammability or rather degree of flammability is material property that characterises the ease with which material catches on fire, and the length of time period during which it will burn, how the material will behave and how it will change during combustion. The degree of flammability of polymers can be characterised by several parameters:

4.1 Reaction of material to fire

Ignition

Fuel source (polymer) ignites and is in the state of stable combustion. See Fig. 26. Initiation of flaming combustion is called flaming ignition. When initiated by a pilot, such as gas particle, electric spark or smouldering wire, we refer to it as piloted ignition. When no pilot is present and mixture of flammable volatiles and gases is ignited from hot surface of solid, we refer to this type of ignition as autoignition. Another type of ignition is spontaneous ignition. This type of ignition takes a long period of time to initiate (hours or days) until it transforms to smouldering or flaming ignition. Spontaneous ignition is occurring when slow oxidation inside of a fuel exposed to air generates heat that exceeds the heat lost to the surroundings. [40]

Growth

Growth of fire is dependent on type of fuel and accessibility to oxygen, temperature might rise to 500°C. Fire spreads to nearby objects. Spreading is utilizing convection, radiation or both mechanisms combined. Convection takes place when flames are in direct contact with object and ignite it. Fire spread by radiation is done by thermal radiation from flames and smoke, that is strong enough to ignite fuel in proximity.

Flashover

Fast transition of fire from growth to fully developed fire. This stage is set off by thermal radiation, where growing fire releases enough heat that objects subjected to it burst into flames. Temperature in this stage reaches about 600°C.

Developed fire

At this point heat release rate (*HRR*) and temperature of the fire are peaking. The Temperature might reach from 900 to 1000°C. Every available combustible fuel is on fire at this point.

Length of this stage is dependent on the amount of fuel and air and produces high amount of CO due to flawed combustion.

Decay

The stage of decay is the last stage of fire, all the fuel has been depleted, or its amounts are decreasing rapidly. Temperature in this stage starts to fall.

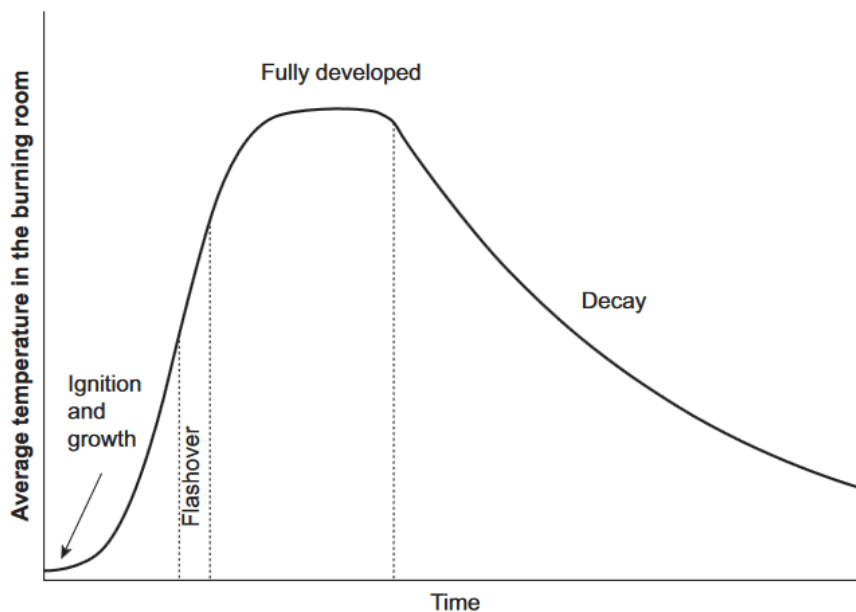


Fig. 26: Stages of fire during combustion of polymer [12].

4.2 Heat release rate (HRR)

Quantitative parameter, expressed as an amount of heat released by a material per area, under constant heat flux radiated by a fire. Its unit is kW/m^2 . HRR is a variable parameter, which changes during time of combustion (see fig. 27). HRR affects fire reaction properties, surface spread of flame and smoke generation [45] [46]. In an open environment, this heat is observed as fire plume above burning fuel. HRR depends on chemical composition of fuel, surface area and the heat or heat flux radiating onto surface area. For this work HRR will be measured with cone calorimeter. The HRR profile changes with time during combustion because of the changes to chemical and structural properties of polymer.

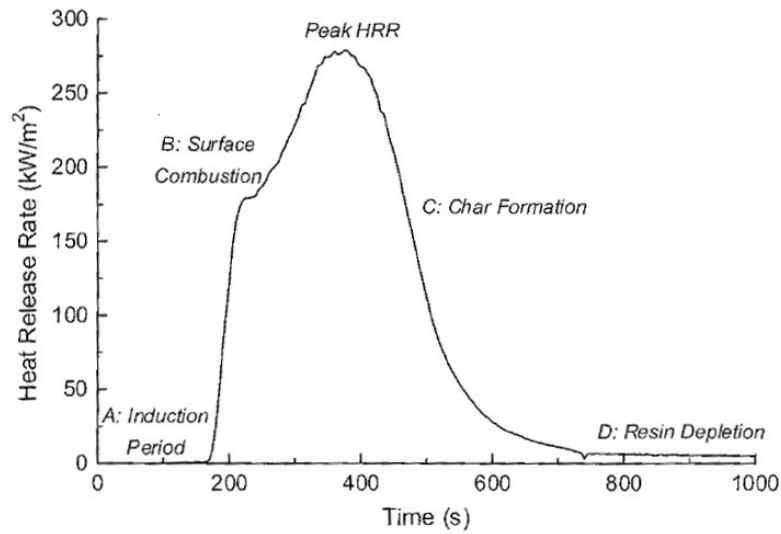


Fig. 27: HRR profile in time. This is a common result of cone calorimeter measurement [43].

HRR is also dependent on thickness of the sample, and increasing thickness can bring results, that show decline in peak and average HRR. From fig. 28 we can see that HRR increases significantly in samples with thickness below 8 mm. Samples thicker than 8 mm on the other hand show only marginal dependence on thickness. [47]

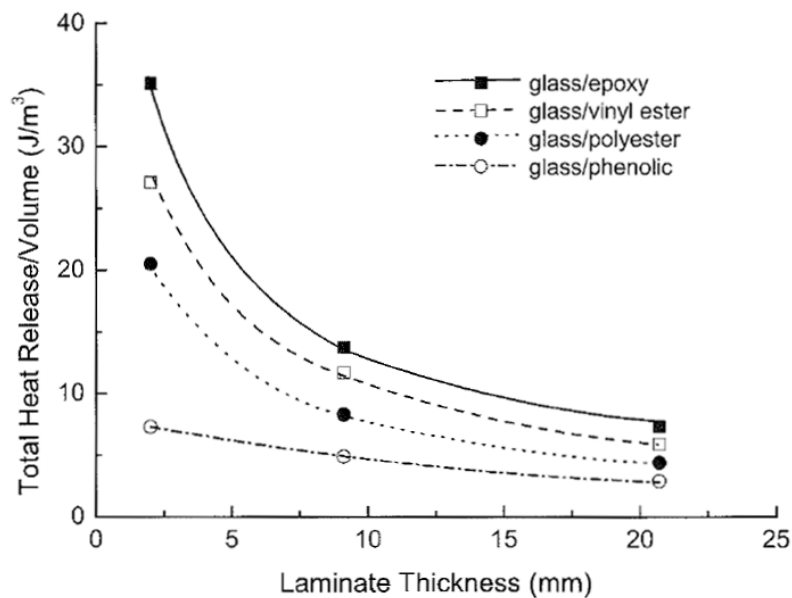


Fig. 28: THR/volume vs. sample thickness [43].

4.3 Peak Heat release rate (PHRR)

PHRR is maximum amount of heat released by a material in combustion. This maximum heat is released in short period of time, usually in less than few seconds. PHRR controls maximum temperature and spread rate of a fire.

4.4 Average heat release rate

The amount of heat released by fire over observed time period.

4.5 Time to ignition

Time period, for which material withstands constant heat flux exposure before igniting. Time to ignition can be affected by material composition, reinforcement content and its type [48], sample thickness [47], oxygen content in atmosphere.

4.6 Flame spread rate

Rate of the flame front traveling over sample surface. This parameter is experimentally measured in horizontal or vertical direction. This property is important in growth stage of a fire, when the flames and heat are beginning to ignite nearby fuel. Spread of flames over solid fuels is classified to two modes according to flow conditions. First mode is called wind-aided flame spread (or flow-assisted) (see fig. 29). This mode occurs when the flame spreads in the same direction as airflow. Second mode is opposite to the first and occurs when the flame spreads against the airflow. Therefore, it is called opposed-flow. Wind-aided flame spread is faster than opposed-flow and also more dangerous, as the heat of the flame extends over larger surface area [41] [49].

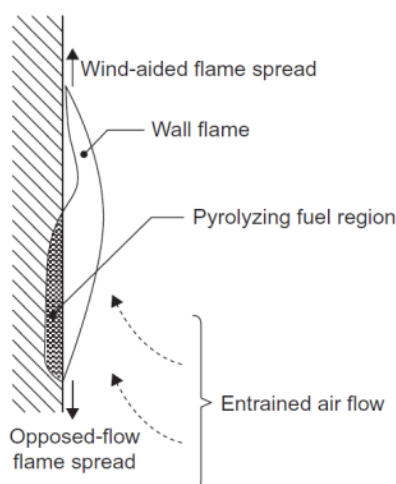


Fig. 29: Wind-aided and opposed-flow modes of surface flame spread [41]

Opposed-flow mode of fire spread is driven mostly by the HRR of the material. [43]

4.7 Limiting oxygen index

Minimum oxygen content needed to sustain combustion in oxygen - nitrogen atmosphere. The result is expressed in % and is compared to amount of oxygen in Earth's atmosphere. LOI value is determined by tests that are covered in standard CSN EN ISO 4589-1:2017.

4.8 Smoke generation, density and toxicity

Contrary to belief that, heat and flames are major cause of death in fires, smoke and toxicity of gas released during combustion are factors, that decrease the chances of survival the most. They contribute to disorientation and incapacitation and eventually to death. Smoke density is defined as a concentration of smoke particles within the plume of fire. Smoke toxicity is defined as a concentration and lethality of fumes released by burning material. Density of smoke can be also quantitatively determined with specific extinction area (SEA). SEA measures conversion effectiveness of volatiles released from sample to smoke. Effective way to suppress smoke generation is to increase char formation by using specific materials or by adding intumescent fire retardants to the compound for example.

Formation of the carbon monoxide (CO), according to Yuan-Wei Yan [17], takes place in early stages of combustion at relatively low temperatures. This is probably due to incomplete combustion of the released volatiles. Then, formation of carbon dioxide (CO₂) is occurring in more developed fires with higher temperatures. Carbon monoxide (CO) proposes bigger threat than Carbon dioxide (CO₂), concentration of only 1500 ppm in the air is needed to cause fatal suffocation, contrary to 100 000 ppm of CO₂ that is needed to cause the same result. [43]

Other than CO and CO₂, many types of gasses can be released from burning material. It depends on composition of used polymer and eventually its filler. Common volatile low molecular weight gasses are propylene, benzene, toluene, styrene, methane, acetone etc. Aromatic compounds and corrosive and toxic gasses are also released from certain types of materials.

Table 4. Contains combustion gasses and their concentration in thermoset and thermoplastic laminates.

Tab. 4: Combustion gasses and their concentration in various types of laminates [50] [51]

| Composite | CO [ppm] | CO ₂ [vol%] | HCN [ppm] | HCl [ppm] |
|----------------------|----------|------------------------|--------------|--------------|
| Glass/Vinyl ester | 230 | 0,3 | not detected | not detected |
| Glass/Epoxy | 283 | 1,5 | 5 | not detected |
| Glass/BMI | 300 | 0,1 | 7 | trace |
| Glass/phenolic | 300 | 1 | 1 | 1 |
| Glass/polyimide | 200 | 1 | trace | 2 |
| Glass/PPS | 70 | 0,5 | 2 | 0,5 |
| Glass/phthalonitrile | 40 | | | |
| Carbon/PEEK | trace | trace | not detected | not detected |

4.9 Mass loss

Mass loss gives quantitative expression on the amount of material that decomposes during combustion. Rate and amount of mass loss can be measured during combustion from changes in sample weight.

4.10 Fire resistance

Fire resistance is ability of material to slow down the burning process and maintain its mechanical properties. Main properties of fire resistance are:

- a) **Heat insulation** – Rate of heat conduction through a material exposed to fire.

- b) **Burn-through resistance** – Time taken until fire penetrates material and surfaces on the other side.
- c) **Mechanical integrity** – Ability of material to maintain mechanical properties (e.g. Stiffness, creep resistance, strength) during and after being exposed to fire.

4.11 Mechanism of combustion

Second part of this chapter gives insight at the flame structure, macroscopic mechanism of combustion and processes at molecular level, that are taking place inside polymers, thermal degradation and pyrolysis

4.11.1 Flame structure

Flame (as seen in fig. 30) is made of three regions, from bottom to the top they are:

- a. **Solid flame region** – Region where most of the heat is generated. Most of solid fuels generate temperature between 830 - 900°C. Hydrocarbon fires and natural gas fires may generate 1150-1250°C.
- b. **Intermittent flame region** – Temperature of this region decreases higher up to tip of a flame. It varies between 300 – 600°C.
- c. **Thermal plume** – Region without visible flame, temperature drops with height. Contains hot gases, vapours and particles that can be carried away by convection. [49]

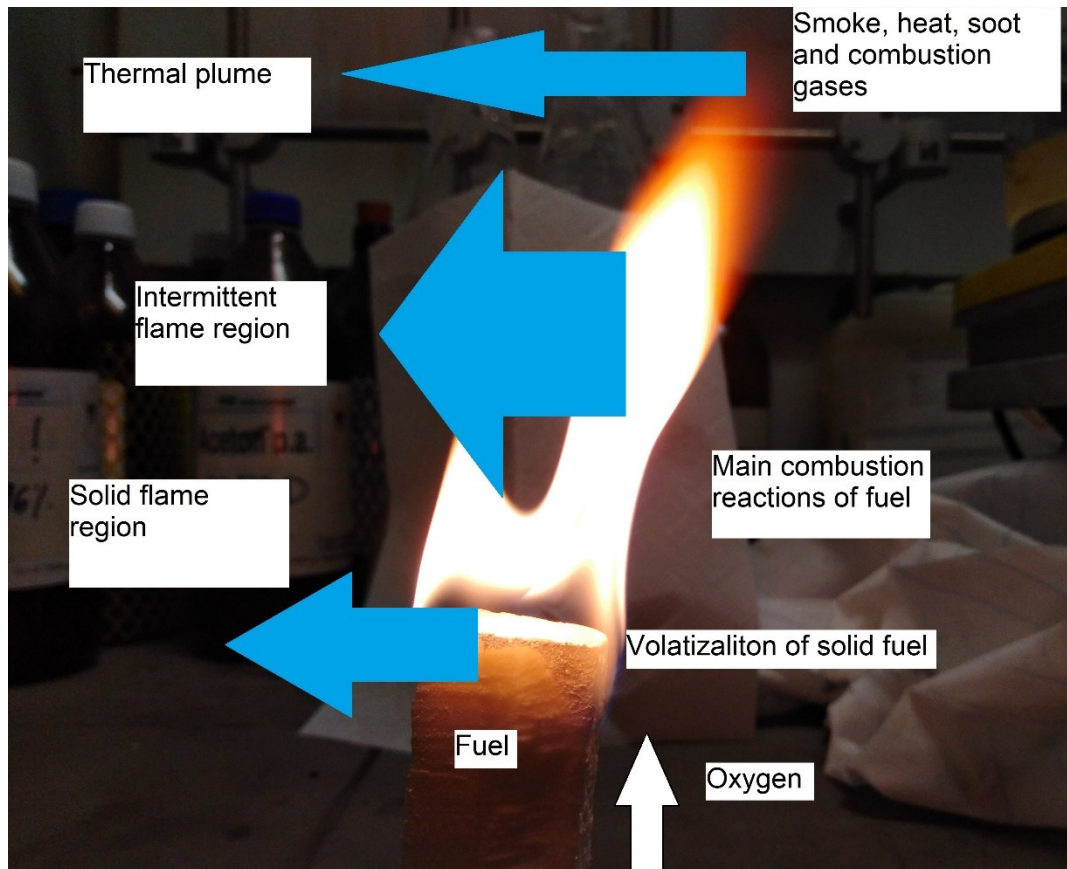
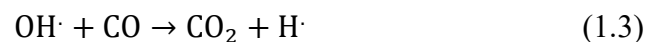
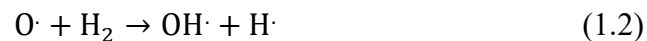


Fig. 30: Schematic of different zones in a flame.

4.11.2 Combustion cycle

Gas combustion is occurring inside solid and intermittent flame regions. Production of highly active hydrogen radicals is undergoing in this process. These radicals combine with oxygen in the flame and produce hydroxyl radicals:



Hydrogen radicals produced in reaction (1.2) and (1.3) are supplied back to the combustion reaction (1.1) and make reaction self-sustaining.

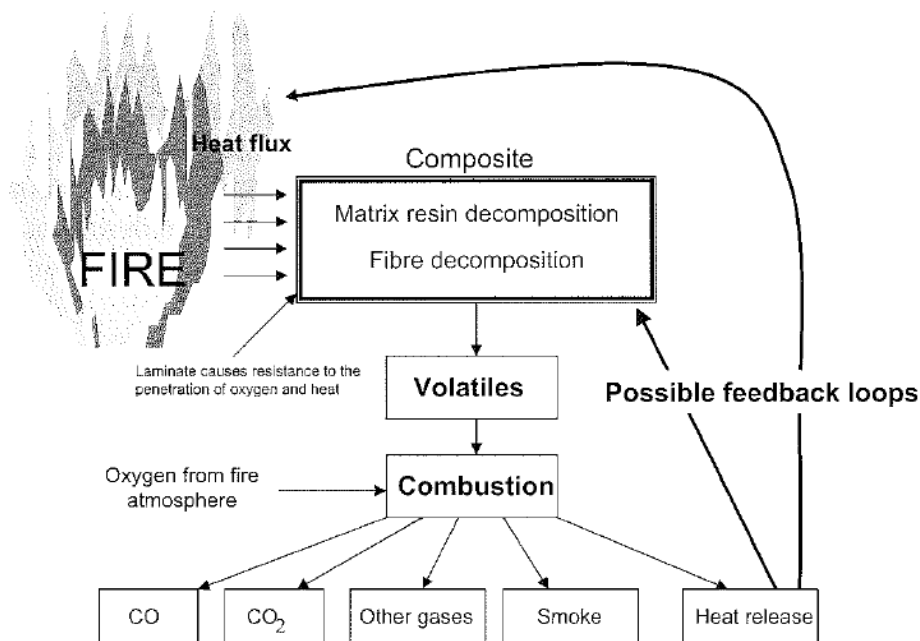


Fig. 31: Schematic picture of thermal decomposition mechanism [43].

Other gases than the mentioned hydrogen radicals, such as: CO, CO₂, smoke and variety of gases leave the combustion cycle. HRR as another product of the combustion is both directly and indirectly fed back to the combustion. Scheme of this HRR feedback can be seen in fig. 31.

The heat flux that is entering the combustion from “outside” of the flame is dependent on the location of the fire. If it is in enclosed compartment, the returning heat flux is greater as if the fire was located in open air.

5 EVALUATION METHODS

In this chapter, all evaluation methods used to describe material properties will be discussed.

5.1 Cone calorimeter

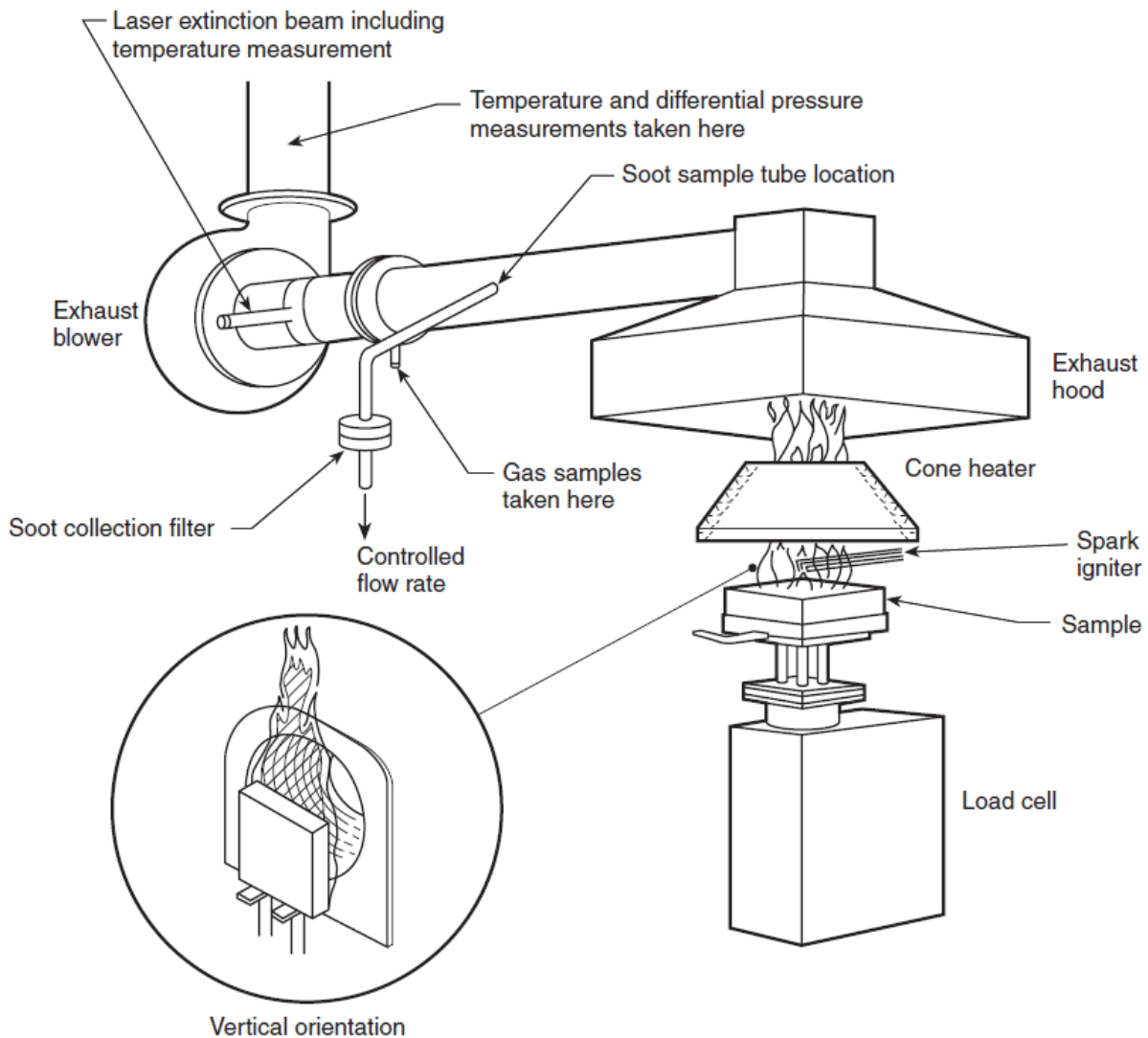


Fig. 32: Scheme of the cone calorimeter [49].

Measurements performed with cone calorimeter were following international standard ISO 5660-1. Cone calorimeter (see fig. 32) is bench-scale instrument for measuring HRR and other fire reaction properties of materials. Due to difficulty of direct and precise measuring of thermal energy, HRR is not measured directly, but rather calculated with the principle of oxygen consumption calorimetry. Equation used for HRR calculation is [52]:

$$\dot{q}(t) = \left(\frac{\Delta h_c}{r_o}\right) (1,10) C \sqrt{\frac{\Delta p}{T_e}} \frac{X_{O_2}^0 - X_{O_2}}{1,105 - 1,5X_{O_2}} \quad (1.1)$$

Where $\left(\frac{\Delta h_c}{r_o}\right)$ is equal to 13.1 MJ, C is calibration constant, Δp is orifice meter pressure differential, T_e is the absolute temperature of gas at the orifice meter, $X_{O_2}^0$ is initial value of oxygen analyser reading, X_{O_2} is oxygen analyser reading, mole fraction of oxygen. The value of 1,10 is the ratio of the molecular masses of oxygen and air.

The key principle states, that the heat of the combustion is proportional to the amount of oxygen, needed for said combustion. It was experimentally established that for 1 kg of oxygen, approximately 13.1 MJ (with $\pm 5\%$ deviance) of heat is needed. [52] This value is constant for breaking similar bonds, hydrogen – hydrogen, hydrogen – carbon and carbon – oxygen of generic fuels. Other fire reaction properties that can be assessed directly are:

- a) Time to ignition
- b) Time of sustained flaming
- c) Effective heat of combustion
- d) Smoke density
- e) Soot yield
- f) Mass loss rate
- g) Yields of CO and CO₂ and other gases produced by combustion.

These fire reaction properties can be determined from single test, using relatively small specimen. Test specimens are burned in ambient air conditions, where the heat from 0 kW/m² to 100 kW/m² is subjected onto them. Specimens should be a good representative of the final product. Shape of the specimen should be a square with sides of 100 mm and thickness from 5 mm to 50 mm. Side which comes to direct contact with irradiation should have flat and even surface. The Burning process proceeds under heating element in a shape of cone (see fig. 33). Heat flux up to the 100 kW/m² is thermostatically controlled by a radiant heater. This heater is an electric rod, coiled into shape of truncated cone.

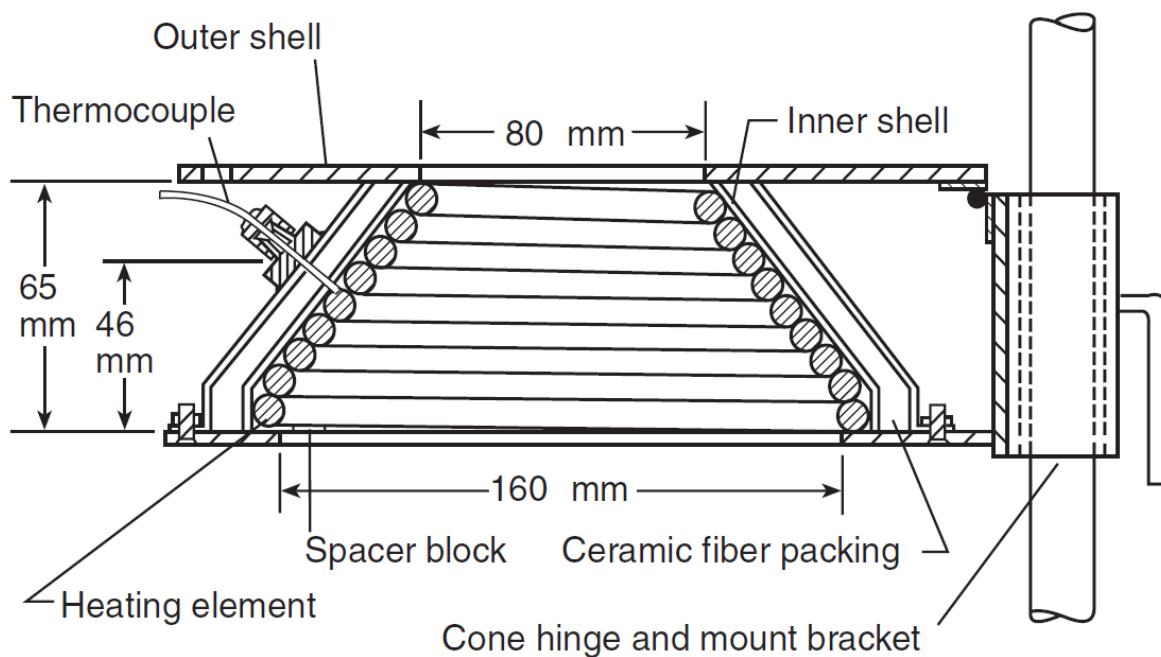


Fig. 33: scheme of cone heater [52].

Tests can be performed in vertical or horizontal position. Steady air flow should be maintained during the burning process, to force all combustible gas released by burning sample to flow up through the exhaust system, where it can be analysed for its composition, toxicity and density.

5.2 Rotational rheometry

Polyurethane as a thermosetting resin shows hardening, due to cross-linking reaction as was already properly described in the chapter 1. For proper investigation of the cross-linking kinetics and to ensure that reaction is not disrupted, rheological investigation upon oscillatory shear mode was utilized.

In this study, temperature dependent behaviour, at constant oscillatory shear conditions was examined. This test falls into oscillation rheometry category, and is also referred to as DMTA dynamic-mechanical thermoanalysis. Basic principle of this measurement is explained by the two plates model (see fig. 34)

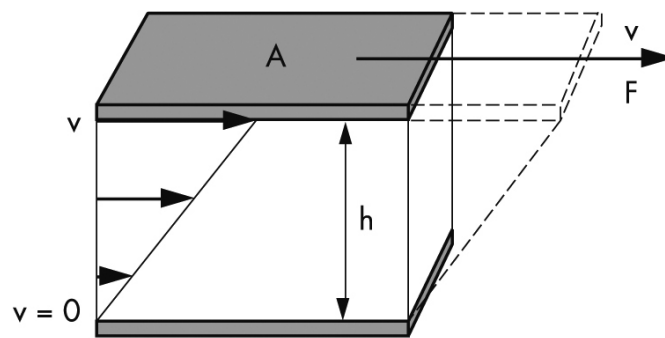


Fig. 34: The two plates model [53].

The bottom plate is stationary while upper oscillating plate is connected to driving wheel. The oscillating plate is moving forward and backwards with force $\pm F$ in angle of $\pm \phi$ range, and produces shearing, that deforms sample in length of $\pm s$. See fig. 35.

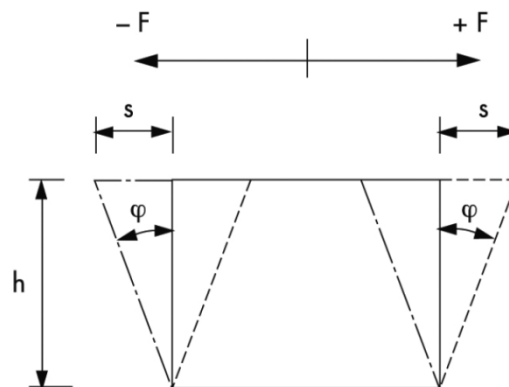


Fig. 35: Scheme of sample deformation during oscillating tests [53].

In this study, main focus was aimed at complex viscosity η^* [Pa.s], storage modulus G' (or elastic modulus) [Pa] and loss modulus G'' (or viscous modulus) [Pa].

Storage modulus is expressed as

$$G' = (\tau_A/\gamma_A) \cdot \cos \delta \quad (5.1)$$

Loss modulus is expressed as

$$G'' = (\tau_A/\gamma_A) \cdot \sin \delta \quad (5.2)$$

Complex viscosity is expressed as

$$|\eta^*| = \sqrt{(\eta')^2 + (\eta'')^2} \quad (5.3)$$

Dependence of complex viscosity on time is important, because it shows the certain processing window for the particular resin and its optimal flow, suitable for coating glass fibre those act as reinforcement in composites e.g. when the fibres are easily impregnated by the resin. This value of viscosity is noted as η^*_{\min} and it can reach two extremes. [53]

- 1) When η^*_{\min} is too low, resin might show creep, that results in inadequate edge protection.
- 2) When η^*_{\min} is too high, resin might not cover reinforcement evenly and create air bubbles.

From dependence of G' and G'' on temperature, we can read temperature at which sol/gel transition starts to occur (see fig. 36). At this point $G' = G''$ and also damping factor $\tan \delta = G'/G'' = 1$.

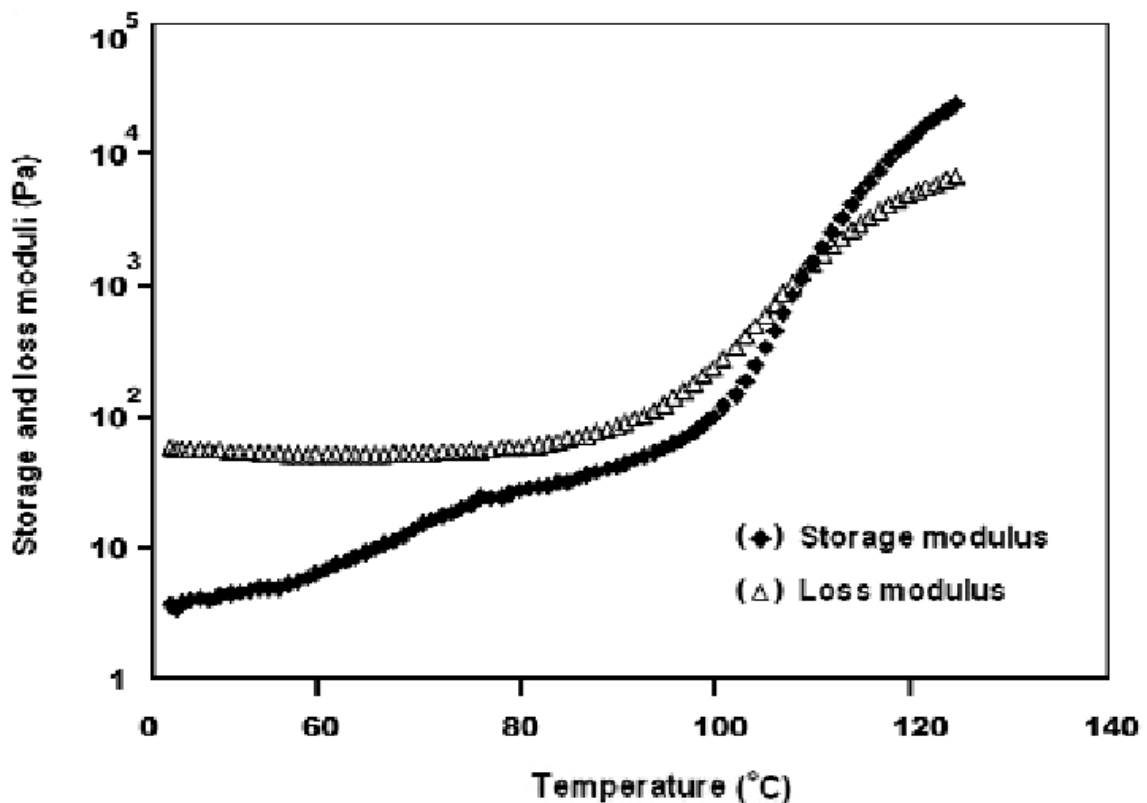


Fig. 36: Dependence of Storage and loss modulus on the temperature from the temperature sweep measurement [54].

5.3 Flammability investigation according to UL-94

UL-94 is test of flammability for plastics used in devices and appliances, it is meant to indicate if the response of material is adequate for its intended use. The test is performed in laboratory conditions on specimens of specific sizes, length of 125 ± 5 mm and width of 13 ± 5 mm. The test may be performed in vertical or horizontal position. In this case vertical position is chosen. Attention is given to specimens behaviour while in combustion and after the combustion, time is measured from ignition to flameout and important events are noted during testing for evaluation. The evaluation classifies the sample to categories V-0, V-1 or V-2. Criteria for each of these categories are listed in table 5. The scheme of equipment setup is shown in fig. 37.

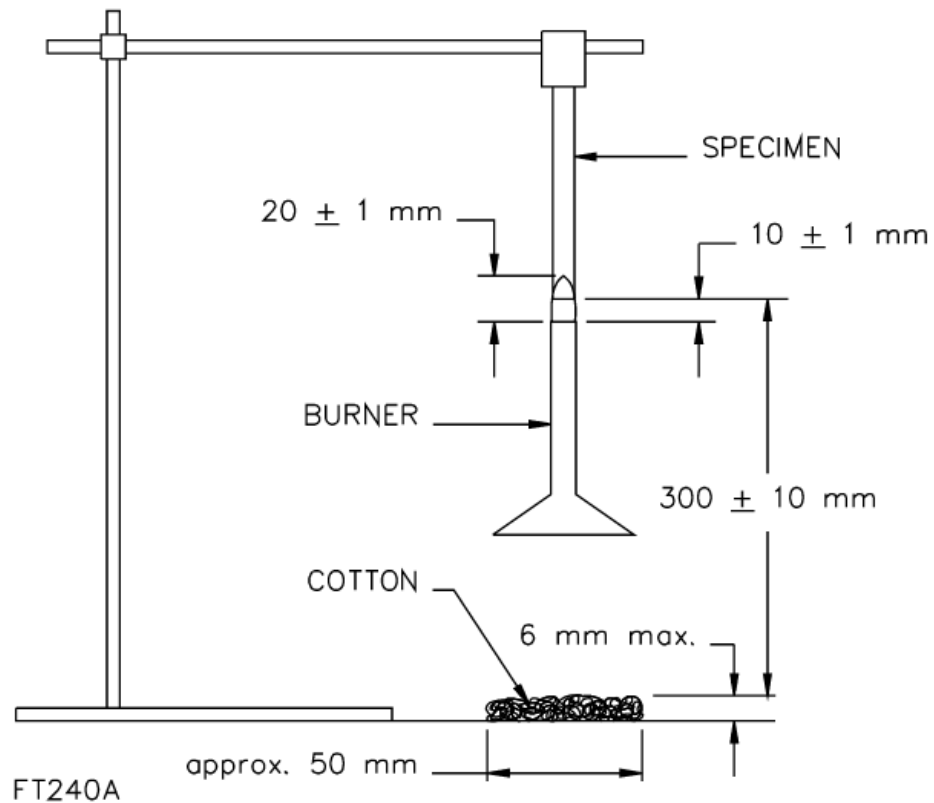


Fig. 37: Scheme of UL 94 Vertical burning test setup [55].

Tab. 5: Classification and their criteria for UL-94 [55].

| Criteria conditions | V-0 | V-1 | V-2 |
|--|-------------|--------------|--------------|
| Afterflame time for each individual specimen t_1 or t_2 | ≤ 10 s | ≤ 30 s | ≤ 30 s |
| Total afterflame time for any condition set (t_1 plus t_2 for the 5 specimens) | ≤ 50 s | ≤ 250 s | ≤ 250 s |
| Afterflame plus afterglow time for each indi- vidual specimen after the second flame appli- cation (t_2+t_3) | ≤ 30 s | ≤ 60 s | ≤ 60 s |
| Afterflame or afterglow of any specimen up to the holding clamp | No | No | No |
| Cotton indicator ignited by flaming particles or drops | No | No | Yes |

5.4 Dynamic mechanical analysis (DMA)

DMA is providing description of mechanical properties of materials in reference to frequency, time and temperature. During the measurement, the sample is subjected to oscillating mechanical stress or strain. The DMA records the value of the force amplitude, the displacement amplitude and the phase difference between each of these values (see fig. 38).

The applied stress or strain must always be in range of linear elasticity of the material as it is defined by Hooke's law. Strain is always the product of stress and due to the viscoelastic character of polymer materials, it always comes after the application of stress. Only in perfectly elastic materials is the strain immediate. The amount of lag between these values is the phase difference, also called the phase angle δ . One of the important values that characterises the material is the complex modulus M^* , which is given by the ratio of peak stress and peak strain. Complex modulus consists of two components, storage modulus M' (the in-phase component) and loss modulus M'' (component out-of-the phase by 90°). Ratio of these components represents the loss factor $\tan \delta$, also called as the "damping factor". High value of the $\tan \delta$ indicates that the material has high viscous component and low values then shows that the material has higher elastic component [56].

Three possible distinctive behaviours of the sample can be then characterised:

- a) Elastic behaviour, $\delta = 0^\circ$. No loss of deformational energy.
- b) Viscous behaviour, $\delta = \pi/2$ (90°). Deformational energy is converted to heat.
- c) Viscoelastic behaviour, viscoelastic sample deformation is delayed to applied stress, $0 < \delta < \pi/2$.

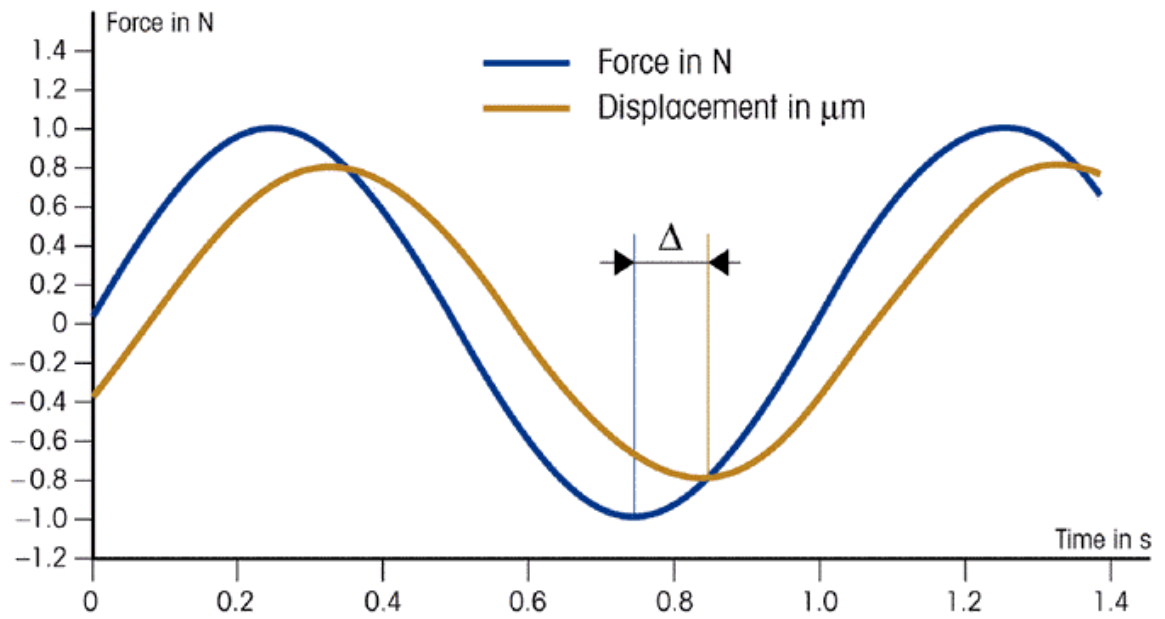


Fig. 38: Force and displacement at $f = 1$ Hz. Deformation is delayed to applied force by time difference Δ . Phase angle $\delta = 2\pi f\Delta$ [56].

Formulas for values characteristic for DMA measurement:

$$\sigma(t) = \sigma_A \sin \omega t = F_A/A \sin \omega t \quad (5.4)$$

$$\varepsilon(t) = \varepsilon_A \sin(\omega t + \delta) = L_A/L_0 \sin(\omega t + \delta) \quad (5.5)$$

$$M^*(\omega) = \sigma(t)/\varepsilon(t) = M' \sin \omega t + M'' \cos \omega t \quad (5.6)$$

$$|M^*| = \sigma_A/\varepsilon_A \quad (5.7)$$

$$M'(\omega) = \sigma_A/\varepsilon_A \cos \delta \quad (5.8)$$

$$M''(\omega) = \sigma_A/\varepsilon_A \sin \delta \quad (5.9)$$

$$\tan \delta = M''(\omega)/M'(\omega) \quad (5.10)$$

5.5 Differential scanning calorimetry (DSC)

Differential scanning calorimetry is a technique used to analyse the thermal properties of polymers, or rather their thermal transitions. The measuring device (fig. 39) is based around two pans, empty reference pan and sample pan with polymer. These pans are heated at the same rate and the difference between heat flow in reference pan and the sample pan is recorded. The measured data are used to determine various properties, heat capacity C_p , glass transition temperature T_g , crystallization temperature T_c , melting temperature T_m or even

determine the degree of crystallinity of the sample or the rate of reaction [57] [58].

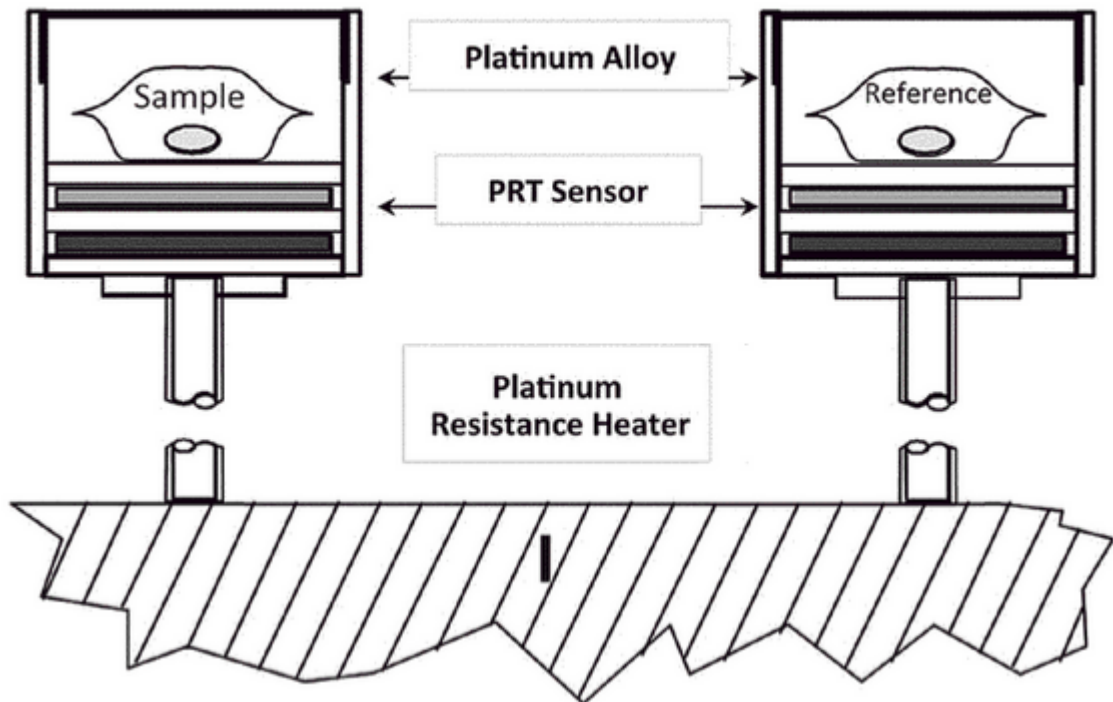


Fig. 39: Scheme of a DSC device [57].

Another important characteristic parameter of polymers, which can be evaluated from DSC, is change of enthalpy ΔH [kJ] propagated by exo- or endo- thermal character of physical or chemical reaction occurring in DSC measurement. The change of enthalpy is given by formula 5.11:

$$\Delta H = \int_{T_1}^{T_2} C_p dT \quad [\text{kJ}] \quad (5.11)$$

Where C_p is the heat capacity of polymer and the temperatures T_1 and T_2 are temperatures in which the transition begins and ends, respectively. Enthalpy represents the area under the peaks of recorded thermogram. On fig. 40, the ideal DSC curve is depicted for semi-crystalline polyolefin with its characteristic transitions.

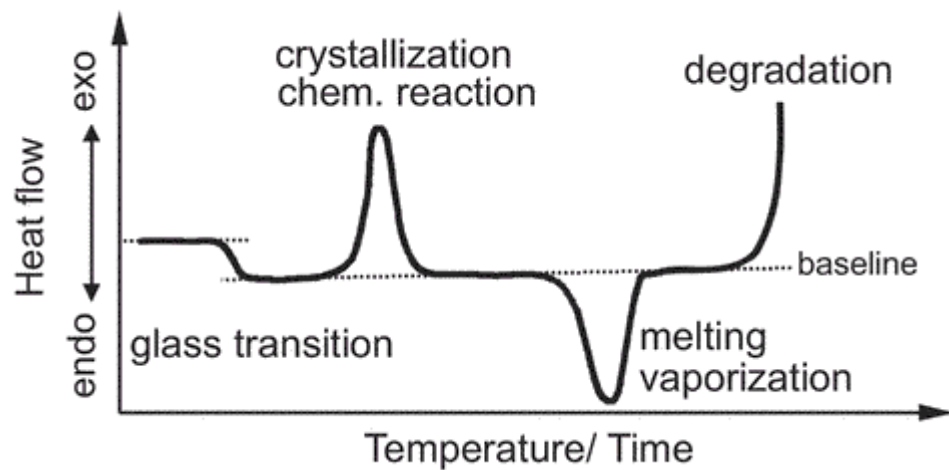


Fig. 40: Idealized DSC curve showing phase transitions of polyolefinic material [59].

5.6 Fourier-transform infrared spectroscopy (FTIR)

FTIR is a method that can be used to determine composition of a sample on a basis of their capability to absorb infrared light of multiple wavelengths. Absorption of the infrared waves is promoted as bond vibrations. These bond vibrations are classified as a valence vibrations (symmetric and asymmetric stretching) and deformational vibrations (β – bending, ρ – rocking, δ – scissoring). [60]

II. ANALYSIS

6 EXPERIMENT

6.1 Materials

6.1.1 Polyurethane components

The isocyanate, Desmodur supplied by 5M (Kunovice, Czech Republic). Polyols used in this work are Letoxit AX437 manufactured and supplied by 5M (Kunovice, Czech Republic). Both, Exolit OP 560, the non-halogenated phosphorous polyol with density of 1,2 [g/cm³], 10 – 13 [%wt] of phosphorous content, with 400 – 500 [mg KOH/g] hydroxyl number and viscosity up to 500 [mPa.s] and Exolit OP 560 is manufactured and supplied by Clariant (Hurth-Knapsack, Germany)

6.1.2 Additive

Flame retarding additive used in this study was Exolit IFR 36, manufactured and supplied by Clariant (Hurth-Knapsack, German). It is an intumescent flame retardant based on ammonium polyphosphate, it is non-halogenated and it is effective through phosphorus /nitrogen synergism. Temperature of its decomposition is above 230 [°C], density is 1,8 [g/cm³], it contains approximately 20 [wt%] and 15 [wt%] of phosphorus and nitrogen respectively. Average particle size is approximately 12 [µm].

6.2 Sample fabrication

Sample preparation was performed in vacuum mixer for 80 [s] with 150 [rpm]. Additive was always added into the polyol, mixed for the first time, then isocyanate was added and mixed for the second time. Same procedure was repeated for mixing samples with two types of polyols.

Tab. 6: Mixing ratios of polyols and isocyanate

| Polyol Letoxit AX 437 | Polyol Exolit OP 560 | Isocyanate Desmodur |
|-----------------------|----------------------|---------------------|
| 100 | 0 | 114,3 |
| 90 | 10 | 114,7 |
| 80 | 20 | 115,1 |
| 70 | 30 | 115,5 |

| | | |
|----|-----|-------|
| 50 | 50 | 116,3 |
| 30 | 70 | 117,1 |
| 0 | 100 | 118,3 |

6.3 Sample preparation

Samples for FTIR were cut-outs from mould left after curing.

Samples for rotational rheometry were liquid PUR blends of corresponding composition according to Table 7 left to cure during temperature sweep scan.

Samples for DSC were liquid PUR blends of corresponding composition according to Table 7 left to cure during dynamic scan.

Samples for DMA test were cut out from one extra UL94 sample using linear precision saw.

Samples for cone calorimeter were prepared by pouring liquid PUR blend into mold with dimension of $100 \times 100 \times 6$ [mm]. Curing reaction was carried out at 160 [°C] for 1 h. Samples were in accordance with ISO 5660-1:2002 requirements.

Samples for UL94 test were prepared by pouring liquid PUR blend into mold with dimensions of $125 \times 13 \times 4$ [mm]. Curing reaction was carried out at 160 °C for 1 h. Samples were prepared in accordance with UL94 requirements.

6.3.1 Sample denotation and composition

Tab. 7: Sample name and composition

| Sample name | Letoxit AX 437 | Exolit OP 560 | Exolit OP 560 [wt%] | Des-modur | Exolit IFR 36 [DSK] | Exolit IFR 36 [wt%] |
|------------------|----------------|---------------|---------------------|-----------|---------------------|---------------------|
| AX_IFR 0 | 100 | - | - | 114,3 | 0 | 0 |
| AX_IFR 10 | 100 | - | - | 114,3 | 10 | 9 |
| AX_IFR 20 | 100 | - | - | 114,3 | 20 | 17 |

| | | | | | | |
|----------------------|-----|-----|----|-------|----|----|
| AX_IFR 30 | 100 | - | - | 114,3 | 30 | 23 |
| AX_IFR 50 | 100 | - | - | 114,3 | 50 | 33 |
| AX_IFR 70 | 100 | - | - | 114,3 | 70 | 41 |
| AX_OP 10 | 90 | 10 | 5 | 114,7 | - | - |
| AX_OP 20 | 80 | 20 | 9 | 115,1 | - | - |
| AX_OP 30 | 70 | 30 | 14 | 115,5 | - | - |
| AX_OP 50 | 50 | 50 | 23 | 116,3 | - | - |
| AX_OP 70 | 30 | 70 | 32 | 117,1 | - | - |
| AX_OP 100 | 0 | 100 | 46 | 118,3 | - | - |

The samples were denoted such as suffix IFR means that the Exolit IFR 36 is used as an additive and suffix OP means that the Exolit OP 560 is used as a partial replacement of AX 437. The number behind the name represents the amount of additive added on top of the 100 % matrix in the case of Exolit IFR 36, or partial amount of polyol AX 437 replaced with Exolit OP 560.

6.4 Experiment methodology

6.4.1 FTIR

FTIR spectroscopy was done with Nicolet iS5 spectrometer equipped with iD5 ATR module with germanium crystal. Total of 64 scans for each sample was performed.

6.4.2 Rotational rheometry

Measurement was performed with Anton Paar rotational rheometer. Temperature sweep from 25 [°C] to 150 [°C] at the heating rate of 5 [°C/min] was performed. Frequency was set to 1 Hz and amplitude was 0,5 % was used. Gap between measuring plates was 1 [mm]. Measurement was performed on Peltier cell with measuring system that has round plate contact plane of 25 [mm] diameter.

6.4.3 Dynamic scanning calorimetry (DSC)

DSC measurement was performed on Mettler Toledo equipment. Dynamic scan was used, in which temperature profile started at 25 [°C] and ended at 250 [°C] with heating rate of 10 [°C/min]. Reaction enthalpy and normalized enthalpy to weight of the sample was recorded and evaluated.

6.4.4 Dynamic mechanical analysis (DMA)

Tension mode, where all measurements were performed at linear viscoelastic region. This region varied from 0.01% to 5%. Then the temperature sweep tests were performed from 30 [°C] up to 220 [°C] with heating rate 3 [°C/min] to show the mechanical performance of the prepared composites as well as changes in glass transition temperatures.

6.4.5 Cone calorimetry

Cone calorimetry was performed on FTT cone calorimeter in horizontal position with 25 [mm] separation between cone heater and sample surface. Heatflux was set to 50 [kw/m²] and was radiated on a surface of 100 [cm²]. Pre measurement calibration measurement itself was carried out as described in ISO 5660-1:2002. Samples prepared for this test were also in accordance to ISO 5660-1:2002.

6.4.6 UL94

This test was performed on samples of 12,5 × 1,5 × 0,3 [cm]. Bunsen burner set to UL94 standard was applied for 10 seconds and then removed from beneath the sample. Right after the self-extinguishing of the samples, the flame was applied for another 10 seconds and then removed. Times of flaming combustion and smouldering combustion were recorded.

7 RESULTS AND DISCUSSION

7.1 FTIR

In order to confirm the presence of the various additives in the PUR samples, FTIR spectroscopy investigation was performed. As can be seen in the Fig. 41, the Exolit IFR 36 additive shows typical and in fact very important peaks at 886 cm^{-1} and 1054 cm^{-1} corresponding to the P-O-C absorption band typically visible in various intumescent systems. Moreover the peak at 3222 cm^{-1} shows also presence of nitrogen containing groups those are also very important in the case of improvement behaviour during burning. The prepared composites showed in Fig. 41 provide increased intensity of the peaks corresponding to P-O-C absorption bands, confirming the increased amount of the additive in the system, only slight increase is visible in case of peaks corresponding to nitrogen containing groups at 3222 cm^{-1} .

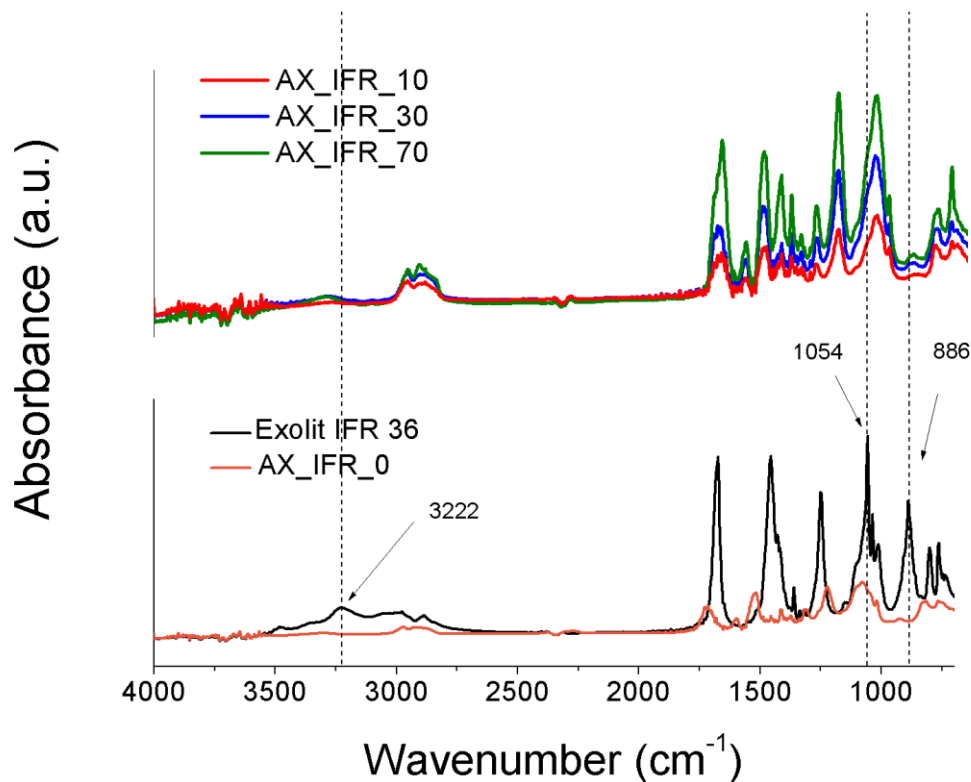


Fig. 41: FTIR spectra of the samples containing various amount of the Exolit IFR 36 additive.

In case of PUR systems with Exolit OP 560 polyol Fig. 42, the situation is very similar to the previous system. This type of polyol shows the presence of the both nitrogen (3383 cm^{-1}) and phosphorus containing groups (1030 cm^{-1} and 890 cm^{-1}). If the amount of the polyol

increase also the peaks intensity increases thus the incorporation of this polyol was successfully confirmed. In both cases, only selected concentrations (smallest, middle and highest) were chosen for presented investigation due to the fact that utilization of whole systems, might be rather unclear for understanding.

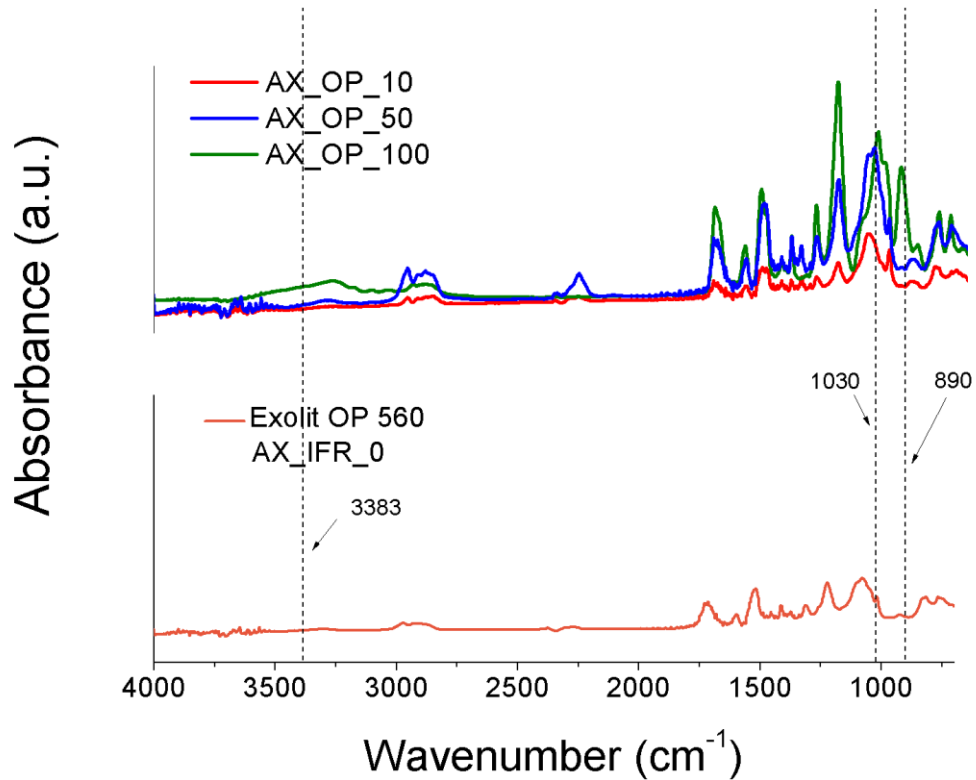


Fig. 42: FTIR spectra of the samples containing various amount of the Exolit OP 560 liquid polyol.

7.2 Rotational rheology

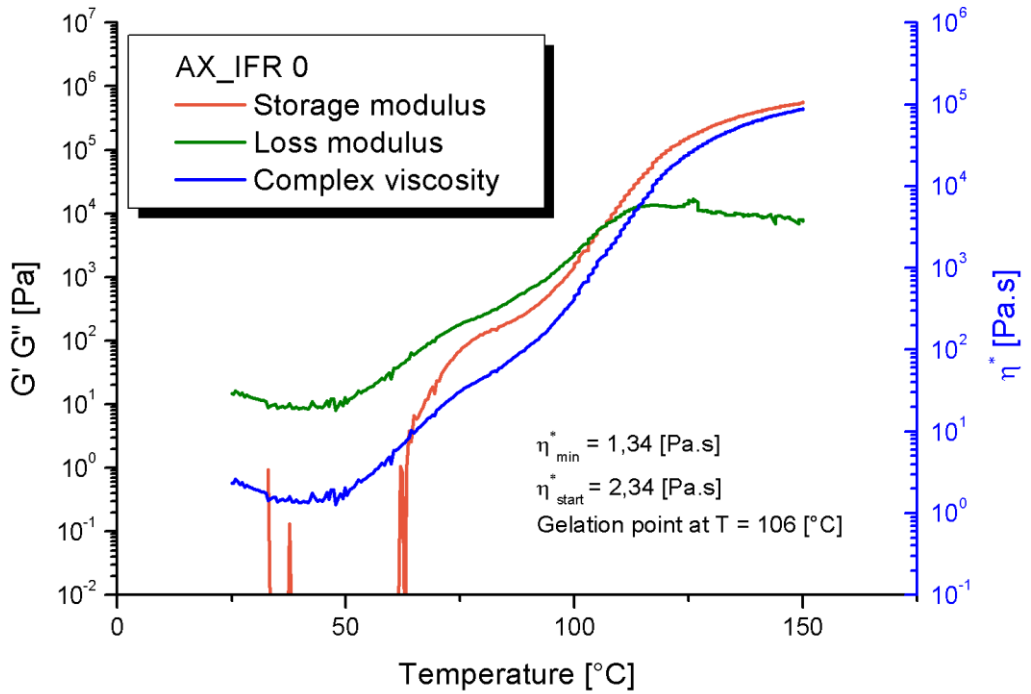


Fig. 43: Record of temperature sweep measurement on sample AX_IFR 0

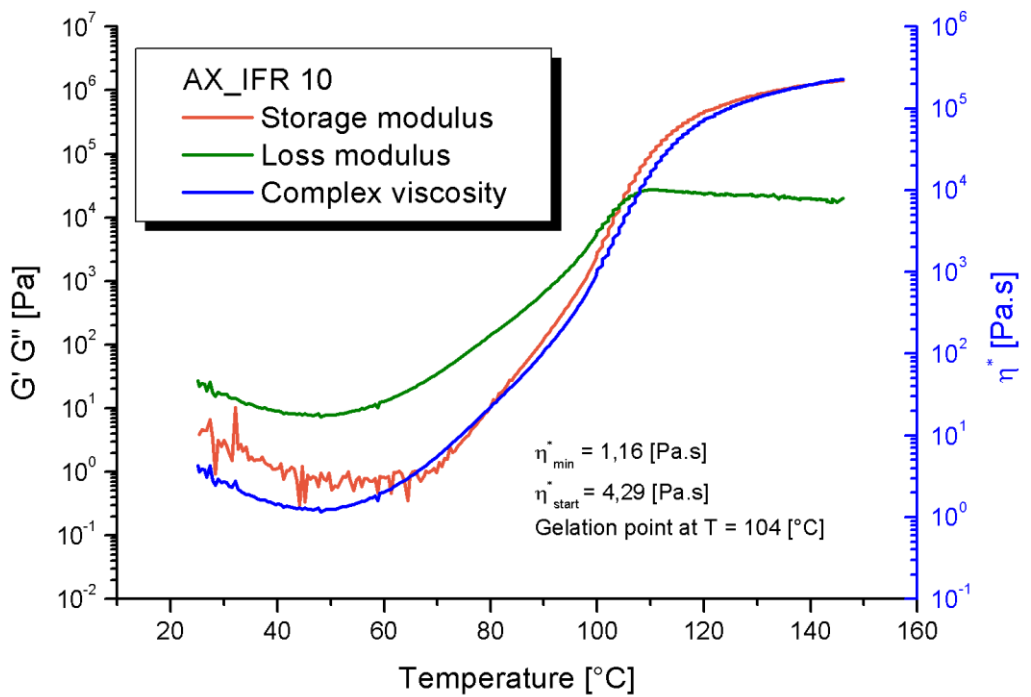


Fig. 44: Record of temperature sweep measurement on the sample AX_IFR 10

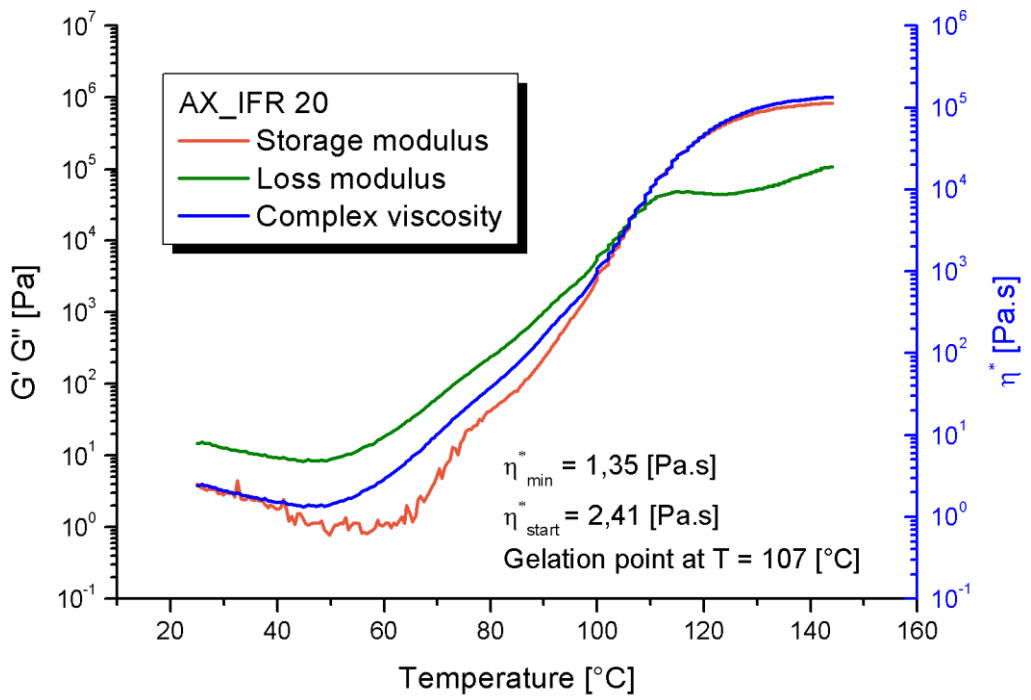


Fig. 45: Record of the temperature sweep measurement on the sample AX_IFR 20

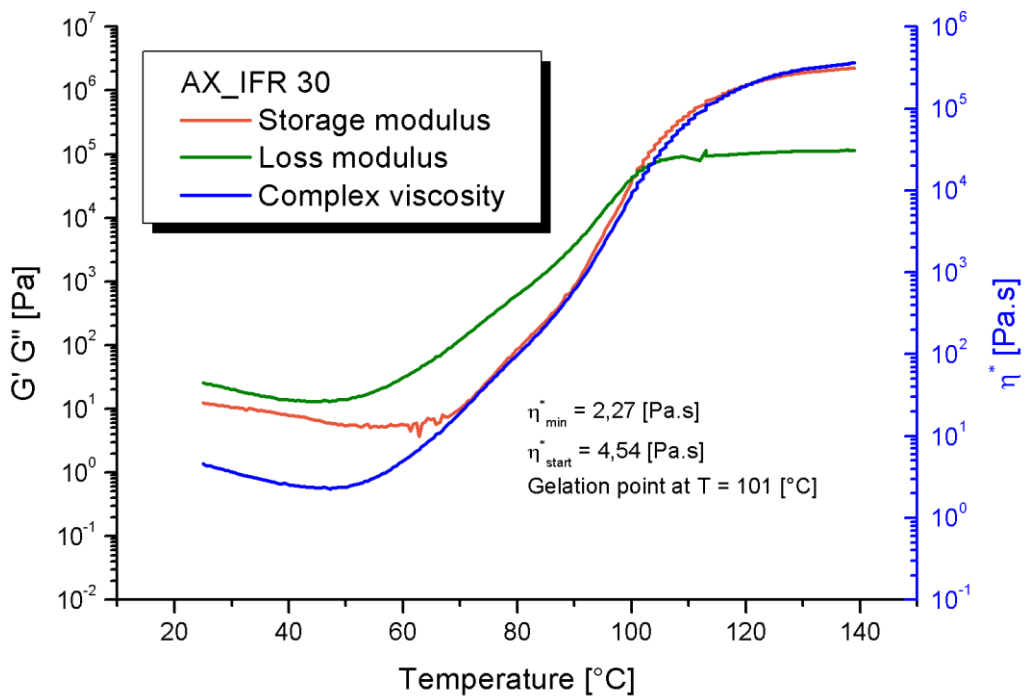


Fig. 46: Record of the temperature sweep measurement on the sample AX_IFR 30

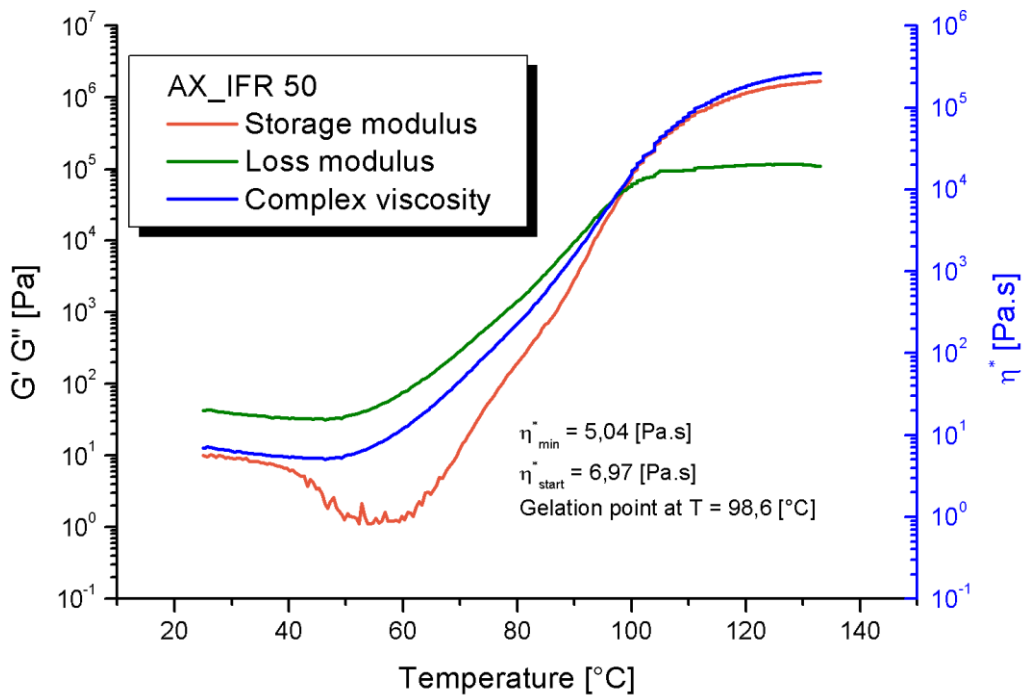


Fig. 47: Record of the temperature sweep measurement on the sample AX_IFR 50

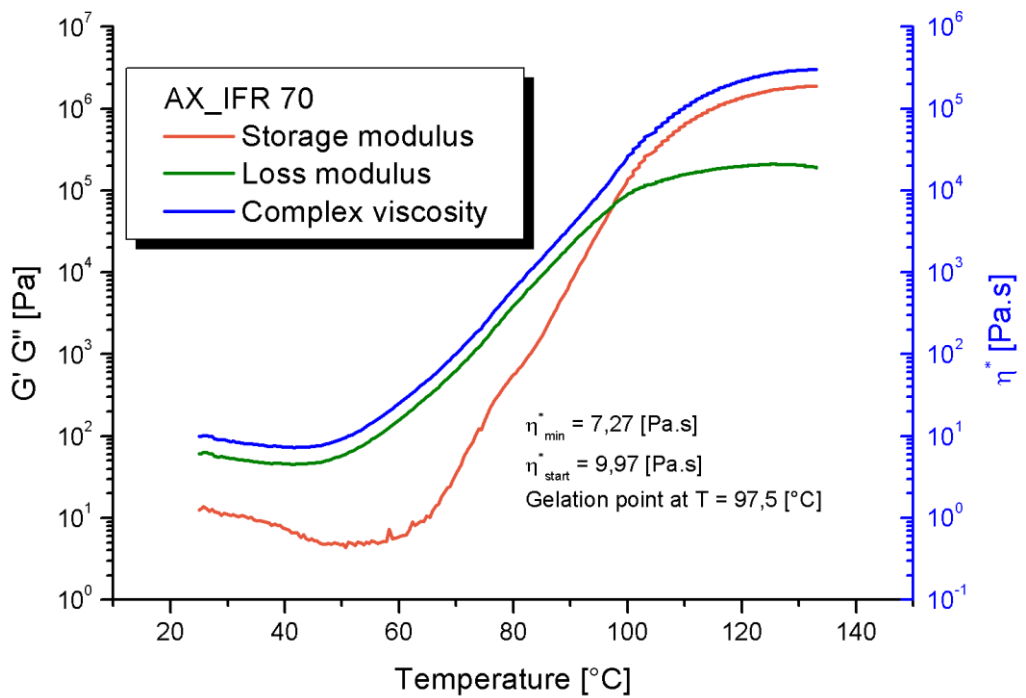


Fig. 48: Record of the temperature sweep measurement on the sample AX_IFR 70

As can be seen from these measurements (fig. 43 – 48), the largely increasing amount of powder additive is increasing the starting and minimal value of complex viscosity η^* . While sample AX_IFR 0 (see fig.41), AX_IFR 10 (see fig. 43) and AX_IFR 20 (see fig. 44) have their η_{\min} in the range of 1,16 to 1,35 [Pa·s] and η_{start} from 2,34 to 4,29 [Pa·s], samples AX_IFR 30, AX_IFR 50 and AX_IFR 70 have their η_{\min} in the range from 2,27 to 7,27 [Pa·s] and η_{start} from 4,54 to 9,97 [Pa·s]. These results show that from 30 [DSK] content, the additive starts to have a significant impact on the processability. Numerical results can be seen in the Tab. 8 below.

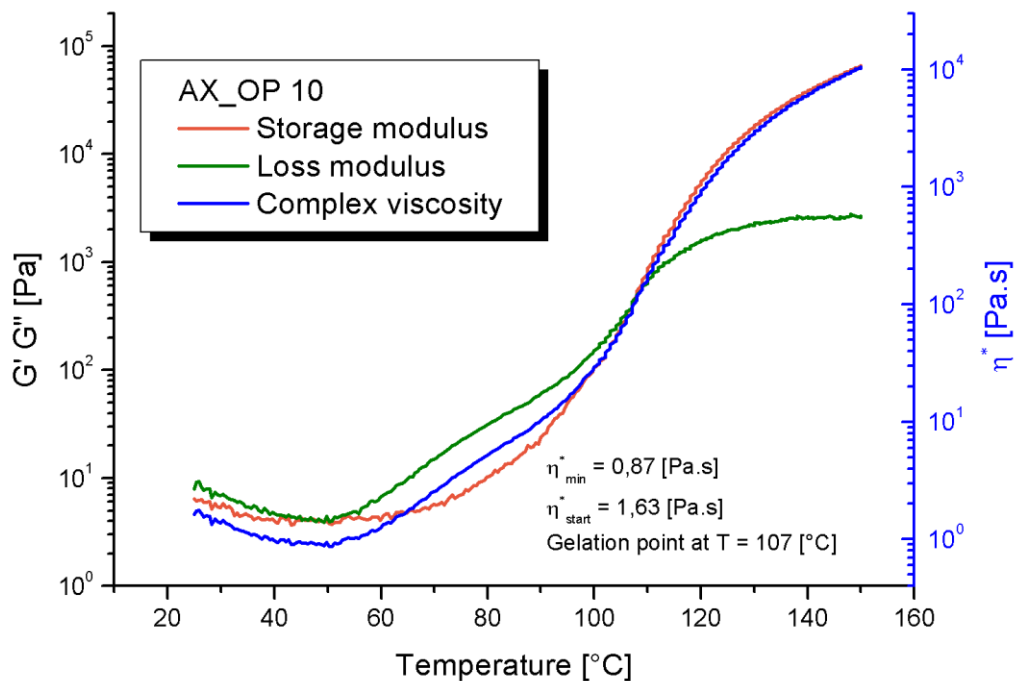


Fig. 49: Record of the temperature sweep measurement on the sample AX_OP 10

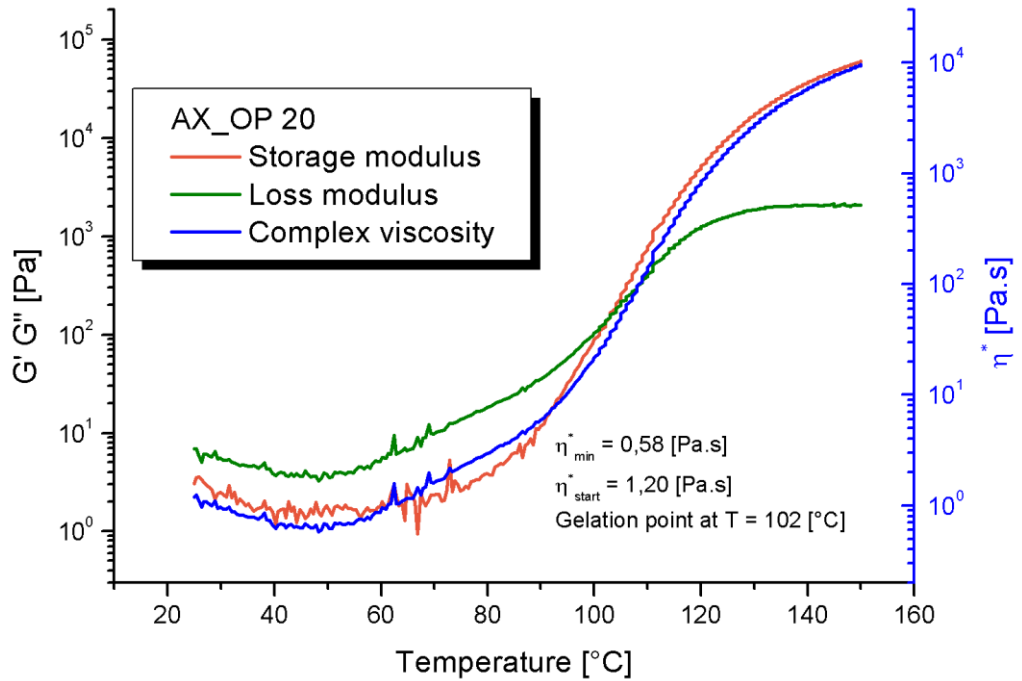


Fig. 50: Record of the temperature sweep measurement on the sample AX_OP 20

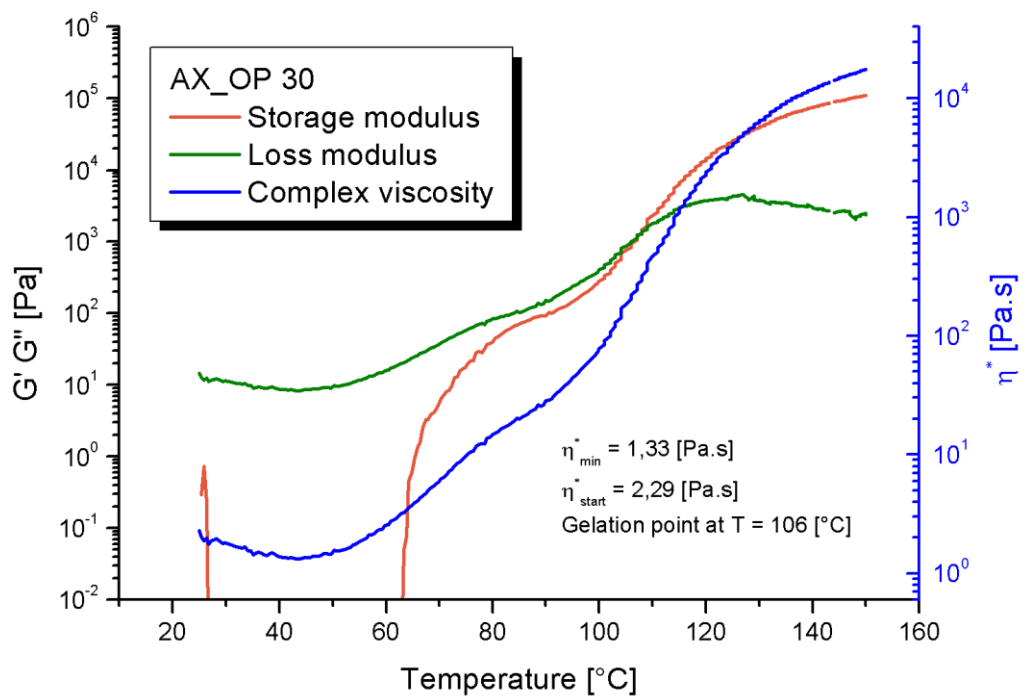


Fig. 51: Record of the temperature sweep measurement on the sample AX_OP 30

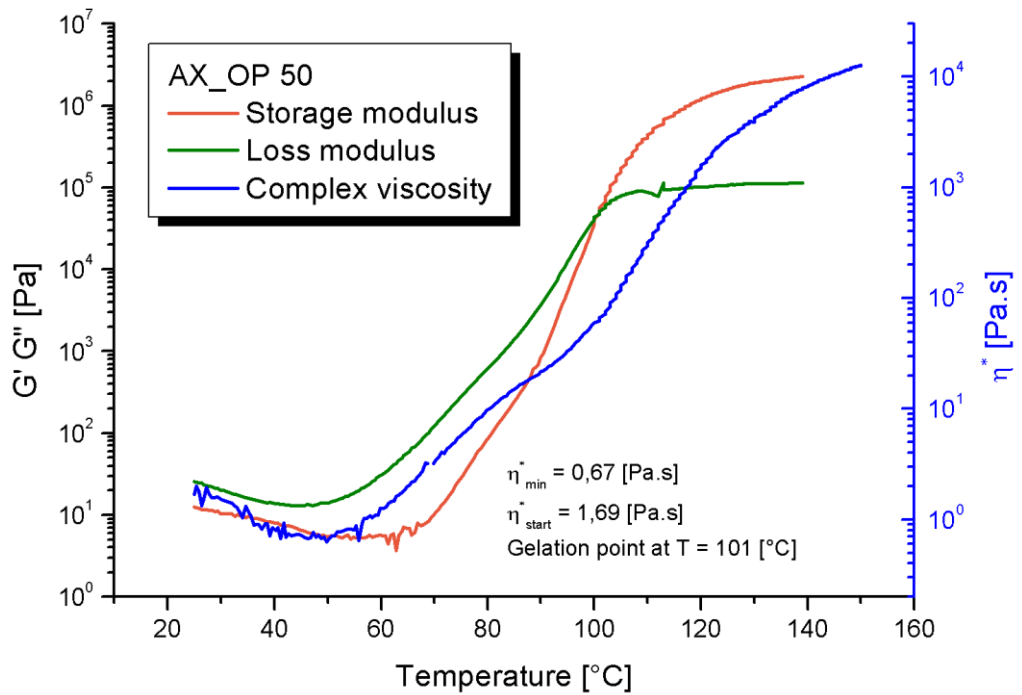


Fig. 52: Record of the temperature sweep measurement on the sample AX_OP 50

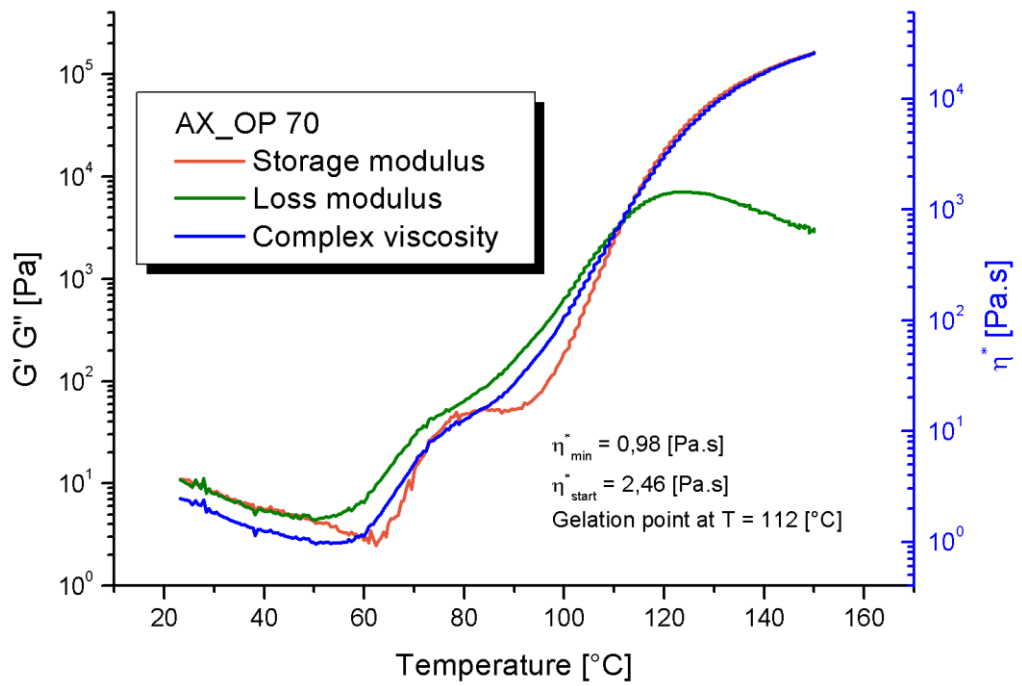


Fig. 53: Record of the temperature sweep measurement on the sample AX_OP 70

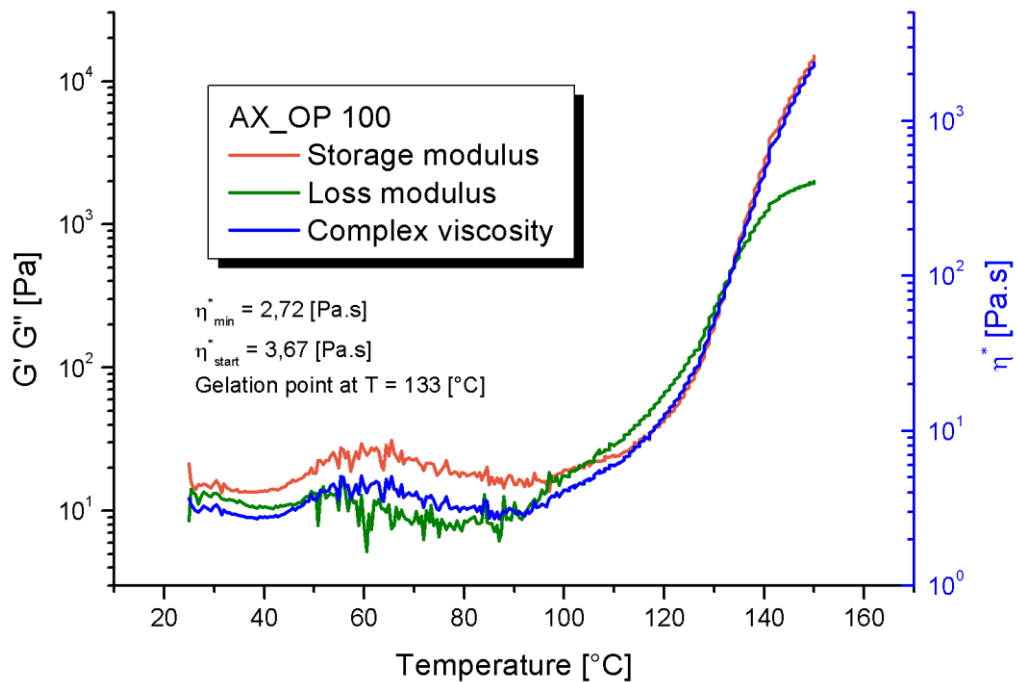


Fig. 54: Record of the temperature sweep measurement on the sample AX_OP 100

From data in Tab. 8 and Figs. (49-54) can be seen that, the replacement of AX 437 by OP 560 lowers the starting viscosity and minimal viscosity. Sample AX_OP 30 does not fall into this trend (see fig. 51). This might be caused by difficulties in measuring storage modulus at the beginning of the measurement. Complex viscosity and temperature of gelation is decreased to the point of 50 % replacement of AX 437 by OP 560 (see fig. 50). For AX_OP 70 (see fig. 53) the starting η^* is higher than in neat AX_IFR 0, but the minimal η^* is still lower. Temperature of gelation is increased to 112 [°C]. For AX_IFR 100 (see fig. 54) all viscosities are higher, especially the minimal η^* is doubled (2,72 [Pa.s]). Gelation point reached point of 133 [°C].

Tab. 8: All measured values of η_{start}^* , η_{min}^* and T_{sg}

| Sample | η_{start}^* [Pa.s] | η_{min}^* [Pa.s] | T_{sg} [°C] |
|-----------|-------------------------|-----------------------|---------------|
| AX_IFR 0 | 2,34 | 1,34 | 106 |
| AX_IFR 10 | 4,29 | 1,16 | 104 |
| AX_IFR 20 | 2,41 | 1,35 | 107 |
| AX_IFR 30 | 4,54 | 2,27 | 101 |
| AX_IFR 50 | 6,97 | 5,04 | 99 |

| | | | |
|------------------|------|------|-----|
| AX_IFR 70 | 9,97 | 7,27 | 98 |
| AX_OP 10 | 1,63 | 0,87 | 107 |
| AX_OP 20 | 1,20 | 0,58 | 102 |
| AX_OP 30 | 2,29 | 1,33 | 106 |
| AX_OP 50 | 1,69 | 0,67 | 101 |
| AX_OP 70 | 2,46 | 0,98 | 112 |
| AX_OP 100 | 3,67 | 2,72 | 133 |

7.3 DSC

Tab. 9: Measured change of enthalpy and peak characterizing temperatures

| Sample | Weight [mg] | ΔH [mJ] | $\Delta H_{\text{normalized}}$ [J/g] | T_{onset} [°C] | T_{peak} [°C] | T_{endset} [°C] |
|------------------|--------------------|-----------------------------------|--|---|--|--|
| AX_IFR 0 | 5,23 | 1167 | 223 | 31 | 57 | 94 |
| AX_IFR 10 | 6,31 | 1557 | 247 | 32 | 57 | 115 |
| AX_IFR 30 | 3,13 | 611 | 191 | 28 | 55 | 135 |
| AX_IFR 50 | 3,57 | 858 | 240 | 25 | 58 | 134 |
| AX_IFR 70 | 3,18 | 722 | 227 | 25 | 89 | 133 |
| Sample | Weight [mg] | ΔH [mJ] | $\Delta H_{\text{normalized}}$ [J/g] | T_{onset} [°C] | T_{peak} [°C] | T_{endset} [°C] |
| AX_OP 10 | 2,66 | 776 | 292 | 30 | 59 | 122 |
| AX_OP 20 | 7,03 | 1032 | 147 | 35 | 63 | 106 |
| AX_OP 30 | 3,40 | 1194 | 351 | 33 | 65 | 122 |
| AX_OP 50 | 5,12 | 1146 | 224 | 30 | 74 | 127 |
| AX_OP 70 | 6,35 | 2520 | 397 | 35 | 76 | 125 |
| AX_OP 100 | 6,44 | 1186 | 184 | 29 | 84 | 124 |

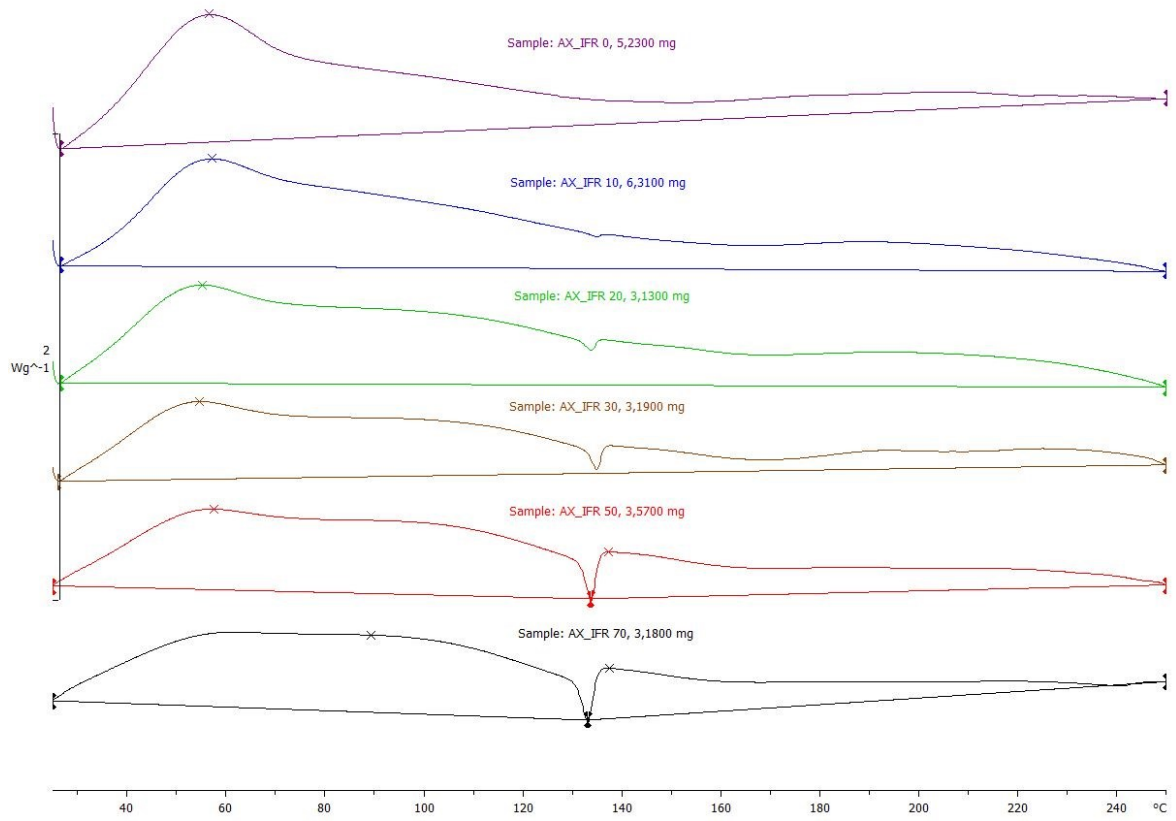


Fig. 55: DSC measurement curves for AX_IFR set of samples

From the Fig. 55 and Tab. 9 it is evident, that increasing concentration of Exolit IFR 36 lowers the onset temperature of curing reaction. Peak and endset temperature is increased and that can be seen from the Figure 55 too, as the peak broadens and shifts towards higher temperatures. Normalized change of enthalpy ΔH does change only marginally and stays in the same range of 191 – 247 [J/g]. Interesting is the signal of endothermic reaction that increases in its intensity as the concentrations increasing. This signal is presumably caused by melting of the organic Exolit IFR 36 additive, which is in a crystalline form. Additionally, this signal might influence the endset temperatures of measurement.

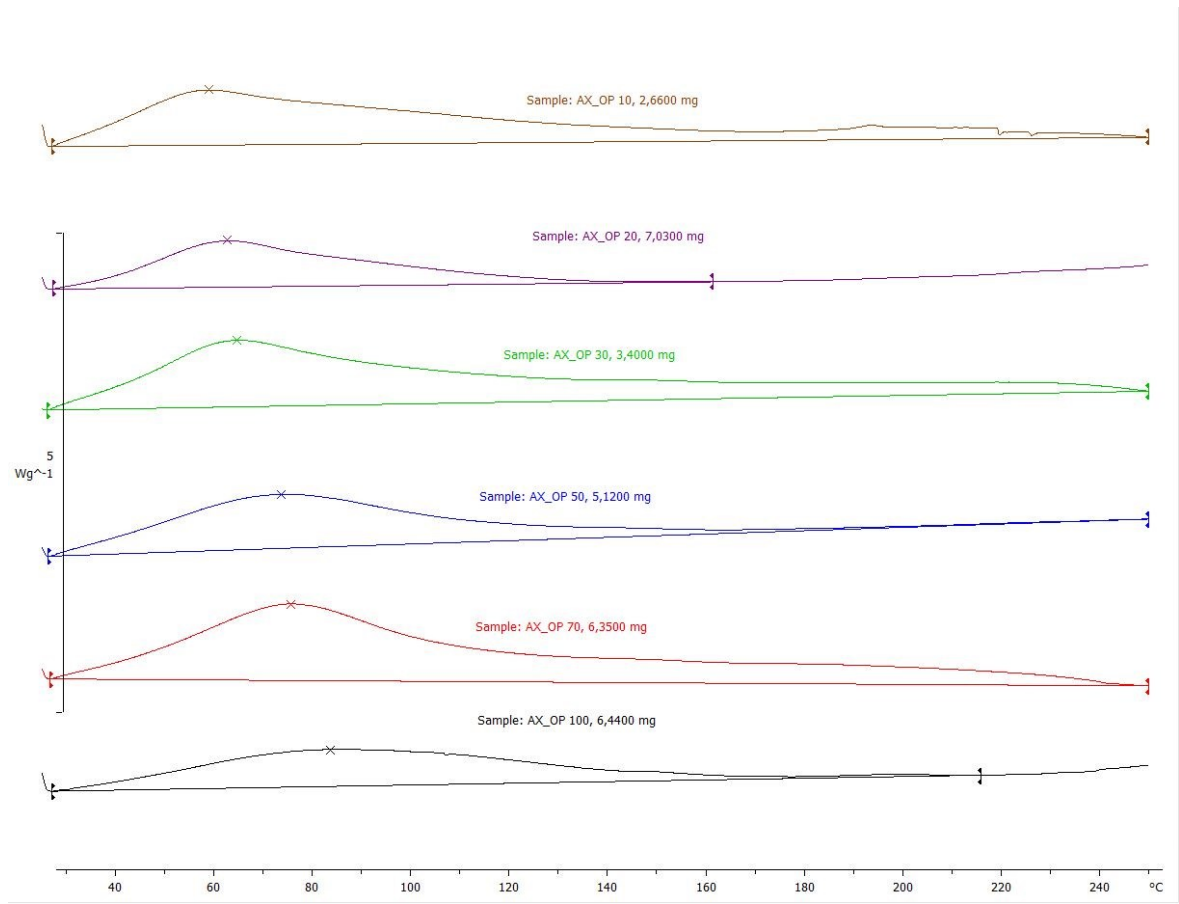


Fig. 56: DSC measurement curves for AX_OP set of samples

From data in Tab. 9 and from Figure 56, a change of peak temperature is clearly seen. As the amount of OP 560 increases and replaces AX 437, T_{peak} is increasing from 59 [°C] in AX_OP 10 to 84 [°C] in AX_OP 100. Onset and endset temperature does not change significantly, only AX_OP 20 appears to be out of trend in terms of these temperatures and normalized change of enthalpy.

7.4 DMA

In order to investigate the impact of the various additives on the mechanical properties, the dynamic mechanical analysis was performed. All samples have relatively similar performance at room temperature, while with the temperature increase the behaviour is miscellaneous. As can be seen in the Fig. 57, the lowest mechanical performance was obtained for neat PUR matrix (AX_IFR 0). Interestingly, the highest mechanical performance was obtained for sample containing only 10 DSK of Exolit IFR 36 additive and with further increasing content the mechanical performance, due to the most probably worse additive dis-

pergation, significantly decreased. The worse dispergation results in the bigger agglomerates those acting as a stress concentrators and thus the considerable disintegration of the prepared samples was achieved. If we also consider, that glass transition temperature can be evaluated as a inflex point of the dependence of storage modulus on the temperature, the highest glass transition was observed for sample AX_IFR 10 while neat PUR matrix (AX_IFR 0) and AX_IFR 70 show the lowest ones

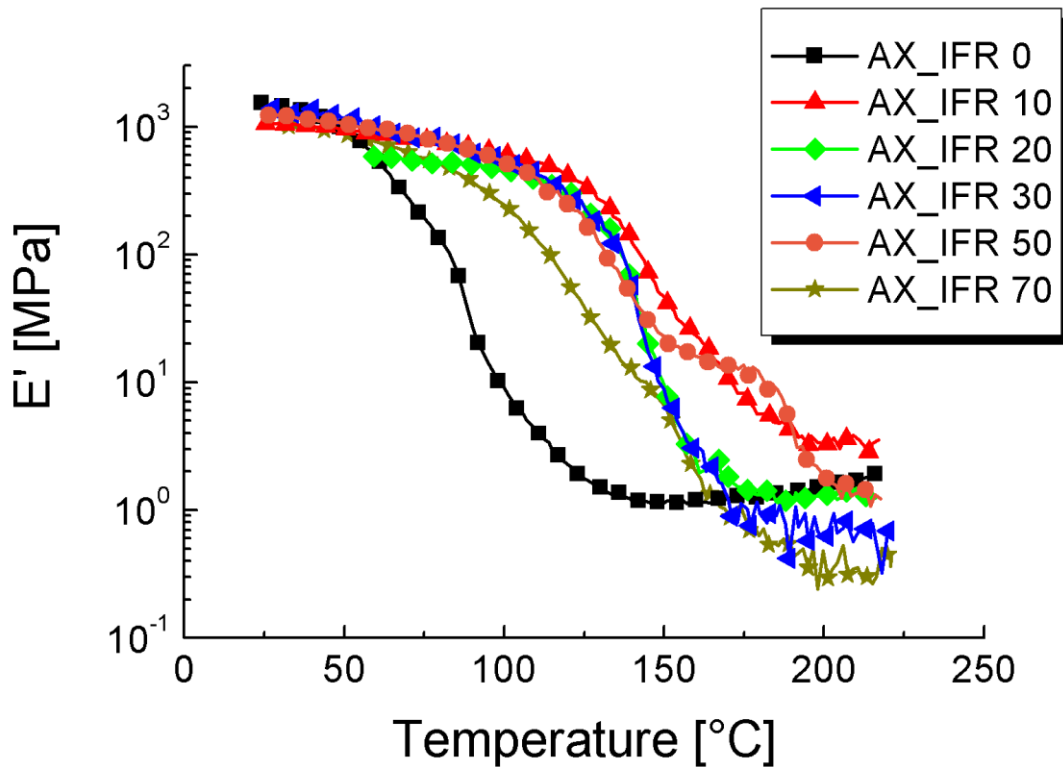


Fig. 57: Dependence of the storage modulus on the temperature for various samples containing Exolit IFR 36 additive.

Very similar behaviour was observed also in the case of samples containing the Exolit OP 560 liquid additive (Fig. 58). In this case, even at room temperature there are significant differences between the prepared samples. The best performance can be seen for neat PUR matrix, however, with increased temperature the PUR matrix loosen its performance very quickly. Also in this case the 10 % of additive OP 560 lead to best mechanical performance, however lower than for 10 DSK of IFR 36. Further increase of additive content just causes the significant decrease in mechanical performance and sample AX_OP 100 shows the worst properties from all investigated samples. The glass transition temperature following the storage modulus results similarly as in the previous case of IFR 36 additive.

Therefore, can be concluded, that utilization of various additives can provide tunability of the mechanical properties and also certain reinforcement, especially at elevated temperatures and when balanced composition of the final system will be achieved.

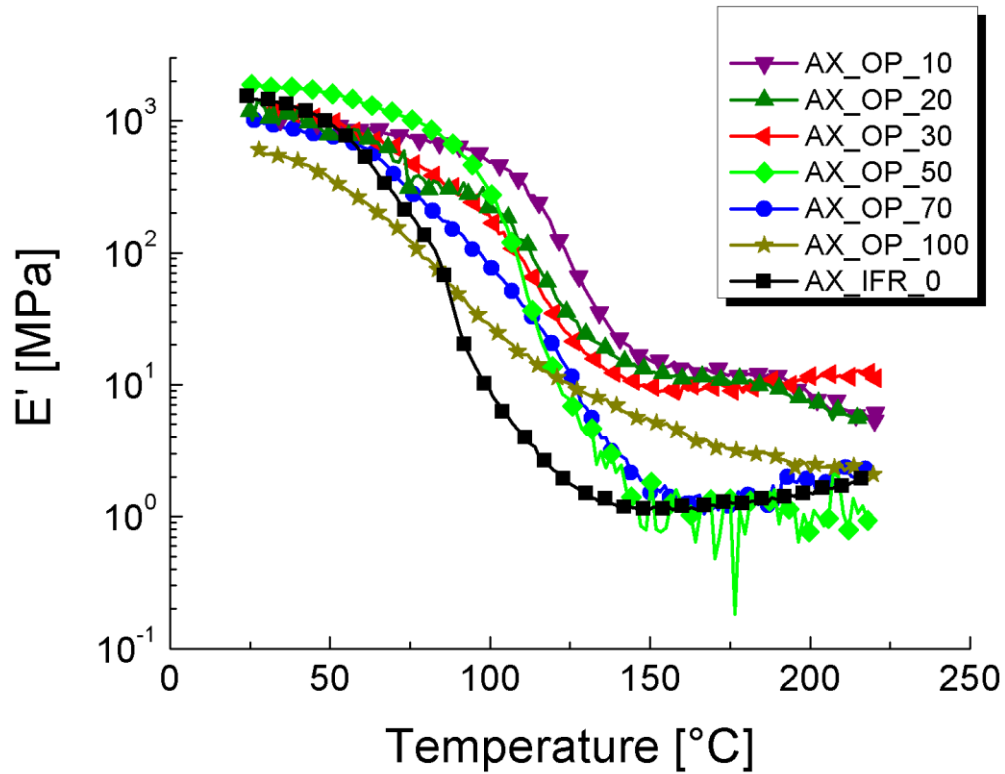


Fig.58: Dependence of the storage modulus on the temperature for various samples containing Exolit OP 560 polyol liquid additive.

7.5 Cone calorimeter

Tab. 10: Important numeric results of cone calorimeter measurement

| Sample | IFR 36 [wt%] | TTI [s] | MARHE [kW/m ²] | mean SEA [m ² /kg] | TSP [m ²] | mean MLR [g/s] | TSF [s] |
|-----------|--------------|---------|----------------------------|-------------------------------|-----------------------|----------------|---------|
| AX_IFR 0 | 0 | 16 | 373,51 | 567,96 | 27,6 | 0,0956 | 509 |
| AX_IFR 10 | 9 | 33 | 240,99 | 470,15 | 25,0 | 0,0671 | 787 |
| AX_IFR 20 | 17 | 23 | 274,92 | 656,87 | 39,0 | 0,1139 | 687 |
| AX_IFR 30 | 23 | 27 | 229,72 | 637,29 | 36,7 | 0,0767 | 753 |
| AX_IFR 50 | 33 | 26 | 191,33 | 647,27 | 33,7 | 0,0714 | 729 |
| AX_IFR 70 | 41 | 29 | 197,08 | 557,28 | 29,9 | 0,0670 | 801 |
| Sample | OP 560 [wt%] | TTI [s] | MARHE [kW/m ²] | mean SEA [m ² /kg] | TSP [m ²] | mean MLR [g/s] | TSF [s] |
| AX_OP 10 | 5 | 23 | 334,42 | 702,00 | 40,3 | 0,0878 | 652 |
| AX_OP 20 | 9 | 21 | 345,93 | 826,99 | 44,4 | 0,0734 | 729 |

| | | | | | | | |
|-----------|----|----|--------|--------|------|--------|-----|
| AX_OP 30 | 14 | 23 | 322,99 | 842,21 | 48,1 | 0,1083 | 527 |
| AX_OP 50 | 23 | 21 | 295,29 | 830,11 | 48,8 | 0,1137 | 519 |
| AX_OP 70 | 32 | 22 | 320,21 | 767,57 | 45,0 | 0,1194 | 493 |
| AX_OP 100 | 46 | 29 | 397,63 | 39,80 | 38,3 | 3,5572 | 361 |

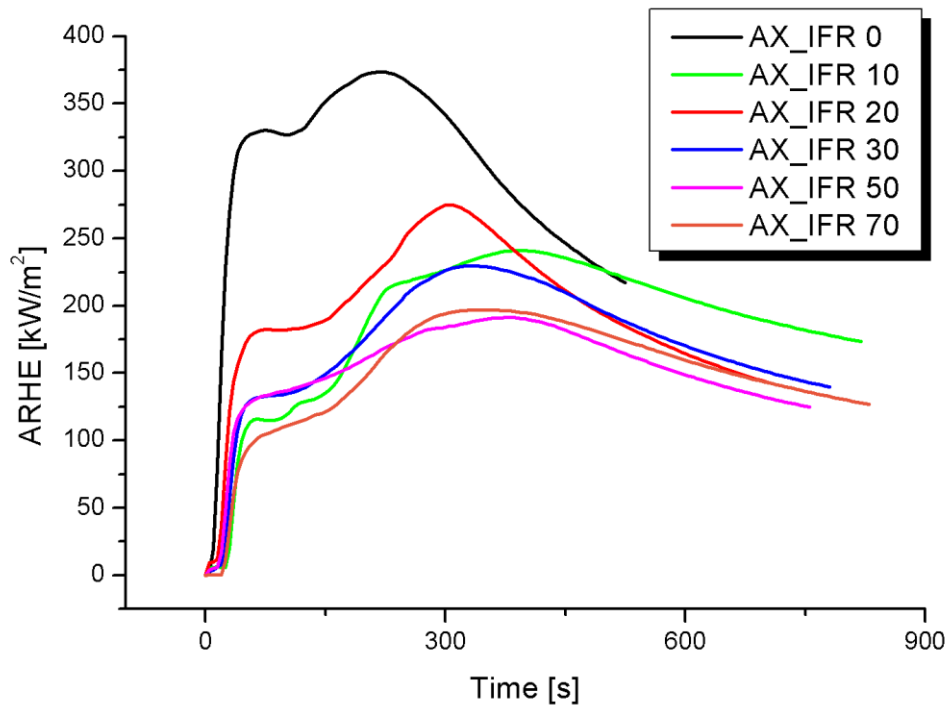


Fig. 59: Average heat release rate in time for AX_IFR set of samples

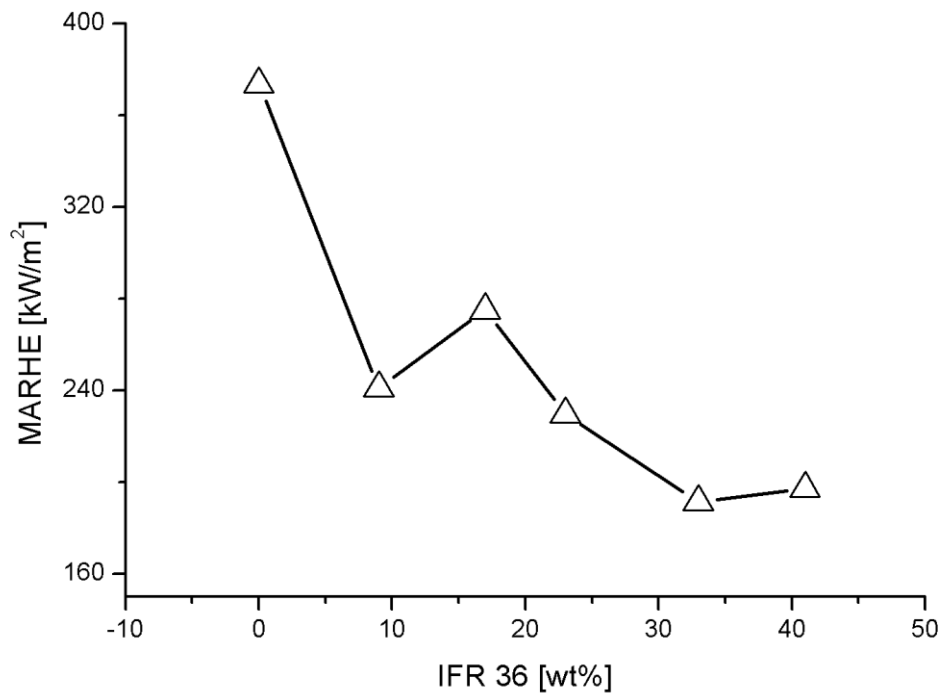


Fig. 60: MARHE values for increasing amount of IFR 36 in matrix

From the numerical and graphical results (see Tab. 10 and Fig. 59), it is evident, that the flammability of the samples reduces with addition of Exolit IFR 36. With very high filling of IFR 36, the MARHE value was lowered by 50% and in the case of all filled samples, the peak shifted right towards the longer time (see Fig. 59). The heat release is diminishing, even though the AX_IFR 20 has MARHE value out of the trend (see Fig. 60). From the heat release point of view, the AX_IFR 10 from its set did not have the lowest MARHE value but the difference from AX_IFR 70 is only about 50 kW/m².

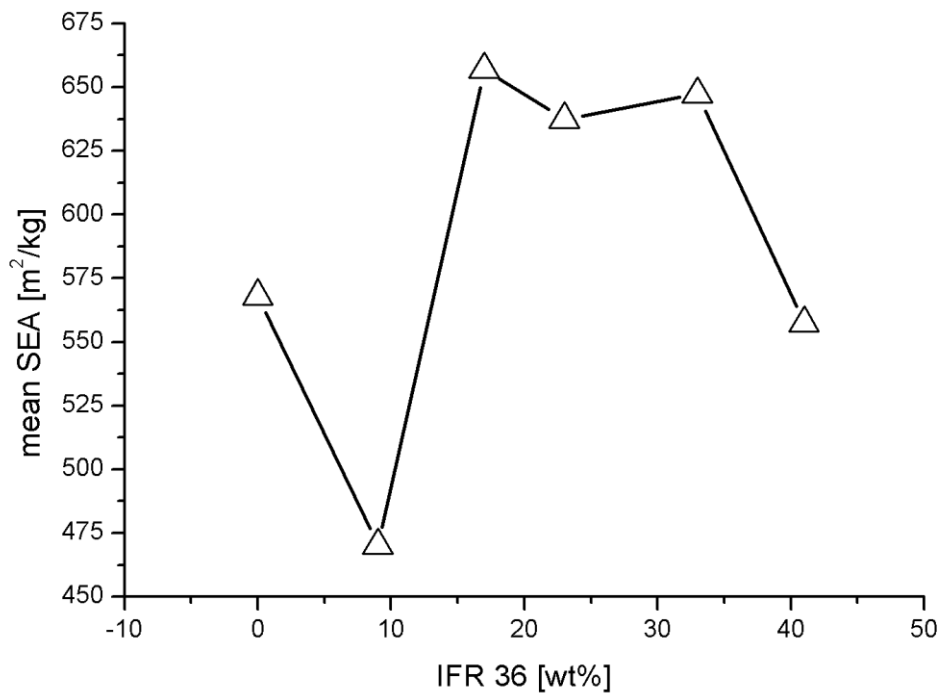


Fig. 61: mean SEA measured for AX_IFR sample set

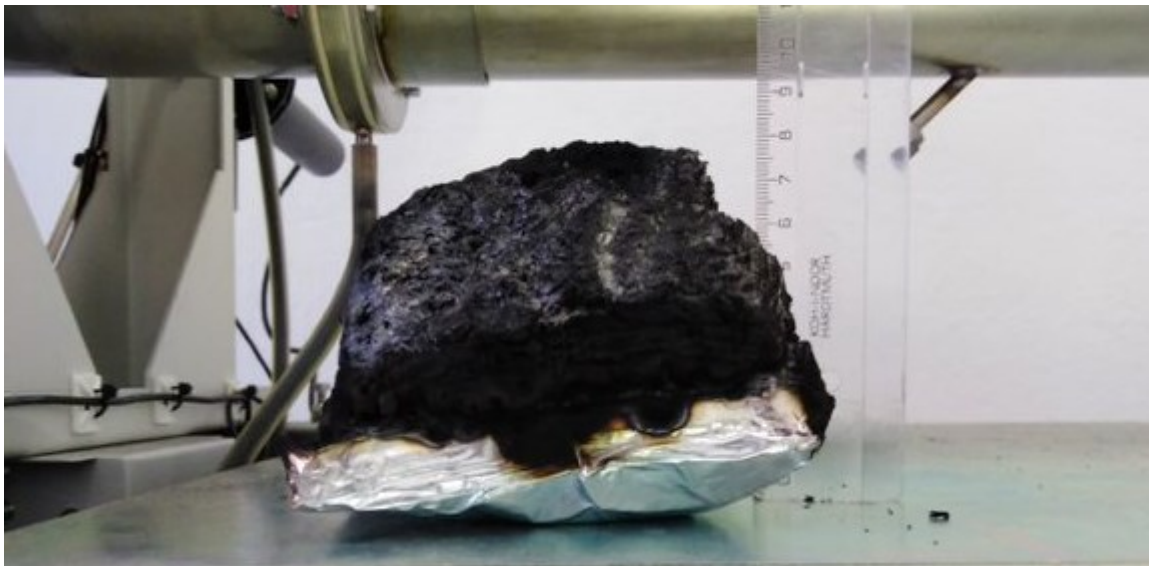


Fig. 62: Remains of sample AX_IFR 10

Important is the aspect of the intumescence, as the AX_IFR 10 was the only sample that managed to perform its intumescent effect as it was supposed to. This was caused mainly due to the proper additive dispersion as was already confirmed from mechanical investigation. The sample has grown up around 7,5 cm (see Fig. 62) while other samples charred but did not grow. This has an important impact on the value of SEA, which characterizes the smokiness

of the sample. AX_IFR 10 had the lowest value of mean SEA (470,15 m²/kg) from the whole Samples AX_IFR 20, 30, 50 have highest SEA values, even preceding the neat AX_IFR 0 (see Tab. 10 and Fig. 61). The AX_IFR 70 has value of SEA in the same range as before mentioned AX_IFR 0. This might be the result of less matrix content in the sample compared to the previous samples.

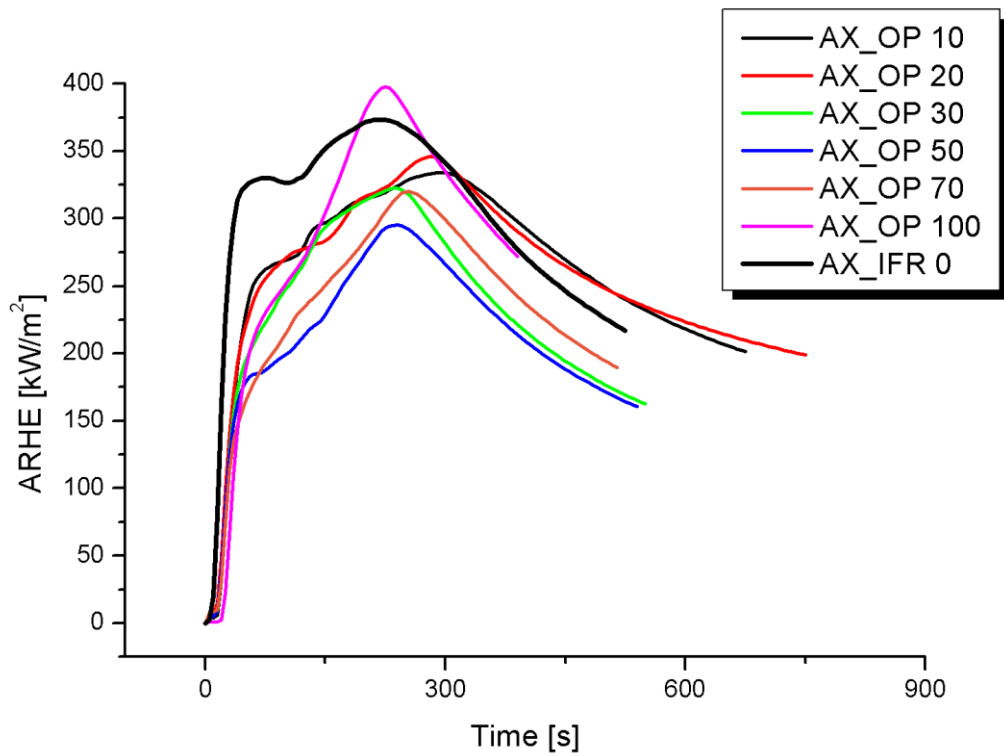


Fig. 63: ARHE in time for AX_OP sample set with AX_IFR 0 for reference.

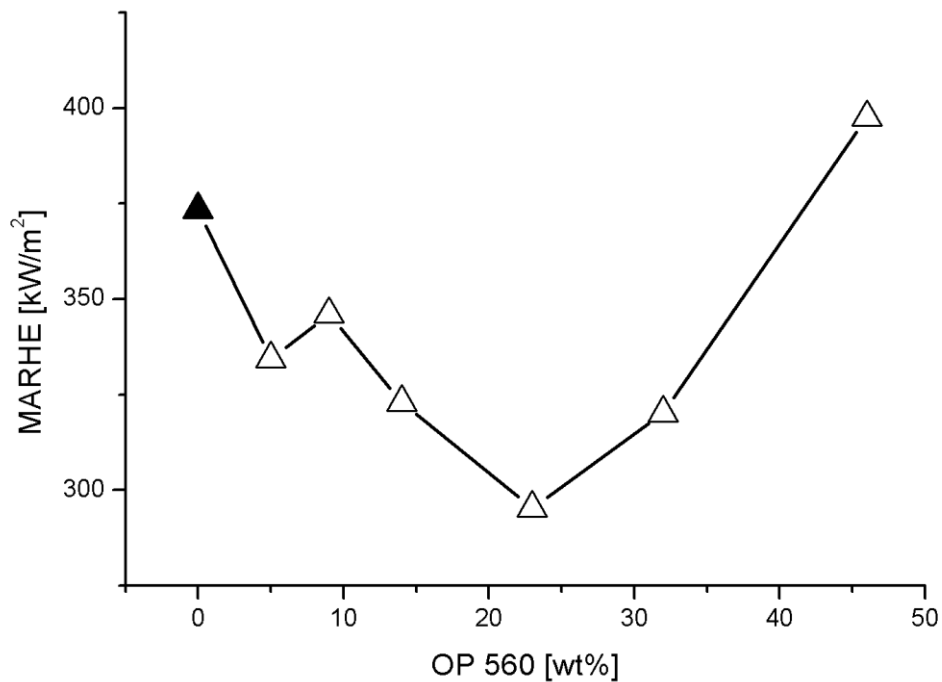


Fig. 64: MARHE values for increasing amount of OP 560. Black point represents AX_IFR 0 for reference

The results of ARHE for AX_OP set of samples show that compared to the neat AX_IFR 0, all samples but one are reducing the released heat and also shift the peak towards the higher time (see Fig. 63). AX_OP 100 scored higher value in MARHE than AX_IFR 0. From heat release point of view, the AX_OP 50 has the lowest MARHE value of this set. Smaller concentrations of OP 560 are not as sufficient and higher concentrations have opposing effect of raising this value (see Fig. 64). Therefore, only the optimized amount of the flame retardant is efficient enough to provide the enhanced flammability resistance.

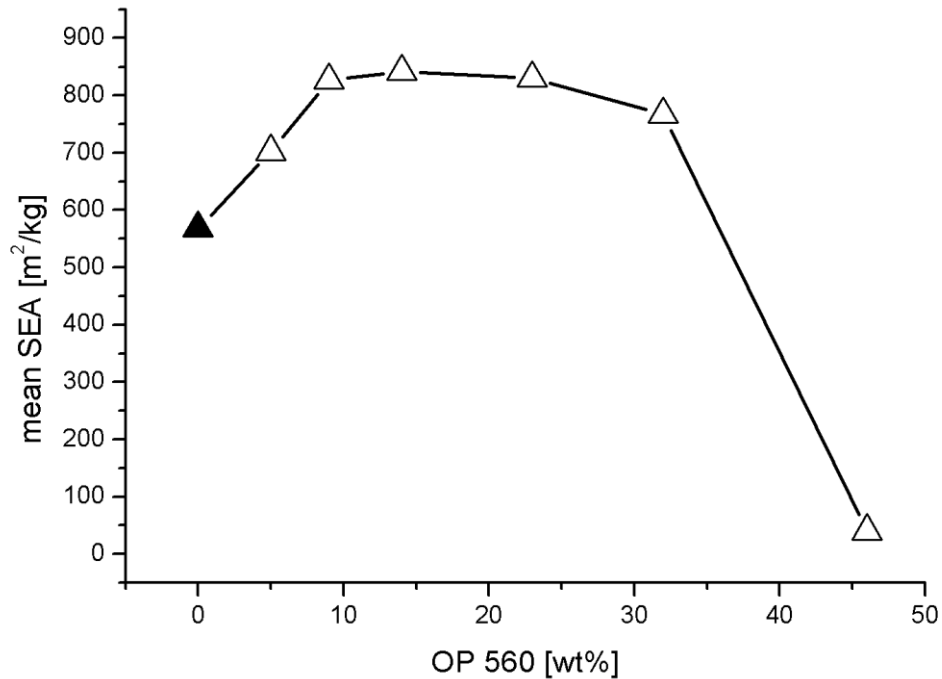


Fig. 65: mean SEA measured for AX_OP sample set with black point representing AX_IFR 0

From SEA evaluation, results for AX_OP 100 are misleading (see Tab. 10 and Fig. 65), because during the measurement, the combustion reaction did become violent to a point where the measurement had to be terminated by lowering the sample from the cone heater. This sample released high amounts of smoke that did not flow into exhaust system but into laboratory. This result is not to be taken into account. The other samples are “smokier” than the neat AX_IFR 0 too and in terms of smoke suppression, they did not prove to be sufficient in any concentration. All samples from this set did expand, on the Fig. 66 remains of the sample AX_OP 50 are shown.

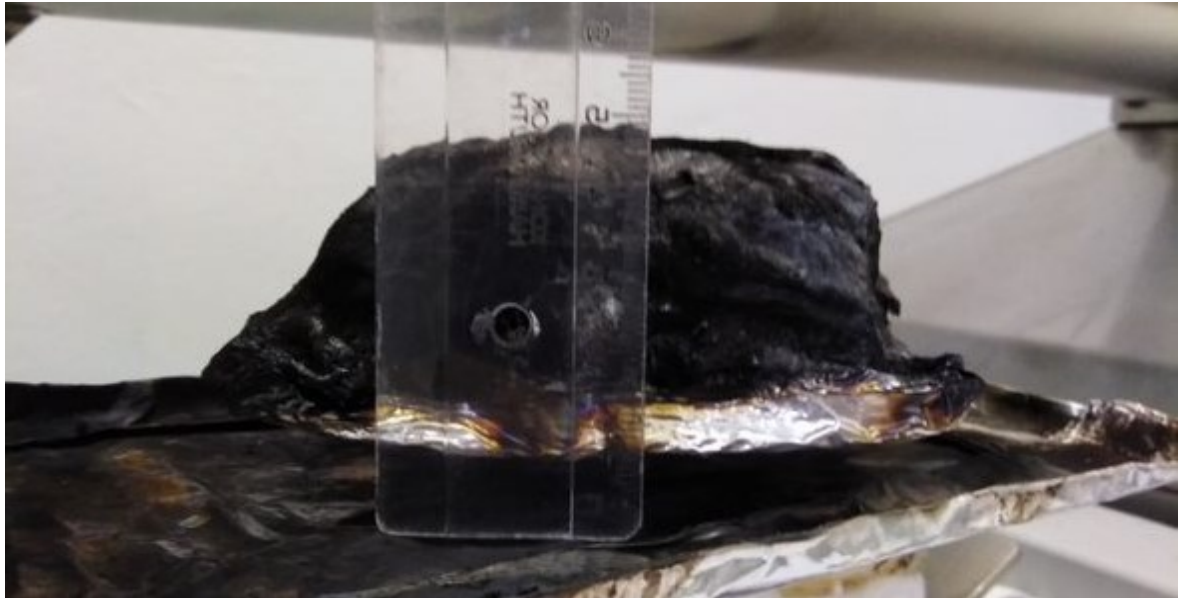


Fig. 66: Remains of AX_OP 50

In regards to the time of sustained flaming (see Tab. 10), from the set of AX_IFR, the AX_IFR 10 achieved the longest time of burning almost 5 minutes longer than AX_IFR 0. From the set of AX_OP, the AX_OP 10 achieved the longest combustion in 729s, which is almost 4 minutes more than AX_IFR 0. The worst result is achieved by AX_OP 100, whole process of burning took only 6 minutes, that is around 2 minutes and 30 seconds less than neat AX_IFR 0.

7.6 UL94

Tab. 11: Recorded times and events from UL94 test for AX_IFR set. With classification.

| Sample | AX_IFR 0 | | | | | AX_IFR 10 | | | | | AX_IFR 20 | | | | |
|---|-----------------------|-----|-----|-----|-----|-----------|----|----|----|----|-----------|----|----|----|----|
| | 1 | 2 | 3 | 4 | 5 | 1 | 2 | 3 | 4 | 5 | 1 | 2 | 3 | 4 | 5 |
| t ₁ | 72 | 75 | 71 | 73 | 71 | 5 | 7 | 6 | 6 | 5 | 0 | 1 | 0 | 1 | 0 |
| t ₂ | 37 | 39 | 36 | 38 | 37 | 3 | 4 | 6 | 5 | 5 | 1 | 0 | 0 | 1 | 1 |
| t ₃ | 8 | 5 | 6 | 8 | 6 | 3 | 1 | 1 | 2 | 1 | 1 | 3 | 1 | 2 | 1 |
| t ₁ + t ₂ whole set | 549 | | | | | 52 | | | | | 5 | | | | |
| t ₂ +t ₃ | 45 | 44 | 42 | 46 | 43 | 6 | 5 | 7 | 7 | 6 | 2 | 3 | 1 | 3 | 2 |
| Fire at clamping point | yes | yes | yes | yes | yes | no | no | no | no | no | no | no | no | no | no |
| Wool fire | no | no | no | no | no | no | no | no | no | no | no | no | no | no | no |
| Classification | Out of classification | | | | | V-1 | | | | | V-0 | | | | |
| Sample | AX_IFR 30 | | | | | AX_IFR 50 | | | | | AX_IFR 70 | | | | |
| | 1 | 2 | 3 | 4 | 5 | 1 | 2 | 3 | 4 | 5 | 1 | 2 | 3 | 4 | 5 |
| t ₁ | 0 | 0 | 0 | 0 | 0 | 0 | 0 | 0 | 0 | 0 | 0 | 0 | 0 | 0 | 0 |

| | | | | | | | | | | | | | | | |
|--|-----|----|----|----|----|-----|----|----|----|----|-----|----|----|----|----|
| t₂ | 1 | 1 | 0 | 2 | 1 | 1 | 0 | 0 | 1 | 0 | 0 | 1 | 0 | 0 | 0 |
| t₃ | 1 | 2 | 1 | 2 | 2 | 1 | 2 | 1 | 0 | 1 | 0 | 0 | 1 | 1 | 0 |
| t₁ + t₂ whole set | 5 | | | | | 2 | | | | | 1 | | | | |
| t₂+t₃ | 2 | 3 | 1 | 4 | 3 | 2 | 2 | 1 | 1 | 1 | 0 | 1 | 1 | 1 | 0 |
| Flame at clamping point | no | no | no | no | no | no | no | no | no | no | no | no | no | no | no |
| Wool fire | no | no | no | no | no | no | no | no | no | no | no | no | no | no | no |
| Classification | V-0 | | | | | V-0 | | | | | V-0 | | | | |

Tab. 12: Recorded times and events from UL94 test for AX_OP set. With classification.

| Sample | AX_OP 10 | | | | | AX_OP 20 | | | | | AX_OP 30 | | | | |
|--|-----------------------|----|----|----|----|----------|----|----|----|----|-----------|----|----|----|----|
| | 1 | 2 | 3 | 4 | 5 | 1 | 2 | 3 | 4 | 5 | 1 | 2 | 3 | 4 | 5 |
| t₁ | 46 | 44 | 42 | 42 | 44 | 5 | 5 | 4 | 5 | 4 | 4 | 3 | 3 | 3 | 3 |
| t₂ | 25 | 21 | 25 | 23 | 21 | 4 | 6 | 4 | 4 | 4 | 0 | 2 | 0 | 1 | 2 |
| t₃ | 4 | 3 | 4 | 3 | 4 | 2 | 3 | 3 | 3 | 4 | 2 | 1 | 2 | 1 | 1 |
| t₁ + t₂ whole set | 333 | | | | | 45 | | | | | 21 | | | | |
| t₂+t₃ | 29 | 24 | 29 | 26 | 25 | 6 | 9 | 7 | 7 | 8 | 2 | 3 | 2 | 2 | 3 |
| Flame at clamping point | no | no | no | no | no | no | no | no | no | no | no | no | no | no | no |
| Wool fire | no | no | no | no | no | no | no | no | no | no | no | no | no | no | no |
| Classification | Out of classification | | | | | V-0 | | | | | V-0 | | | | |
| Sample | AX_OP 50 | | | | | AX_OP 70 | | | | | AX_OP 100 | | | | |
| | 1 | 2 | 3 | 4 | 5 | 1 | 2 | 3 | 4 | 5 | 1 | 2 | 3 | 4 | 5 |
| t₁ | 0 | 1 | 1 | 0 | 1 | 0 | 0 | 0 | 0 | 0 | 0 | 0 | 0 | 0 | 0 |
| t₂ | 1 | 1 | 1 | 1 | 1 | 0 | 0 | 0 | 0 | 0 | 2 | 1 | 2 | 1 | 1 |
| t₃ | 2 | 3 | 2 | 2 | 1 | 1 | 2 | 1 | 2 | 0 | 2 | 3 | 1 | 1 | 1 |
| t₁ + t₂ whole set | 8 | | | | | 0 | | | | | 7 | | | | |
| t₂+t₃ | 3 | 4 | 3 | 3 | 2 | 1 | 2 | 1 | 2 | 0 | 4 | 4 | 3 | 2 | 2 |
| Flame at clamping point | no | no | no | no | no | no | no | no | no | no | no | no | no | no | no |
| Wool fire | no | no | no | no | no | no | no | no | no | no | no | no | no | no | no |
| Classification | V-0 | | | | | V-0 | | | | | V-0 | | | | |

In the case of the UL94 test of flammability majority of samples from both sets achieved the best rating V-0 (see Tab. 11 and Tab. 12). These samples attenuated and stopped their flaming right away or in a few seconds after removing the flame source. Smouldering combustion was quenched also right away or after a few seconds. Neat PUR matrix (AX_IFR 0) and AX_OP 10 did not passed classification in UL94. Flames burning the AX_IFR 0 climbed up to the clamping point, which renders not possible for any classification in UL94 vertical

ratings and also the time of combustions were too long. AX_OP 10 did not pass solely because of the long combustion times. Another sample that did not pass for the perfect score was AX_IFR 10, this sample missed the V-0 classification by 2 seconds and falls into the second category, V-1.

CONCLUSION

In this thesis, two sets of six samples of Polyurethane matrix filled with additive intumescent flame retardant Exolit IFR 36 and reactive flame retardant polyol Exolit OP 560 were prepared. Basic characterization of the samples was done with FTIR spectroscopy to show that increase amount of the individual additives in the proposed formulations are in good correlation with increasing intensity of the specific absorption bands for flame retardant additives in the presented spectra.

From rotational rheometry results it can be assumed that the increasing amount of Exolit IFR 36 raises the starting and minimal complex viscosity η^*_{\min} . The most significant impact on processability is occurring from loading of 30 DSK (23 wt%) and above, in term of viscosity and sol – gel transformation temperature. Therefore, the suitable additive concentration for processing is 10 and 20 DSK. In set of AX_OP samples have relatively small $\eta^*_{\min} = 0,58 - 1,33$ Pa·s. The only difference is with AX_OP 100, that has $\eta^*_{\min} = 2,72$ Pa·s. The rest of the samples from this set show promising values from the processability point of view.

Comparative characterisation method for reaction kinetics was DSC in which the impact of the additive on kinetics of the curing reaction was investigated. It was found out, that the change of enthalpy $\Delta H_{\text{normalized}}$ has maximum difference of 14 % (for AX_IFR 30) in relation to neat PUR matrix AX_IFR 0. Onset temperatures T_{onset} did decrease with more concentration of IFR 36. T_{peak} increased only for the AX_IFR 70. Endset temperature has increased from 94 °C to 133 °C. This information might be misleading, because this value is affected by the melting peak that occurred around 130 °C in all samples filled with IFR 36. Signal of this peak increases with the concentration of IFR 36 in samples. Presumably this signal is a consequence of crystalline form of ammonium polyphosphate on which this intumescent flame retardant is based on.

For set of AX_OP samples the changes in $\Delta H_{\text{normalized}}$ are more evident, but there is no significant trend in measured data. The most affected property is T_{peak} that increased with addition of OP 560, which can be a consequence of addition of liquid polyol additive.

To evaluate mechanical properties of fabricated material, the DMA was used. In set of AX_IFR samples, the worst mechanical performance was obtained by neat PUR matrix AX_IFR 0, while the best ones were found for AX_IFR 10 and a trend that shows that the increasing amount of IFR 36 significantly influencing the mechanical properties, due to the presence of the high additive content and most probably bad additive dispergation. AX_OP

set shows that even at the room temperature, the samples have different behaviour, and these differences are even pronounced at elevated temperatures. The sample AX_OP 10 shows the best mechanical performance from this set. Just as in previous case, further addition of OP 560 decreases the mechanical properties of matrix, most probably due to the poor incorporation of the liquid polyol. Therefore can be concluded that possible tunability of mechanical performance with utilizing both IFR 36 and OP 560 can be achieved.

In cone calorimetry measurement of heat release, the best result belongs to the AX_IFR 10 from set of IFR 36 filled PUR matrix. Only this sample shows significant intumescent effect, has longest TTI and therefore best resistivity to fire, mean MLR is lowest in this set just as mean SEA. MARHE value is not the lowest but in comparison to the lowest value obtained by AX_IFR 70 the difference is marginal.

In AX_OP set, the MARHE result is best for the AX_OP 50. Trend shows that the MARHE value decreases right to this amount of used OP 560, further addition increases this value. Intumescent effect in these samples was present but not significant. Mean SEA values are high, exceeding even the neat AX_IFR 0. Time of sustained flaming for samples in this set is smaller than for those from set of AX_IFR.

The last characterisation of material was done by the standard UL 94 method. In this test two samples, AX_IFR 0 and AX_OP 10 did not achieve any classification. One sample AX_IFR 10 obtained V-1 classification, and the rest of the samples obtained V-0 classification.

BIBLIOGRAPHY

- [1] CAVACO, Luís Inácio. *Polyurethane: Properties, Structure and Applications*. B.m.: Nova Science Publishers, 2012. ISBN 978-1-61942-453-1.
- [2] CSN EN 45545-2:2013. *Drážní aplikace - Protipožární ochrana drážních vozidel - Část 2: Požadavky na požární vlastnosti materiálů a součástí*. Praha: Úřad pro technickou normalizaci, metrologii a státní zkušebnictví, 2014.
- [3] PRISACARIU, Cristina. *Polyurethane Elastomers: From Morphology to Mechanical Aspects* [online]. Wien: Springer-Verlag, 2011 [vid. 2019-02-11]. ISBN 978-3-7091-0513-9.
- [4] PASCAULT, Jean-Pierre; Sautereau. *Thermosetting polymers: Plastics engineering*. Hoboken: Marcel Dekker Inc, 2002. ISBN 978-0-8247-4405-2.
- [5] STOKLASA. *Makrololekulární chemie*. Skripta Univerzita Tomáše Bati. Zlín, 2005.
- [6] SONNENSCHNEIN, Mark F. *Polyurethanes: Science, Technology, Markets, and Trends*. B.m.: John Wiley & Sons, 2014. ISBN 978-1-118-73783-5.
- [7] SZYCHER, Michael. *Szycher's Handbook of Polyurethanes*. B.m.: CRC Press, 2012. ISBN 978-1-4398-6313-8.
- [8] SARDON, Haritz, Ana PASCUAL, David MECERREYES, Daniel TATON, Henri CRAMAIL a James L. HEDRICK. Synthesis of Polyurethanes Using Organocatalysis: A Perspective. *Macromolecules* [online]. 2015, **48**(10), 3153–3165.
- [9] O'SICKEY, Matthew J. Characterization of Structure-Property Relationships of Poly(urethane-urea)s for Fiber Applications [online]. 2002 [vid. 2019-03-25].
- [10] THOMAS, Sabu, Janusz DATTA, Jozef HAPONIUK a Arunima REGHUNADHAN. *Polyurethane Polymers: Composites and Nanocomposites*. B.m.: Elsevier Science, 2017. ISBN 978-0-12-804065-2.
- [11] LI, Wu, Anthony J. RYAN a Ingrid K. MEIER. Morphology Development via Reaction-Induced Phase Separation in Flexible Polyurethane Foam. *Macromolecules* [online]. 2002, **35**(13), 5034–5042.
- [12] PAPASPYRIDES, Constantine D. a Pantelis KILIARIS. *Polymer Green Flame Retardants*. B.m.: Newnes, 2014. ISBN 978-0-444-53809-3.

- [13] LAOUTID, F., L. BONNAUD, M. ALEXANDRE, J. -M. LOPEZ-CUESTA a Ph. DUBOIS. New prospects in flame retardant polymer materials: From fundamentals to nano-composites. *Materials Science and Engineering: R: Reports* [online]. 2009, **63**(3), 100–125.
- [14] WEIL, Edward D. a Sergei V. LEVCHIK. *Flame Retardants for Plastics and Textiles: Practical Applications*. B.m.: Hanser, 2009. ISBN 978-3-446-41652-9.
- [15] LIU, Lei a Zhengzhou WANG. Synergistic effect of nano magnesium amino-tris-(methylenephosphonate) and expandable graphite on improving flame retardant, mechanical and thermal insulating properties of rigid polyurethane foam. *Materials Chemistry and Physics* [online]. 2018, **219**, 318–327.
- [16] LU, Hongdian a Charles A. WILKIE. Study on intumescent flame retarded polystyrene composites with improved flame retardancy. *Polymer Degradation and Stability* [online]. 2010, **95**(12), 2388–2395.
- [17] YAN, Yuan-Wei, Li CHEN, Rong-Kun JIAN, Shuang KONG a Yu-Zhong WANG. Intumescence: An effect way to flame retardance and smoke suppression for polystyrene. *Polymer Degradation and Stability* [online]. 2012, **97**(8), 1423–1431.
- [18] HORROCKS, A. Richard, D. PRICE a Dennis PRICE. *Fire Retardant Materials*. B.m.: Woodhead Publishing, 2001. ISBN 978-1-85573-419-7.
- [19] DUQUESNE, S., M. JIMENEZ a S. BOURBIGOT. Chapter 16 Fire Retardancy and Fire Protection of Materials using Intumescent Coatings – A Versatile Solution? In: *Fire Retardancy of Polymers: New Strategies and Mechanisms* [online]. B.m.: The Royal Society of Chemistry, 2009, s. 240–252. ISBN 978-0-85404-149-7.
- [20] CHEN, Xiao-Yu, Zong-Hou HUANG, Xiu-Qi XI, Jia LI, Xin-Yu FAN a Zhan WANG. Synergistic effect of carbon and phosphorus flame retardants in rigid polyurethane foams. *Fire and Materials* [online]. 2018, **42**(4), 447–453.
- [21] LI, Jie, Xuehua MO, Yi LI, Huawei ZOU, Mei LIANG a Yang CHEN. Influence of expandable graphite particle size on the synergy flame retardant property between expandable graphite and ammonium polyphosphate in semi-rigid polyurethane foam. *Polymer Bulletin* [online]. 2018, **75**(11), 5287–5304.
- [22] GERARD, Caroline, Gaele FONTAINE a Serge BOURBIGOT. Synergistic and antagonistic effects in flame retardancy of an intumescent epoxy resin. *Polymers for Advanced Technologies* [online]. 2011, **22**(7), 1085–1090.

- [23] ELBASUNEY, Sherif. Novel multi-component flame retardant system based on nanoscopic aluminium-trihydroxide (ATH). *Powder Technology* [online]. 2017, **305**, 538–545.
- [24] CAMINO, G., A. MAFFEZZOLI, M. BRAGLIA, M. DE LAZZARO a M. ZAMMARANO. Effect of hydroxides and hydroxycarbonate structure on fire retardant effectiveness and mechanical properties in ethylene-vinyl acetate copolymer. *Polymer Degradation and Stability* [online]. 2001, **74**(3), 457–464.
- [25] HAPUARACHCHI, T. D. a T. PEIJS. Aluminium trihydroxide in combination with ammonium polyphosphate as flame retardants for unsaturated polyester resin. *Express Polymer Letters* [online]. 2009, **3**(11), 743–751.
- [26] LIU, Jichun, Yingbin GUO, Haibo CHANG, Hang LI, Airong XU a Bingli PAN. Interaction between magnesium hydroxide and microencapsulated red phosphorus in flame-retarded high-impact polystyrene composite. *Fire and Materials* [online]. 2018, **42**(8), 958–966.
- [27] WANG, Chunfeng, Yongliang WANG a Zhidong HAN. Enhanced flame retardancy of polyethylene/magnesium hydroxide with polycarbosilane. *Scientific Reports* [online]. 2018, **8**(1), 14494.
- [28] HORROCKS, A. Richard, Gill SMART, Shonali NAZARE, Baljinder KANDOLA a Dennis PRICE. Quantification of Zinc Hydroxystannate** and Stannate** Synergies in Halogen-containing Flame-retardant Polymeric Formulations. *Journal of Fire Sciences* [online]. 2010, **28**(3), 217–248.
- [29] SALAMOVA, Amina a Ronald A. HITES. Brominated and Chlorinated Flame Retardants in Tree Bark from Around the Globe. *Environmental Science & Technology* [online]. 2013, **47**(1), 349–354
- [30] GAGNÉ, Pierre-Luc, Marlène FORTIER, Marc FRASER, Lise PARENT, Cathy VAILLANCOURT a Jonathan VERREAULT. Dechlorane Plus induces oxidative stress and decreases cyclooxygenase activity in the blue mussel. *Aquatic Toxicology* [online]. 2017, **188**, 26–32.
- [31] KEFENI, Kebede K., Jonathan O. OKONKWO, Olubiyi I. OLUKUNLE a Ben M. BOTHA. Brominated flame retardants: sources, distribution, exposure pathways, and toxicity. *Environmental Reviews* [online]. 2011, **19**, 238–253.

- [32] VAN DER VEEN, Ike a Jacob DE BOER. Phosphorus flame retardants: properties, production, environmental occurrence, toxicity and analysis. *Chemosphere* [online]. 2012, **88**(10), 1119–1153.
- [33] REALINHO, Vera, David ARENCÓN, Marcelo ANTUNES a José Ignacio VELASCO. Effects of a Phosphorus Flame Retardant System on the Mechanical and Fire Behavior of Microcellular ABS. *Polymers* [online]. 2019, **11**(1), 30.
- [34] WANG, Shaofeng, Yuan HU, Ruowen ZONG, Yong TANG, Zuyao CHEN a Weicheng FAN. Preparation and characterization of flame retardant ABS/montmorillonite nanocomposite. *Applied Clay Science* [online]. 2004, **25**(1), 49–55.
- [35] XING, Weiyi, Wei YANG, Wenjie YANG, Qihang HU, Jingyu SI, Hongdian LU, Benhong YANG, Lei SONG, Yuan HU a Richard K. K. YUEN. Functionalized Carbon Nanotubes with Phosphorus- and Nitrogen-Containing Agents: Effective Reinforcer for Thermal, Mechanical, and Flame-Retardant Properties of Polystyrene Nanocomposites. *ACS Applied Materials & Interfaces* [online]. 2016, **8**(39), 26266–26274.
- [36] YAKUSHIN, Vladimir, Arnis ABOLINS, Dzintra VILSONE a Irina SEVASTYANOVA. Polyurethane coatings based on linseed oil phosphate ester polyols with intumescent flame retardants. *Fire and Materials* [online]. 2019, **43**(1), 92–100.
- [37] ZAGHLOUL, Moustafa Mahmoud Yousry Mahmoud. Mechanical properties of linear low-density polyethylene fire-retarded with melamine polyphosphate. *Journal of Applied Polymer Science* [online]. 2018, **135**(46), 46770.
- [38] AHMED, Lubna, Bin ZHANG, Ruiqing SHEN, Robert J. AGNEW, Haejun PARK, Zhengdong CHENG, M. Sam MANNAN a Qingsheng WANG. Fire reaction properties of polystyrene-based nanocomposites using nanosilica and nanoclay as additives in cone calorimeter test. *Journal of Thermal Analysis and Calorimetry* [online]. 2018, **132**(3), 1853–1865.
- [39] TROITZSCH, Jürgen. *Plastics Flammability Handbook - Principles, Regulations, Testing, and Approval (3rd Edition)*. B.m.: Hanser Publishers, 2004. ISBN 978-1-56990-356-8.
- [40] HURLEY, Morgan J., Daniel T. GOTTUK, John R. Hall JR, Kazunori HARADA, Erica D. KULIGOWSKI, Milosh PUCHOVSKY, Jose' L. TORERO, John M. Watts JR a

- Christopher J. WIECZOREK, ed. *SFPE Handbook of Fire Protection Engineering* [online]. 5. vyd. New York: Springer-Verlag, 2016 [vid. 2019-03-21]. ISBN 978-1-4939-2564-3.
- [41] KUTZ, Myer. *Handbook of Environmental Degradation of Materials* [online]. B.m.: Elsevier, 2012 [vid. 2019-03-21]. ISBN 978-1-4377-3455-3.
- [42] PIELICHOWSKI, Krzysztof a James NJUGUNA. *Thermal Degradation of Polymeric Materials*. B.m.: Smithers Rapra Technology, 2005. ISBN 978-1-85957-498-0.
- [43] MOURITZ, A. P. a A. G. GIBSON. *Fire Properties of Polymer Composite Materials* [online]. B.m.: Springer Netherlands, 2006 [vid. 2019-03-21]. Solid Mechanics and Its Applications. ISBN 978-1-4020-5355-9.
- [44] CHATTOPADHYAY, D. K. a Dean C. WEBSTER. Thermal stability and flame retardancy of polyurethanes. *Progress in Polymer Science* [online]. 2009, **34**(10), 1068–1133.
- [45] SORATHIA, U., R. LYON, T. OHLEMILLER a A. GRENIER. A review of fire test methods and criteria for composites. *Sampe Journal*. 1997, **33**(4), 23–31.
- [46] MOURITZ, A. P., Z. MATHYS a A. G. GIBSON. Heat release of polymer composites in fire. *Composites Part A: Applied Science and Manufacturing* [online]. 2006, **37**(7), Special Issue on Fire Behaviour of Composites, 1040–1054.
- [47] SCUDAMORE, M. J. Fire performance studies on glass-reinforced plastic laminates. *Fire and Materials* [online]. 1994, **18**(5), 313–325.
- [48] FATEH, Talal, Charles KAHANJI, Paul JOSEPH a Thomas ROGAUME. A study of the effect of thickness on the thermal degradation and flammability characteristics of some composite materials using a cone calorimeter. *Journal of Fire Sciences* [online]. 2017, **35**(6), 547–564.
- [49] HURLEY, Morgan J., Daniel T. GOTTUK, John R. Hall JR, Kazunori HARADA, Erica D. KULIGOWSKI, Milosh PUCHOVSKY, Jose' L. TORERO, John M. Watts JR a Christopher J. WIECZOREK, ed. *SFPE Handbook of Fire Protection Engineering* [online]. 5. vyd. New York: Springer-Verlag, 2016 [vid. 2019-03-21]. ISBN 978-1-4939-2564-3.
- [50] SORATHIA, U., T. DAPP a J. KERR. *Flammability Characteristics of Composites for Shipboard and Submarine Internal Applications*. Covina: Soc Advancement Material & Process Engineering, 1991. ISBN 978-0-938994-56-5.

- [51] SASTRI, S. B., J. P. ARMISTEAD, T. M. KELLER a U. SORATHIA. Phthalonitrile-glass fabric composites. *Polymer Composites* [online]. 1997, **18**(1), 48–54.
- [52] ISO 5660-1:2002. *Reaction-to-fire tests - Heat release, smoke production and mass loss rate - Part 1: Heat release rate (cone calorimeter method)*. Geneva: International organization for standardization, 2002.
- [53] MEZGER, Thomas G. *The Rheology Handbook, 4th Edition*. B.m.: Vincentz Network, 2014. ISBN 978-3-86630-842-8.
- [54] HADDADI, Hamed, Navid FAMILI, Ehssan NAZOKDAST a Sadegh MORADI. Chemorheological analyses of a reaction injection moulding polyurethane formulation. *Iranian Polymer Journal (English Edition)*. 2006, **15**. 967-977.
- [55] UL 94. *Test for Flammability of Plastic Materials for Parts in Devices and Appliances*. Northbrook: Underwriters Laboratories Inc., 1996.
- [56] WAGNER, Matthias. *Thermal Analysis in Practice: Fundamental Aspects*. B.m.: Carl Hanser Verlag GmbH & Company KG, 2017. ISBN 978-1-56990-644-6.
- [57] GAISFORD, Simon, Vicky KETT a Peter HAINES. *Principles of Thermal Analysis and Calorimetry: 2nd Edition*. B.m.: Royal Society of Chemistry, 2016. ISBN 978-1-78262-051-8.
- [58] ATKINS, Peter a Julio de PAULA. *Atkins' Physical Chemistry*. B.m.: OUP Oxford, 2010. ISBN 978-0-19-954337-3.
- [59] EHRENSTEIN, Gottfried W., Gabriela RIEDEL a Pia TRAWIEL. *Thermal Analysis of Plastics: Theory and Practice*. B.m.: Carl Hanser Verlag GmbH & Company KG, 2012. ISBN 978-3-446-43414-1.
- [60] GRIFFITHS, Peter a James A. De HASETH. *Fourier Transform Infrared Spectrometry*. B.m.: John Wiley & Sons, 2007. ISBN 978-0-471-19404-0.

LIST OF ABBREVIATIONS

PUR – Polyurethane

THF – Tetrahydrofuran

PTMEG – polytetra-methylene ether glycol

PBT – polybutylene terephthalate

DMC – dimethyl carbonate

PC – polycarbonate

TDI – toluene-based isocyanate

MDI – aniline or formaldehyde-based isocyanate

pMDI – polymeric form of MDI

HDI – hexamethylene diisocyanate

IPDI - isophorone diisocyanate

H12DI - 4,4'-diisocyanatodicyclohexylmethane

HCN – hydrogen cyanide

MDA – 4,4'-Methylenedianiline

pMDA – polymeric form of MDA

HS – hard segment

SS – soft segment

FRS – flame retardant system

HFR – Halogen flame retardant

HRR – Heat release rate

ARHE – average rate of heat emission

MARHE – maximum average rate of heat emission

SEA – Specific extinction area

MLR – Mass loss rate

TSP – Total smoke produced

ATH – alumina trihydrate

MDH – magnesium hydroxide

BFR – bromine flame retardant

CFR – chlorine flame retardant

TBBPA – tetrabromobisphenol-a

ABS – acrylo butadiene styrene

HIPS – high impact polystyren

PBDE – polybromodiphenylether

EU – European union

HBCD – hexabromocyclododecane

TBPA – tetrabromophtalic anhydride

DP – Dechlorane plus

PFR – phosphorus-based flame retardant

APP I – Ammonium polyphosphate type 1

APP II – Ammonium polyphosphate type 2

IFR – intumescent flame retardant

Mel – Melamine

EG – expandable graphite

MPP – melamine polyphosphate

PE – polyethylene

LDPE – low density polyethylene

HDPE – High density polyethylene

PP – polypropylene

PVC – polyvinylchloride

HCl – hydrochloric acid

PET – polyethyleneterephthalate

PMMA – Polymethylene metacrylate

POM – polyoxymethylene

PC – polycarbonate

TGA – thermogravimetric analysis

PTFE – polytetrafluorethylene

MMT – montmorillonite

M_w – molecular weight

C – calibration constant obtained from methane flow calibration for cone calorimeter

$X_{O_2}^0$ – initial amount of oxygen

X_{O_2} – amount of oxygen at given time

Δp - Pressure difference at the orifice of cone calorimeter exhaust

T_e - total temperature at the orifice

$\dot{q}(t)$ – Heat flow

Δh_c – net heat of combustion

r_o – stoichiometric oxygen/fuel ratio

CO – carbon monoxide

CO₂ - carbon dioxide

η^* - complex viscosity

G' - storage modulus

G'' - loss modulus

C_p – heat capacity

T_g – glass transition temperature

T_m – melting temperature

T_c – crystallization temperature

T_{sg} - gelation temperature

DSC – dynamic scanning calorimetry

DMA – dynamic mechanical analysis

ΔH – change of enthalpy

LIST OF FIGURES

- Fig. 1:** Schematic representation of polyurethane chain and its segmented character [3]
- Fig. 2:** Mechanisms of isocyanate and alcohol reaction a) without catalyst b) with base or nucleophilic activator and c) acid or electrophilic activator. [8]
- Fig. 3:** Polyether [6]
- Fig. 4:** Schematic synthesis of polyether polyol [7]
- Fig. 5.:** Common polyether polyols [7]
- Fig. 6:** Polyester [6]
- Fig. 7:** Synthesis of polyester polyol [6]
- Fig. 8:** Synthesis of caprolactane polyester [7]
- Fig. 9:** Preparation of PC polyol from phosgene and dimethyl carbonate [6]
- Fig. 10:** Production of TDI [7]
- Fig. 11:** MDI and pMDI production schematic [7]
- Fig. 12:** Structures of common aliphatic isocyanates [6]
- Fig. 13:** Effect of intumescence and charring
- Fig. 14:** Expansion of intumescent used in coating of PUR foam. [19]
- Fig. 15:** HRR results on neat rigid PUR foam and rigid PUR foam filled with FR mixture of expandable graphite and guanidinium phosphate in various concentrations [20]
- Fig. 16:** Effect of ATH and APP on unsaturated polyester resin [25]
- Fig. 17:** HRR data of neat MDH and MDH modified with polycarbosilane [27]
- Fig. 18:** Structure of APP I and APP II [13]
- Fig. 19:** Effect of Melamine (Mel), APP and expandable graphite (EG) on HRR of speciality polyol [36]
- Fig. 20:** HRR of neat PS and PS filled with MMT and nanosilica [38]
- Fig. 21:** TGA scan of PE and PP [41]
- Fig. 22:** TGA scan for PET and PMMA [41]
- Fig. 23:** TGA scan for Acetal, Nylon 6 and PC under air and nitrogen atmosphere [41]

- Fig. 24:** Mechanics of PUR thermal degradation [44]
- Fig. 25:** Mechanics of N substituted PUR thermal degradation [44]
- Fig. 26:** Stages of fire during combustion of polymer [12]
- Fig. 27:** HRR profile in time. This is a common result of cone calorimeter measurement [43]
- Fig. 28:** THR/volume vs. sample thickness [43]
- Fig. 29:** Wind-aided and opposed-flow modes of surface flame spread [41]
- Fig. 30:** Schematic of different zones in a flame
- Fig. 31:** Schematic picture of thermal decomposition mechanism [43]
- Fig. 32:** Scheme of the cone calorimeter [49]
- Fig. 33:** scheme of cone heater [52]
- Fig. 34:** The two plates model [53]
- Fig. 35:** Scheme of sample deformation during oscillating tests [53]
- Fig. 36:** Dependence of Storage and loss modulus on the temperature from the temperature sweep measurement [54]
- Fig. 37:** Scheme of UL 94 Vertical burning test setup. [55]
- Fig. 38:** Force and displacement at $f = 1$ Hz. Deformation is delayed to applied force by time difference Δ . Phase angle $\delta = 2\pi f\Delta$. [56]
- Fig. 39:** Scheme of a DSC device [57]
- Fig. 40:** Idealized DSC curve showing phase transitions of polyolefinic material [59]
- Fig. 41:** FTIR spectra of the samples containing various amount of the Exolit IFR 36 additive.
- Fig. 42:** FTIR spectra of the samples containing various amount of the Exolit OP 560 liquid polyol.
- Fig. 43:** Record of temperature sweep measurement on sample AX_IFR 0
- Fig. 44:** Record of temperature sweep measurement on the sample AX_IFR 10
- Fig. 45:** Record of the temperature sweep measurement on the sample AX_IFR 20
- Fig. 46:** Record of the temperature sweep measurement on the sample AX_IFR 30

Fig. 47: Record of the temperature sweep measurement on the sample AX_IFR 50

Fig. 48: Record of the temperature sweep measurement on the sample AX_IFR 70

Fig. 49: Record of the temperature sweep measurement on the sample AX_OP 10

Fig. 50: Record of the temperature sweep measurement on the sample AX_OP 20

Fig. 51: Record of the temperature sweep measurement on the sample AX_OP 30

Fig. 52: Record of the temperature sweep measurement on the sample AX_OP 50

Fig. 53: Record of the temperature sweep measurement on the sample AX_OP 70

Fig. 54: Record of the temperature sweep measurement on the sample AX_OP 100

Fig. 55: DSC measurement curves for AX_IFR set of samples

Fig. 56: DSC measurement curves for AX_OP set of samples

Fig. 57: Dependence of the storage modulus on the temperature for various samples containing Exolit IFR 36 additive.

Fig. 58: Dependence of the storage modulus on the temperature for various samples containing Exolit OP 560 polyol liquid additive.

Fig. 59: Average heat release rate in time for AX_IFR set of samples

Fig. 60: MARHE values for increasing amount of IFR 36 in matrix

Fig. 61: mean SEA measured for AX_IFR sample set

Fig. 62: Remains of sample AX_IFR 10

Fig. 63: ARHE in time for AX_OP sample set with AX_IFR 0 for reference.

Fig. 64: MARHE values for increasing amount of OP 560. Black point represents AX_IFR 0 for reference

Fig. 65: mean SEA measured for AX_OP sample set with black point representing AX_IFR 0

Fig. 66: Remains of AX_OP 50

LIST OF TABLES

- Tab. 1:** Some of the most commonly used glycols, polyols and acids for polyester polyol production [6]
- Tab. 2:** Differences between MDI and pMDI [7]
- Tab. 3:** Common chain extenders [7]
- Tab. 4:** Combustion gasses and their concentration in various types of laminates [50] [51]
- Tab. 5:** Classification and their criteria for UL-94
- Tab. 6:** Mixing ratios of polyols and isocyanate
- Tab. 7:** Sample name and composition
- Tab. 8:** All measured values of η_{start} , η_{min} and T_{sg}
- Tab. 9:** Measured change of enthalpy and peak characterizing temperatures
- Tab. 10:** Important numeric results of cone calorimeter measurement
- Tab. 11:** Recorded times and events from UL94 test for AX_IFR set. With classification.
- Tab. 12:** Recorded times and events from UL94 test for AX_OP set. With classification.

APPENDICES

APPENDIX P I: APPENDIX TITLE